

GKSS Forschungszentrum
Institut für Werkstoffforschung
Abteilung Makromolekulare Strukturforchung

Development of new antimicrobial peptides based on the synthetic peptide NK-2

Dissertation zur Erlangung des Doktorgrades der Fakultät für
Mathematik, Informatik und Naturwissenschaften der Universität
Hamburg

vorgelegt von
Sebastian Linser

Geesthacht im Jahre 2006

Erster Gutachter der Arbeit:
Professor Doktor Ulrich Hahn

Zweiter Gutachter der Arbeit:
Privat Dozentin Doktor Regine Willumeit

Tag der Annahme der Dissertation: Freitag, 28.04.2006
Tag der Disputation: Freitag, 03.11.2006

Table of contents

1. Summary	5
2. Introduction	6
2.1. Adapted and innate immunity	6
2.2. Antibiotics (<i>Greek: against something living</i>)	7
2.3. Antimicrobial peptides	8
2.3.1. Mechanisms of action of antimicrobial peptides	11
2.3.2. Antimicrobial peptidomimetics	12
2.4. The antibacterial peptide NK-2	13
2.5. Bio-membranes	15
2.5.1. Lipid composition of bio-membranes	16
2.5.2. Lipid phase behaviour	17
3. Materials and Methods	19
3.1. Chemicals	19
3.2. Instruments	19
3.3. Buffers	20
3.4. Peptides and peptidomimetics	20
3.5. Lipids	21
3.6. Bacterial culture	25
3.6.1. Overnight and growth cultures	25
3.6.2. Microsusceptibility assay	26
3.7. Hemolysis	26
3.8. Mass spectroscopy	27
3.10. Preparation of liposomes for SAXS experiments	30
3.11. Small Angle X-ray Scattering (SAXS)	31
4. Description of the peptides	36
4.1. NK-2	36
4.2. Substitutions of reactive amino acids	38
4.2.1. NK-CS	38
4.2.2. NKCS-[MS]	38
4.3. Shortened analogues of NK-CS	39
4.4. Amino acid substitutions within the unstructured region of NK-CS ..	40
4.5. A modification predicted by computational modelling	41
4.6. Summary of important peptide parameters	41
5. Results	42
5.1. Structure-Function correlation for the peptide NK-2	42
5.2. Results for NK-CS	50
5.2.2. Investigation of shortened analogues of NK-CS	62
5.2.3. Results for peptides with modifications in the possible unstructured region	69
5.3. NKCS-[AA] – predicted by computational biology	72
5.4. Peptidomimetics	77
5.5. Summary of peptide parameters	82
6. Discussion	84
7. Conclusion	92
8. References	93
8.1. Own publications	93
8.2. Articles and books	94
8.3. Useful internet addresses	102
9. Acknowledgements	103

Abbreviations

AIDS	acquired immune deficiency syndrome
AMP	antimicrobial peptides
ATCC	American type culture collection
<i>B. megaterium</i>	<i>Bacillus megaterium</i>
B cells	bursa of fabricius (origin) lymphocytes
CD	Circular dichroism
CE	capillary electrophoresis
CFU	colony forming unit
CMC	critical micelle concentration
CPP	critical packing parameters
DMSO	Dimethyl sulfoxide
DiPOPE	1,2-dipalmitoleoyl-phosphatidylethanolamine
DOPE-trans	1,2-dielaidoyl-phosphatidylethanolamine
DPPC	1,2-dipalmitoyl-phosphatidylcholine
DSC	differential scanning calorimetry
<i>E. coli</i>	<i>Escherichia coli</i>
ESI	Electrospray ionization
FDA	food and drug administration
Fig	figure
GC	gas chromatography
HIV-1	human immunodeficiency virus 1
HPLC	high pressure liquid chromatography
IgG	immunoglobulin G
LPS	Lipopolysaccharid
MIC	minimal inhibitory concentration
MS	Mass spectroscopy
NaP	sodium phosphate buffer
NK cells	natural killer cells
NKL	NK-lysin
NMR	nuclear magnetic resonance
OD	optical density
<i>P. aeruginosa</i>	<i>Pseudomonas aeruginosa</i>
PBS	phosphate buffered saline
PDB	protein data bank
POPC	1-palmitoyl-2-oleoyl-phosphatidylcholine
POPE	1-palmitoyl-2-oleoyl-phosphatidylethanolamine
POPG	1-palmitoyl-2-oleoyl-phosphatidylglycerin
PPB	potassium phosphate buffer
RD	repeat distance
RT	room temperature
<i>S. aureus</i>	<i>Staphylococcus aureus</i>
<i>S. carnosus</i>	<i>Staphylococcus carnosus</i>
SAXS	small angle X-ray scattering
SDS	sodium dodecyl sulfate
T cells	thymus (origin) lymphocytes
TOF	time-of-flight
Tris	Tris[hydroxymethyl]aminomethane

1. Summary

Summary

The objective of this thesis was to develop derivatives of the antimicrobial peptide NK-2 and to correlate their activity with a structural description of their membrane interaction.

Eleven new antimicrobial peptides were synthesized and characterized with respect to their antibacterial and hemolytic activity, peptide structure and their impact on biological model membranes. For all tested peptides a correlation between the antibacterial activity and the impact on the inverse hexagonal phase transition of phosphatidylethanolamine lipids promoting a positive membrane curvature was found. This phase transition and the resulting polymorphism of phosphatidylethanolamine lipids is a prerequisite for cell division, fusion and probably also membrane protein function.

Additionally, in a parallel approach, the peptidomimetic molecule LA-03-149 was investigated. The concept of mimicking basic properties of antimicrobial peptides in order to achieve a similar biological effect was proven to be correct for this molecule which exhibits a good activity and interacts with model membranes in a peptide-comparable fashion affecting the inverse hexagonal phase transition of phosphatidylethanolamine lipids. Contrary to the findings described above, the peptidomimetic LA-03-149 decreased the transition temperature and thus promoted a negative membrane curvature.

Zusammenfassung

Ziel der vorliegenden Arbeit war die Entwicklung und das Verständnis der Wirkweise neuer antimikrobieller Peptide auf Basis des antimikrobiellen Peptides NK-2. Elf neue Peptide wurden synthetisiert und ihre antibakterielle und hämolytische Aktivität, die Struktur der Peptide und ihr Einfluss auf Modellmembranen untersucht. Für alle getesteten Peptide wurde ein Zusammenhang zwischen der antibakteriellen Aktivität und der Stärke des Einflusses auf den invers hexagonalen Phasenübergang von Phosphatidylethanolamin Lipiden entdeckt. Dieser Phasenübergang und der daraus resultierende Polymorphismus der Phosphatidylethanolamine ist eine Voraussetzung für die Zellteilung, die Zellfusion und eventuell auch für die Funktion von Membranproteinen. Alle entwickelten Peptide verstärkten die positive Membrankrümmung der Lipide, was sich in der Erhöhung der Phasenübergangstemperatur äußerte.

Zusätzlich zu den antibakteriellen Peptiden wurde ein peptidomimetisches Molekül charakterisiert. Die Idee, grundsätzliche Eigenschaften antimikrobieller Peptide mit peptidomimetischen Substanzen zu imitieren um damit denselben biologischen Effekt zu erzielen, hat sich durch die gute antibakterielle Aktivität und eine den Peptiden ähnliche Wechselwirkung mit Modellmembranen des kleinen Moleküls LA-03-149 bestätigt. Im Gegensatz zur oben erwähnten Unterstützung einer positiven Membrankrümmung induziert das Molekül LA-03-149 jedoch eine negative Membrankrümmung, zu erkennen an der Herabsetzung der hexagonalen Phasenübergangstemperatur.

2. Introduction

2.1. Adapted and innate immunity

The immune system is a complex network of specialized cells, organs and molecules that has evolved to defend the body against attacks by "foreign" invaders. When functioning properly, it fights off infections by bacteria, viruses, fungi, and parasites. When it malfunctions, it can unleash many diseases, from allergy to arthritis to cancer to AIDS.

The body has devised different astonishingly intricate defences that are divided into two types: Adapted and innate immunity. Already in the 5th century B.C., Greek physicians noted that people who had recovered from the plague would never get it again - they had acquired immunity. The reason for this is the astonishing feature of the *adapted immune system* to be distinct between self and nonself particles or cells. Any substance that is recognized as nonself will trigger an immune response and is called an antigen. An antigen announces its foreignness by means of intricate and characteristic epitopes, which are shown on its surface and will activate T and B cells. Some of the cells become "memory" cells which prime the immune system upon encounter of that same antigen, to destroy it quickly. So called "active or adapted" immunity (classified by mounting an immune response) can be triggered by both infection and vaccination. Vaccines contain micro organisms that have been altered so they will produce an immune response but will not be able to induce full-blown disease. In abnormal situations, the immune system can wrongly identify self as nonself and execute a misdirected immune attack. The result is a so-called autoimmune disease such as rheumatoid arthritis or systemic lupus erythematosus.

The second, and for this work more important mechanism of response against intruders, is the *innate or passive immunity* (Janeway, C.A., Jr. et al. 2002 and Zasloff, M., N. Engl. J. Med. 2002). The genetically based innate immunity system is what we are born with and it is nonspecific; all antigens are attacked pretty much equally. The first barriers of this system are mechanical obstacles that avoid the introduction of microorganisms and pathogens. The most important barrier is the skin; it cannot be penetrated by most organisms unless it already has an opening, such as a scratch or a cut. Other pathogens are expelled from the lungs by ciliary action; coughing and sneezing abruptly eject both living and nonliving things from the respiratory system; the flushing action of tears, saliva and urine also force out pathogens, as does the sloughing off of skin. Furthermore, sticky mucus in the respiratory and gastrointestinal tracts traps many microorganisms and after all, the stomach is a formidable obstacle insofar as its mucosa secretes hydrochloric acid ($0.9 < \text{pH} < 3.0$) and protein-digesting enzymes that kill many pathogens. The innate immunity is not separated from the adaptive immunity, but involved in the cascade of the adaptive immune response (Janeway, C.A., Jr and Medzhitov, R. Sem. Immunol. 1998; see also references therein). Beside the mechanical barriers there are more biochemical ways to inhibit infections by pathogens. Infants are born with relatively weak immune responses. They have, however, a natural "passive" immunity; they are protected during the first months of life by means of antibodies they receive from their mothers. The antibody IgG, which travels across the placenta, makes them immune to the same microbes to which their mothers are immune. In parallel NK (Natural Killer) cells, which are activated by lymphokines released from T cells, are able to secrete molecules that can kill bacteria. The T and NK cells play, together with neutrophils and macrophages, a key role in the innate immune system. All of those cells are known to contain multiple molecules for example in granules. Some

of these substances are called antimicrobial peptides or **peptide antibiotics** (AMPs) and are abundant in all species. A speciality of some of the peptides is their membrane activity without needing a protein receptor. Because of their widespread abundance and their huge variety a short overview about peptides from different origin will be given in the next paragraphs.

2.2. Antibiotics (*Greek: against something living*)

In September 1923 the British physician Alexander Fleming discovered by accident a substance that was able to kill bacteria - that substance was named lysozyme. Shortly after he isolated the antibiotic substance penicillin from the fungus *Penicillium notatum* (Fleming, A. Br. J. Exp. Pathol. 1929), for which he shared a Nobel Prize in 1945. After that amazing discovery, medicine was revolutionized and many scientists concentrated on finding more of these substances. Until now a huge variety of antibiotics are used to cure bacterial infections. They are one of the most used drugs worldwide and about 8000 different substances are known today. A classification can be done in different categories; an example by their mechanism of action is given below (taken and modified from Alberts, B. et al. 1994 and see also <http://www.wikihealth.com/Antibiotic>). In general these antibiotics are receptor bound (either protein or DNA/RNA specific).

- *Antibiotics which interfere with cell-wall synthesis*
 - Beta-lactams, including penicillins and cephalosporins; mono-lactams, such as imipenem; vancomycin, bacitracin
- *Antibiotics which interfere with bacterial protein synthesis*
 - *Antibiotics which bind to the 50S ribosomal unit*
 - Lincosamides/lincosides including clindamycin and lincomycin; chloramphenicol, macrolides
 - *Antibiotics which interfere the 30S ribosomal unit*
 - Tetracyclines; aminoglycosides including gentamicin
- *Drugs which inhibit folate synthesis*
 - Sulfonamides and trimethoprim
- *Drugs which interfere with DNA synthesis*
 - Metronidazole, quinolones, novobiocin
- *Drugs which interfere with RNA synthesis*
 - Rifampin (rifampicin)

Antibiotics are highly potent and relatively cheap drugs for treatment of infections. Unfortunately, their witless and abundant (mis)use eventually led to the severe problem of development of antibiotic resistance by bacteria. By the year 1984 half of the people with active tuberculosis in the United States of America had a strain that resisted at least one antibiotic (<http://www.wikihealth.com/Antibiotic>). In more affected locations like hospitals and some child-care places, the rate of antibiotic resistance is much higher than normal and low cost antibiotics are virtually useless for treatment of regularly seen infections. For example, the number of vancomycin resistant infections in US hospitals increased from the year 1987 to 2002 from 1% to 25%, while the methicillin resistant infections even increased over 20 years until 2002 from 3% to 60% (Leeb, M. Nature. 2004). The financial burden coming with the medication of all infectious diseases is enormous. In the United States of America alone, twenty billion dollars are spent for therapies annually (Nature Biotech., 2000).

Therefore it is necessary to search for alternatives to conventional antibiotic therapies. Two new candidates have emerged; on the one side carbohydrate agents and second, more important for this work, peptide antimicrobials (Hancock, R.E.W. Lancet. 1997). The discovery of these AMPs could open up a new strategy if, from this new class of 'antibiotics', potent candidates for drug development can be identified.

These peptide antibiotics, which are in the centre of this work, are molecules of the innate immune system that have mechanisms to kill bacteria that differ from conventional antibiotics. Their interaction is membrane lipid specific and no further protein receptor is necessary. In contrast to the given examples of antibiotics, so far there is no clinical application of a peptide antibiotic. The first treatment using the peptide antibiotic magainin against diabetic foot ulcers was rejected in 1999 by the FDA (see <http://www.diabetes-mellitus.org/locilex.htm>). Currently several synthetic peptide antibiotics are under clinical trial (see Bush, K. et al. Curr. Opin. Microbiol. 2004 and <http://www.genaera.com/clinicaltrials.html>). One example out of this overview is the synthetic analogue of the naturally occurring antimicrobial peptide protegrin-1, Isegranon (Giles, F.J. et al. Expert Opin. Investig. Drugs. 2002).

2.3. Antimicrobial peptides

Several hundreds of peptide antibiotics have been discovered in the recent years (a small selection is described in table 1; see also Vizioli, J. and Salzet, M., Trends Pharmacol. Sci. 2002 and Hancock, R.E.W., Lancet. 1997). The peptides differ in size, sequence, charge, hydrophobicity and their ability to interact with membranes. But they all are amphipathic, charged molecules which can kill bacteria and fungi. Examination of these peptides has shown only general trends but little sequence homology, and this suggests that each peptide has evolved to act optimally in the environment in which it is produced and against local micro organisms. On the other hand, the lack of sequence homology makes it difficult to predict the activities and mechanisms of action of the peptides. That fact also makes it challenging to design potent synthetic antimicrobial peptides which have the desired *in vivo* activities for example for clinical applications (Hancock, R.E.W. and Chapple, D.S. Antimicrob. Agents Chemother. 1999).

Antimicrobial peptides can be distinguished in non-ribosomally synthesized peptides, such as the gramicidins, polymyxins, bacitracins, glycopeptides, etc., and ribosomally synthesized (natural) peptides. The non-ribosomally synthesized peptides are largely produced by bacteria, whereas the ribosomally synthesized peptides are produced by all species (including bacteria) as a major component of natural host defence molecules (Hancock, R.E.W. and Chapple, D.S. Antimicrob. Agents Chemother. 1999). AMPs are present within the granules of neutrophils, in mucosal or skin secretions from epithelial cells, or as the degradation products of proteins. It is known that neutrophils contain a range of antimicrobial proteins and peptides including cationic antimicrobial proteins, lysozyme, lactoferrin, bactenecins, defensins, indolicidins, and cathelicidins. Many other cell types including epithelial cells and platelets (which produce platelet microbicidal proteins) also produce different antimicrobial substances. Thoroughly studied mammalian peptides are the defensins (Ganz, T. Science. 1999). Furthermore, the proteolytic degradation of cationic proteins is thought to contribute to the formation of antimicrobial peptides.

Table 1: Overview of antimicrobial peptides.

CLASS	EXAMPLE	ORIGIN	REFERENCE
Anionic peptides	Maximin H5	amphibians	Lai, R. et al (2002)
	Dermicidin	human	Schittek, B. et al (2001)
Cationic α-helical peptides	Cecropin (A)	insects	Steiner, H. et al (1981)
	Melittin	insects	Habermann, E. (1972)
	Magainin-II	amphibians	Zasloff, M. (1987)
	Dermaseptin	amphibians	Pouny, Y. et al (1992)
	Buforin-II	amphibians	Park, C.B. et al (2000)
	LL-37	human	Johansson, J. et al (1998)
Cationic peptides with an abundance of specific amino acids	Abaecin (Proline-rich)	honeybee	Boman, H.G. (1995)
	Apidaecins (Proline- and Arginine-rich)	honeybee	Boman, H.G. (1995)
	Bactenectins (Proline- and Arginine-rich)	cattle, sheep and goats	Shamova, O. et al (1999)
	PR-39 (Proline- and Arginine-rich)	pig	Boman, H.G. et al (1993)
	Prophenin (Proline- and Phenylalanine-rich)	pig	Zhao, C. et al (1995)
	Hymenoptaecin (Glycine-rich)	honeybee	Boman, H.G. (1995)
	Celeopteracin (Glycine- and Proline-rich)	beetle	Boman, H.G. (1995)
	Indolicidine (Tryptophan-rich)	cattle	Selsted, M.E. et al (1992)
Peptides and Proteins that form disulphide bridges	Brevinins (one disulphide bridge)	amphibians	Basir, Y.J. et al (2000)
	Tachyplesin (two disulphide bridges)	horseshoe crab	Kokryakov, V.N. et al (1993)
	Defensins (three disulphide bridges)	human, rabbit, rat, cattle mice, pig, goat, poultry, monkey	Ganz, T. (2003) Lehrer, R.I. (2004) Tang, Y.Q. et al (1999)
	NK-lysin (three disulphide bridges)	pig	Andersson, M. et al (1995)
	Drosomycin (more than three disulphide bridges)	fruit fly	Fehlbaum, P. et al (1994)
Peptides that are fragments of larger proteins	Lactoferricin (from Lactoferrin)	-	Kuwata, H. et al (1998)
	Casocidin (from casein)	human	Zucht, H.D. et al (1995)

Ribosomally synthesized peptides are of high interest because of their high potency to become a new class of antibiotics. For example, frog skin has been used for medicinal purposes for centuries and is still used today in South American countries. The isolation of bombinin (Csordas, A. and Michl, H. Monatsheft Chem. 1970) and subsequently the class of magainins from *Xenopus* species (Zasloff, M. PNAS. 1987) led to the investigation and discovery of peptides throughout many amphibian species. Alone within *Xenopus* over a dozen antibiotic peptides, which are expressed not only within the granular glands of the skin but also in the cells of the gastric mucosa and intestinal tract, have been discovered (Kreil, G. Ciba Found. Symp. 1994). For peptides from amphibians, synergy is observed with combinations of the peptides. All known amphibian peptides have been shown or predicted to form cationic amphipathic alpha-helices, e.g., magainins, dermaseptins, and buforin-II or are cysteine-disulfide loop peptides, as it was found for ranalexin and the brevinins from the *Rana* frog species. In 1972, the small antimicrobial and hemolytic peptide melittin was isolated from bee venom (Habermann, E. Science. 1972) and became the basis for extensive research into the structure and mechanism of action of this type of cationic antimicrobial peptide. Insect antimicrobial peptides in general are isolated from two sources. Some are secreted within the insect, as for example, the cecropins which are found within the hemolymph of the cecropia moth. Some are found outside the body like melittin in the bee venom (Hancock, R.E.W. and Chapple, D.S. Antimicrob. Agents Chemother. 1999). Although both classes are found to be antimicrobial, the venoms also tend to have cytotoxic activities.

The focus within this work was put on membrane active ribosomally synthesized peptides, due to their potent antibacterial activity and also due to the probable mechanism of action. It is thought that these cationic and amphiphilic peptides act by a direct impact on the bacterial membranes, and from this reason the hope arised that no resistance against the AMP will occur. To understand the selectivity and the exact mode of action of antibacterial membrane active peptides, synthetic peptides have been synthesized by systematic variation of naturally occurring peptides, by variation of model peptide sequences predicted to form amphipathic alpha-helices or by random processes. By creating a synthetic peptide based on a naturally occurring peptide, it is possible to improve antibacterial activity and at the same time give insight into the mechanism of action ((Hancock, R.E.W. and Chapple, D.S. Antimicrob. Agents Chemother. 1999).

The start was done by searching for analogues of cecropins with improved antibacterial activity and low cytotoxicity, and for this reason cecropin-melittin hybrids were developed (Boman, H.G. et al. FEBS lett. 1989). Analogous modification experiments have been undertaken to design peptides based on both sequence and amphipathicity. An alpha-helical antibacterial model peptide was synthesized by determining the most frequent amino acids in the first 20 positions for over 80 different natural sequences (Tossi, A. et al. Eur. J. Biochem. 1997). As found for many other α -helical peptides, this peptide was unstructured in water but readily adopts an α -helix in a hydrophobic environment. Synthetic peptides are also designed in order to improve factors such as specificity, stability, and toxicity. These studies have been based on naturally occurring peptides. But it is also possible to discover potent antimicrobial peptides randomly. Combinatorial libraries allow the systematic examination of millions of peptides. Investigators have identified a number of tetra- and hexapeptides composed of L-, D-, and unnatural amino acids which exhibit antimicrobial activities against *Staphylococcus aureus* (Blondelle, S.E. et al. Antimicrob. Agents Chemother. 1996).

The approach in this work is the knowledge based design of more potent antibacterial peptides taking into account the structure-function relation.

2.3.1. Mechanisms of action of antimicrobial peptides

The focus of this work was concentrated on cationic alpha-helical peptides, because the peptide that was investigated at first (NK-2; see chapter 1.4.) can be classified into this category. Cationic antimicrobial peptides can be specific for Gram negative or Gram positive bacteria only, or display a broad spectrum activity in nature. The most potent peptides have good MICs (minimal inhibitory concentrations of 1 to 8 µg/ml) against a wide range of bacteria (Hancock, R.E.W. Lancet. 1997). Beside their ability to kill bacteria, some, for example a cecropin-melittin hybrid, can neutralize endotoxin (Piers, K. et al. Antimicrob. Agents Chemother. 1994) and show a high synergy with conventional antibiotics especially against resistant mutants (Hancock, R.E.W., Lancet. 1997). For these reasons peptide antibiotics appear to have excellent potential in the fight against antibiotic-resistant bacterial pathogens.

It is very difficult to predict the activity of a peptide from its sequence. Most peptides without disulfide bridges have random structures in water, and only in the proximity of a membrane or other hydrophobic environments, these peptides form a structure (Bello, J. et al. Biochem. 1982 and Falla, T.J. et al. J. Biol. Chem. 1996). For example melittin folds into amphipathic α -helices in membranous environments. So far it is known that both the cationic and amphipathic nature of the peptides is important for the initial interaction between the peptide and bacterial membrane. The charge and the hydrophobicity of the peptides promotes an interaction and binding with bacterial outer and cytoplasmic membranes. That is possible due to increased electrostatic and hydrophobic interactions between the lipid headgroups, their acyl chains and the hydrophobic helix core (Wieprecht, T. et al. FEBS Lett. 1997).

The first step is the approach of the peptides to the membranes. In Gram negative bacteria, it is hypothesized that cationic peptides interact with the highly negatively charged outer membrane. The surface of the membrane contains magnesium ions which function to neutralize the charge and it is believed that the cationic peptides displace these magnesium ions (Hancock, R.E.W. Lancet Infect. Dis. 2001). The peptides then either bind tightly to the negatively charged membrane lipopolysaccharide (LPS) or neutralize the charge over an area of membrane subsequently distorting the membrane structure (Hancock, R.E.W. Lancet Infect. Dis. 2001). Once this occurs the peptides can translocate across the outer membrane.

The bacterial cytoplasmic membrane is also negatively charged. Cationic peptides can insert in a position parallel to the membrane lipids and fold into membrane-bound structures leading to multiple possible mechanisms of membrane disruption: Defensins, cecropins and bacteriocins form voltage-dependent ion-permeable channels in planar lipid bilayer membranes. This is the so called '**barrel stave mechanism**', first proposed to explain the interaction of the peptide alamethicin (see on the left side within the figure 1). For this mechanism (also called helical-bundle model) monomers of the peptide bind to the membrane and will eventually insert into the membrane, subsequently followed by recruitment of additional monomers. At a threshold concentration the helices of the peptides are bundled into the membrane to form a pore (Brodgen, K.A. Nature Rev.. 2005). The formation of a pore is strongly dependent on the lipid bilayer composition and the number of peptides involved (Cantor, R.S. Biophys. J. 2002).

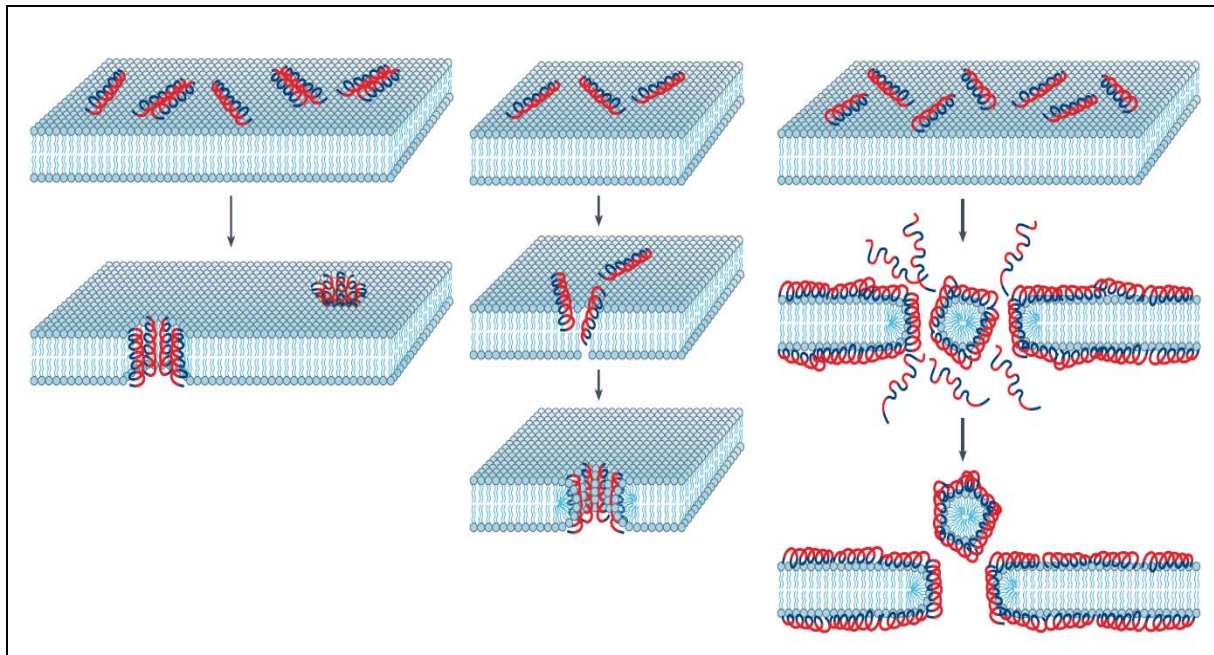


Figure 1: Comparison of different antimicrobial mechanisms: Left side: Barrel stave model. Center: Toroidal Pore and right side: Action of membrane disrupting by the carpet model. Modified after Brodgen, K.A. Nature Reviews (2005).

The evidence that these peptides form channels has been widely disputed, and alternative models have been proposed, for example the **carpet model** (figure 1; right side), in which peptide molecules saturate the surface of the cytoplasmic membrane before causing a wholesale disruption of the membrane permeability barrier (Pouny, Y. et al. Biochem. 1992). Peptides like dermaseptin and ovosporin are electrostatically attracted to anionic phospholipid head groups and orientate parallel to the bilayer surface (Bechinger, B. BBA. 1999). They cover the surface like a carpet until a threshold peptide concentration is reached and the disruption is started. The curvature of the membrane is distorted, the membrane disintegrates, and micelles are formed as shown in figure 1 (Shai, Y. BBA. 1999).

AMPs like magainin-II, protegrin-I and LL-37 tend to form a **toroidal pore** that differs from the two mechanisms described above (figure 1; in the middle). Here the peptides insert their helices into the membranes and effect that the lipid monolayer bend into the pore that the water core is lined by both the inserted peptide and the lipid head groups (Matsuzaki, K. et al. Biochem. 1996). In the end the peptides associate with the polar head groups of the lipids even when they insert into the bilayer (Yang, L. et al. Biophys. J. 2001), in contrast to the barrel stave pore that was described above.

2.3.2. Antimicrobial peptidomimetics

AMPs can be a potent alternative to so far used antibiotics. Still they also have some disadvantages. They have only a low stability due to fast proteolysis after application; a poor absorption due to their hydrophilicity and if they resist the proteolysis there is also a relatively fast secretion from the kidneys and the liver. For these reasons there is a strong interest to develop synthetic substances that mimic the properties of AMPs, but are not as damageable as AMPs (Giannis, A. and Kolter, T. Angew. Chem. 1993). Recent developments of peptidomimetics can be classified into beta-

peptides (Porter, E.A. et al. Nature. 2000 and Liu, D. and DeGrado, W.F. J. Am. Chem. Soc. 2001), peptoids, which are thought to mimic for example standard antimicrobial peptides like magainin (see Patch, J.A. and Barron, A.E. J. Am. Chem. Soc. 2003), cyclic and noncyclic D- and L-amino acids (Oren, Z. and Shai, Y. Biochem. 1997), arylamides (Tew, G.N. et al. Proc. Natl. Acad. Sci. U.S.A. 2002) and phenylene ethynyls (Arnt, L. et al. J. Polym. Sci. A Polym. Chem. 2004). Many of these substances share the feature of selectivity with antimicrobial peptides and beside these AMPs some other important drugs have been developed by imitating peptides or proteins, for example the production of a potent proteases inhibitor in therapies against HIV infections was possible (Böhm, H.J. et al. 1996 and Böhm, H.J. J. Comput-Aided Mol. Design, 1996).

The design of peptidomimetics focuses on the physicochemical properties of the AMPs, mainly the charge and the amphiphilic structure of the peptide. A typical arrangement of side groups (that are charged, polar or nonpolar) is necessary (figure 2). Substances that match this scheme tend to be rather amphiphilic and in case of a phenylene ethynyl backbone they exhibit a strong antimicrobial activity and a good selectivity (Arnt, L., Rennie, J.R., Linser, S., Willumeit, R. and Tew, G.N. J. Phys. Chem. B. 2006).

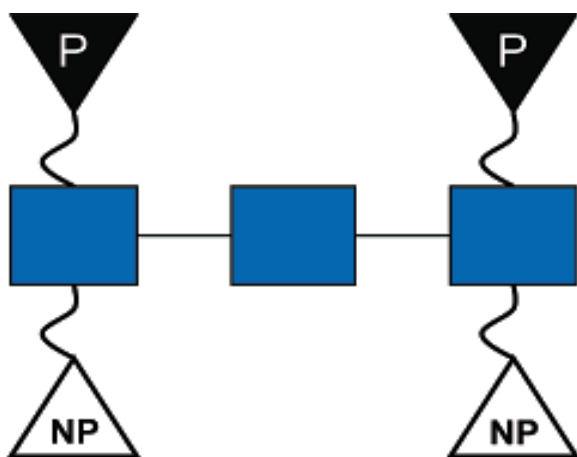


Figure 2: Arrangement of polar (P) and nonpolar (NP) groups that are directed to opposite sides from the backbone (blue boxes) of a structure. Taken from Arnt, L. et al. J. Phys. Chem. B. 2006.

2.4. The antibacterial peptide NK-2

The peptide NK-2 was derived from the natural occurring protein NK-lysin by Andrä and Leippe (Andrä, J. and Leippe, M. Med. Microbiol. Immunol. 1999). NK-lysin is a 78 amino acid residue protein (for sequence see figure 3) that was first isolated from porcine small intestine (Andersson, M. et al. EMBO J. 1995). NK-lysin is an element of the cytotoxic machinery of T and NK cells, where it works as an effector peptide to kill target cells.

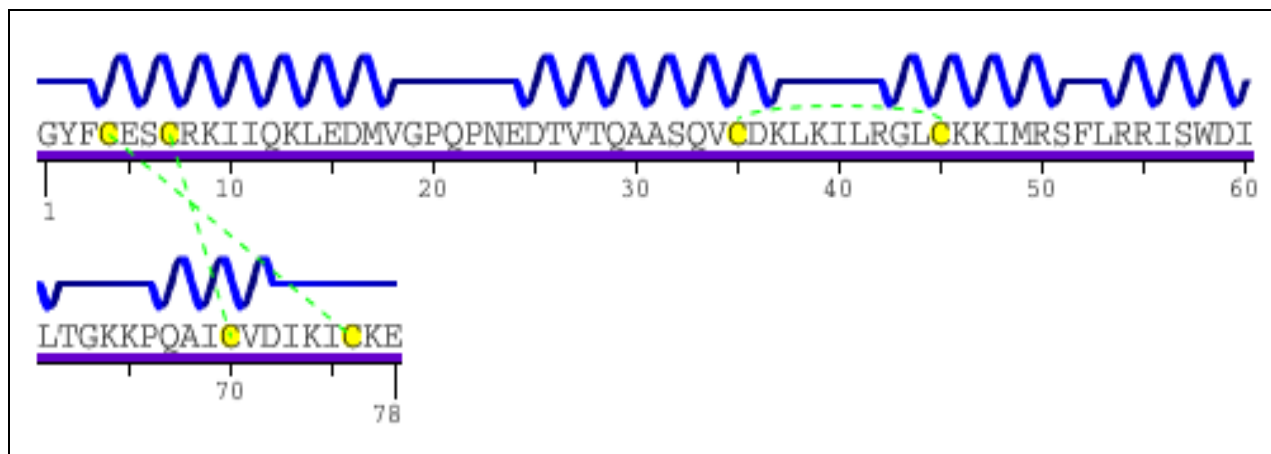


Figure 3: Amino acid sequence of NK-lysin taken from the Protein Data Bank (PDB 1NKL; Liepinsh, E. et al., Nature Struct. Biol. 1997). Disulfide bridges are indicated by the green truncated lines.

Andersson and colleagues already found that NK-lysin has a high activity against *Escherichia coli* (lethal concentration (LC) against the strain D21 was 0,5 μ M, respectively 8 μ M when bacteria were cultured without medium E) and *Bacillus megaterium* (LC was 1,6 μ M, respectively 0,8 μ M when bacteria were cultured without medium E) and also a moderate antifungal activity against *Candida albicans* (LC of 30 μ M) in a range that was found earlier for the human peptide defensin NP-2 (Lehrer, R.I. et al. Annu. Rev. Immunol. 1993). These two molecules show a simple homology although NK-lysin, with a molecular weight close to 9 kDa is larger than the defensins. NK-lysin does not develop activity against *Pseudomonas aeruginosa*, *Staphylococcus aureus* and the *Salmonella* strain LT-2 (Garcia-Penarrubia, P. 1992). The selectivity of NK-Lysin is good because it does not show activity against sheep red blood cells up to a concentration of 170 μ M (Andersson, M. et al. EMBO J. 1995).

In 1997 the three dimensional structure of NK-lysin was determined by NMR spectroscopy (figure 4). NK-lysin consists of five α -helices folded into a single globular domain.

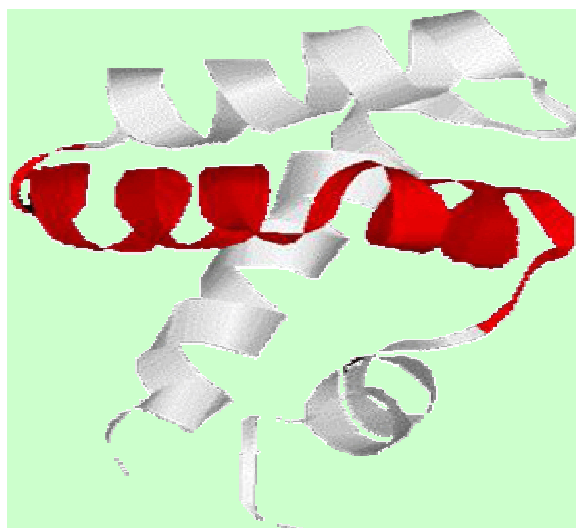


Figure 4: Three dimensional NMR structure of NK-lysin. The α -helices marked in red belong to the short fragment of NK-lysin, called NK-2 (with three modifications, see text). The structure was published by Liepinsh, E. et al. Nature Struct. Biol. 1997.

Functional studies of NK-lysin fragments showed that the lytic activity of the protein is caused by the amino acids residues 39-65 only (Andrä, J. PHD thesis. 1996). Exchange of three amino acids created a more potent peptide which was called NK-2 (see figure 5). This sequence corresponds to the third and fourth helices of the NK-lysin structure. Further investigations against a broader selection of bacteria, fungi and mammalian cells showed a high selectivity against pathogens and NK-2 was suggested to be a potent member of the uprising class of peptide antibiotics (Andrä, J. and Leippe, M. Med. Microbiol. Immunol. 1999).



Figure 5: Sequence of NK-2 (corresponding to the sequence of NK-lysin: Amino acids 39-65). The red labeled amino acids differ from the sequence of NK-lysin. The Lysine at position six was replaced by a Valine, the Serine at position thirteen was replaced by a Threonine and Tryptophan at position 20 was replaced by Lysine.

In this work the mechanism of the NK-2's interaction with the target cell is studied and antibacterial active derivatives are developed.

2.5. Bio-membranes

The cell membranes of bacteria (Gram positive and Gram negative) differ in their composition significantly from mammalian cell membranes (see table 2). Furthermore, for Gram positive bacteria like *Bacillus subtilis* or *Staphylococcus carnosus* only one lipid bilayer connected to a peptidoglycan network has to be taken into account. Gram negative bacteria like *Escherichia coli* have a second lipid bilayer consisting of lipopolysaccharide reaching into the extracellular space. This lipopolysaccharide (LPS) is very important in bacterial infections. When it is released from the membrane it can cause sepsis. Therefore a potent antimicrobial peptide should inhibit the release of LPS by Gram negative bacteria, either by killing the bacteria very fast before the LPS is secreted or by neutralizing the bacterial endotoxin after its release.

The cell membrane itself is a lipid bilayer with a variety of functional proteins, carbohydrates and their complexes (figure 6). The membranes are filled with proteins that pass through the membrane or are embedded into the bilayer; some of those proteins build pores or channels through the membrane. The so called 'Fluid Mosaic Model' suggested in 1972 by Singer and Nicholson was the first description of the membrane structure. The formation of a lipid bilayer in water is a self-assembling process involving rearrangements of water and lipid molecules such that the overall free energy change for the reaction is at an optimum. The reactants involved must attain a state of minimum energy and maximum entropy. In order to accomplish this, the hydrocarbon chains of the lipids are taken away from water whereas the polar head groups are in contact with water.

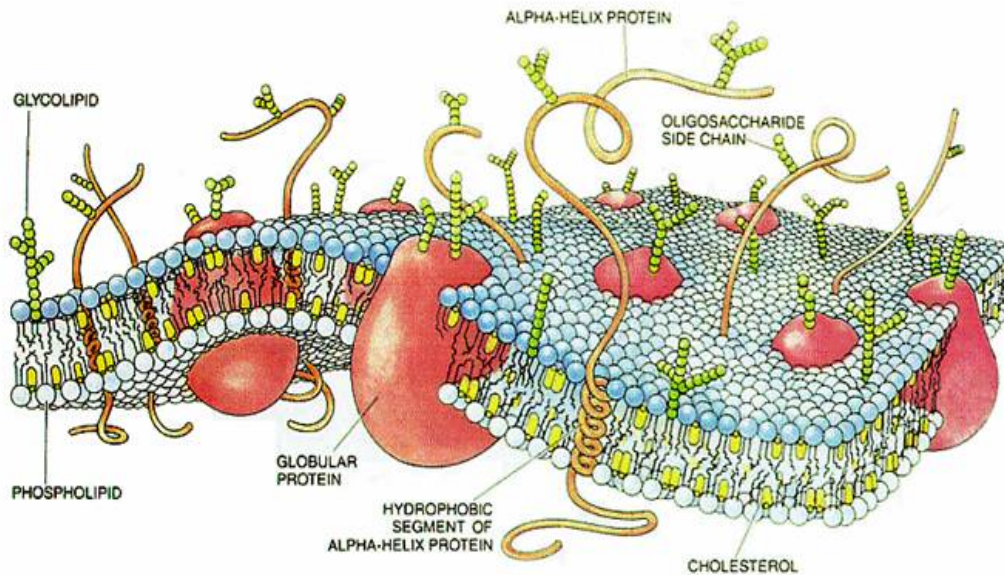


Figure 6: Schematic picture of a cell membrane sequestered with proteins (modified after Singer, S.J. and Nicholson, G.L. Science. 1972).

The cell membrane plays a pivotal role in energy conversion, material translocation, signal transduction and information processing. Most membranes are semi-permeable, meaning they are permeable to water but only selectively permeable to various solvents (for example glucose, ions, etc.). Therefore, transmembrane activities are driven by gradients of chemical and electrochemical potentials.

2.5.1. Lipid composition of bio-membranes

One of the principal classes of lipids in bio-membranes are phospholipids. These molecules have a potent reactive phosphate group that is connected to a glycerol which is connected to the hydrocarbon tails (this molecule is called a phosphatidyl). The top region is the polar headgroup. It is connected to the phosphate group and subsequently a glycerol is bound. The following two fatty acid tails are component of the nonpolar part of the molecule. Due to these hydrophobic and hydrophilic regions, lipids are amphipathic molecules where the headgroup interacts with water and the nonpolar acyl chains are repelled by water. For this reason lipids are able to structure in highly ordered supra molecular aggregates (Israelachvili, J.N. et al. Q. Rev. Biophys. 1980). The main suprastructure of a single lipid is the formation of a lipid bilayer where hydrogen bonds between polar groups stabilize the bilayer structure.

The thickness (that varies from 6 to 10 nm (Frömter, E. 1982) and electrostatic properties of a bilayer depend on the lipid composition which varies for cell types (see table 2) and on the saturation of the chains, which has important influences on the packing and movement of the lipids in the lateral plane of the membrane.

The multilayers can be analysed with different techniques; in this work SAXS measurements were done to determine the repeat distance of the investigated lipids (figure 7). This correlation of the reflections indicates an aggregate of multilamellar stacks; in this case d stands for the length of the lamellar cell or the repeat distance (figure 7). The repeat distance indicates the distance between two lipid double layers including the in between lying water layer and indicates the molecular ordering of the multilamellar vesicles.

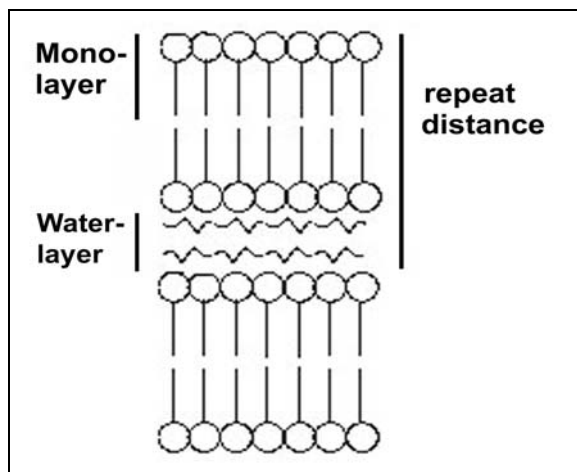


Figure 7: Schematic picture of the repeat distance.

Table 2: Lipid composition of biological membranes. The values are given as weight percent of total lipid. Source: Alberts, B. et al. 1994.

Lipid	Human Erythrocyte	Human Myelin	Beef Heart Mitochondria	<i>E. coli</i>
Phosphatidylcholine	17	10	39	0
Phosphatidylethanolamine	18	15	35	70
Phosphatidylserine	7	9	2	0
Sphingomyelin	18	8	0	0
Glycolipids	3	28	0	0
Cholesterol	23	22	3	0
others	13	8	21	30

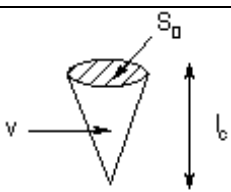

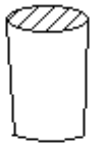
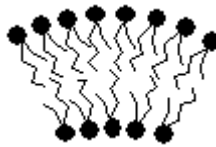


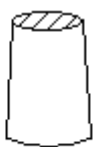

It is the chemical composition of a given membrane which determines its biophysical properties, and this composition differs from membrane to membrane. Beside this, the structure of a membrane is also depending on the surrounding medium, and thereby water and salts are of importance to determine the lipid configuration.

2.5.2. Lipid phase behaviour

One astonishing feature of a membrane is its fluidity that strongly influences the functional properties of the membrane. The mobility of the lipid molecules within the flexible plane of the membrane permits also mobility and flexibility of protein molecules. The lipid composition, the total saturation of the acyl chains and the interaction of the membrane lipids with proteins or peptides can change the fluidity and the phase behaviour of the bilayer. In addition, in model systems, the structure and biophysical properties of a bilayer can also be altered by temperature (Cotterill, R. 2004). Several lipid structures are known: L_c , L_β , $L\beta'$, $P\beta'$, L_α , H_i , H_{II} , and different cubic structures. In general these phase transitions are reversible. The gel state (L_β) (and the sub-gel state (L_c)) to the liquid crystalline state (L_α) transition corresponds to the melting of the hydrocarbon chains (main transition), which means the membrane becomes more fluid. Sometimes this temperature dependent transition is interrupted by an intermediate structure called ripple phase $P\beta'$, before the bilayer becomes more fluid. In the liquid crystal state, hydrocarbon chains are disordered and in constant motion. In the gel state the fatty acids are fully extended, the lipid packing is highly ordered and van der Waals interactions between adjacent chains are maximal. One way in which membranes can respond to, for example, lateral stress is by forming non-planar (lamellar) geometries, including the inverted hexagonal (H_{II}) phase and cubic phases.

Every lipid has specific phases that depend on the status of the hydrocarbon chains and the nature of the head group. The phase transitions can be investigated among other by Differential Scanning Calorimetry (DSC) or by Small Angle X-ray Scattering (SAXS), which was used in this work. DSC is used because the transitions are accompanied by a heat change in the system that can be measured as the enthalpy of this reaction. The phase transition behaviour, which is determined by the head groups and the fatty acid composition, is closely related to the packing of the lipids in a bilayer, vesicle or a liposome. Typical structures are explained by means of the critical packing parameter (CPP), which is the ratio of effective volume v , head group area S_0 and chain length l_c ($CPP = v/S_0 l_c$). The CPP determines the preferred structure assumed for each molecular shape. In table 3 the typical molecular shapes, phase arrangements and CPPs are shown for the most prominent phospholipids (Cecv, G. and Marsh, D. 1987).

Table 3: Molecular shapes and CPPs of important phospholipids. Modified and taken from Cecv, G. and Marsh, D. 1987 and Gennis, R.B. 1989. PC is phosphatidylcholine, PG is phosphatidylglycerin, PS is phosphatidylserine, PI is phosphatidylinositol, PA is phosphatidylacid, SPM is Sphingomyelin and PE is phosphatidylethanolamine.

Molecular shape	critical packing parameters (CPP)	Phase	Lipid
 <p>Cone</p>	$< 1/3$ (spheres) $1/3 - 1/2$ (rods)		Free fatty acids (e.g. oleate, stearate etc.)
 <p>Truncated cone</p>	$1/2 - 1$ (lamellar and vesicles)		Lipids with two fatty acids and large head groups (PC, PG, PS, PI, PA, SPM)
 <p>Cylinder</p>	~ 1 (lamellar and planar bilayers)		Lipids with two fatty acids with small head group areas; anionic lipids and saturated chains (PE, PS + Ca^{2+})
 <p>Inverted truncated cone</p>	> 1 (hexagonal H_{II})		Lipids with two fatty acids with small head group areas, non-ionic lipids and polyunsat. chains: PE (unsat.), PA + Ca^{2+} , PS (pH<4)

The phase transitions change the properties of the membrane what results in a different packing of the lipids and an enhancement of the fluidity. The transition temperatures that are indicted for POPE are specific for every lipid and depend on the shape and the composition of the polar head group but also on the composition and saturation of the hydrocarbon chains. Thus, a longer acyl chain can lead to an increase of the transition temperature while another double bond in the chains decreases the temperature (Silvius, J.R. Lip. Prot. Interact. 1982).

3. Materials and Methods

3.1. Chemicals

Acetone	Merck, Darmstadt, Germany
Acetonitrile	Merck, Darmstadt, Germany
Agarose	Sigma-Aldrich, Deisenhofen, Germany
Bacto Agar	Becton Dickinson, Heidelberg, Germany
Bacto Peptone (meat)	Becton Dickinson, Heidelberg, Germany
Bacto Peptone (Casein-digest)	Becton Dickinson, Heidelberg, Germany
Bacto Tryptone	Becton Dickinson, Heidelberg, Germany
Chloroform	Merck, Darmstadt, Germany
Dimethyl sulfoxide (DMSO)	Fluka, St. Louis, USA
EDTA	Merck, Darmstadt, Germany
Ethanol	Merck, Darmstadt, Germany
Glucose	Fluka, St. Louis, USA
Hydrochloric acid (1N)	Merck, Darmstadt, Germany
Meat extract	Merck, Darmstadt, Germany
Methanol	Merck, Darmstadt, Germany
Morpholinoethanesulfonic acid	Merck, Darmstadt, Germany
Potassium chloride	Merck, Darmstadt, Germany
Potassium dihydrogen phosphate	Merck, Darmstadt, Germany
Sodium Chloride	Merck, Darmstadt, Germany
Di-sodiumhydrogenphosphate	Merck, Darmstadt, Germany
Sodiumdihydrogenphosphate	Merck, Darmstadt, Germany
Sodium dodecyl sulphate (SDS)	Fluka, St. Louis, USA
Sodiumhydroxide (1N)	Merck, Darmstadt, Germany
Trifluoroacetic acid	Fluka, St. Louis, USA
Trypticase Soy Broth	Becton Dickinson, Heidelberg, Germany
Tween 20	Merck, Darmstadt, Germany
Water	double distilled, Milli-Q bioceel, Billerica, USA
Yeast extract	Becton Dickinson, Heidelberg, Germany

All chemicals were purchased in p.a. quality.

3.2. Instruments

Bacterial culture:

Bacteria counter: BZG30, WTW, Weilheim, Germany
Photometer: Helios, Thermo Spectronic, Waltham, USA
Micro plate reader: Sunrise, Tecan, Crailsheim, Germany

Mass spectroscopy:

Capillary-liquid chromatography system: Agilent 1100 series, Waldbronn, Germany.
Reversed-phase column: Zorbax SB C18, Agilent, Waldbronn, Germany.
Quadropole time-of-flight mass spectrometer: Qstar pulsar I, Applied Biosystems, Darmstadt, Germany.

Circular dichroism spectroscopy:

Spectrophotometer: Jasco J-715, Easton, USA

3.3. Buffers

PBS	8g NaCl 0,2g KCl 1,44g Na ₂ HPO ₄ ad 1l H ₂ O, pH 7,4
MES	20mM Morpholinoethanesulfonic acid 140mM NaCl pH 5,5
Sodium phosphate Buffer (NaP)	10mM sodiumphosphate pH 7,4 (the pH value was adjusted by mixing NaH ₂ PO ₄ and Na ₂ HPO ₄).
Potassium phosphate Buffer (PPB)	10mM potassium phosphate pH 7

3.4. Peptides and peptidomimetics

The peptide NK-2 was synthesized by WITA GmbH (Berlin, Germany) and Biosyntan (Berlin, Germany). All other modified peptides and magainin-II-amide were purchased from Biosyntan. The peptides were ordered with an amidated C-terminus and 95 % purity, guaranteed by analytical RP-HPLC (Lichrospher 100 RP 18, 5 µm columns, Merck, Darmstadt, Germany) and MALDI-TOF (instrument from Bruker Daltonik GmbH, Bremen, Germany) performed by the companies. Melittin was purchased from Sigma-Aldrich (Deisenhofen, Germany). The peptides were stored at -20°C. Directly before use they were solved in double distilled water to a final concentration of 1mM. Between the experiments the peptide solutions were also stored at -20°C. A more detailed description of the used peptides will be given in chapter 4.

The poly(phenylene ethynylene) peptidomimetic LA-03-149 (figure 8) was purchased from and synthesized by the group of G.N. Tew at the university of Massachusetts, Amherst, USA.

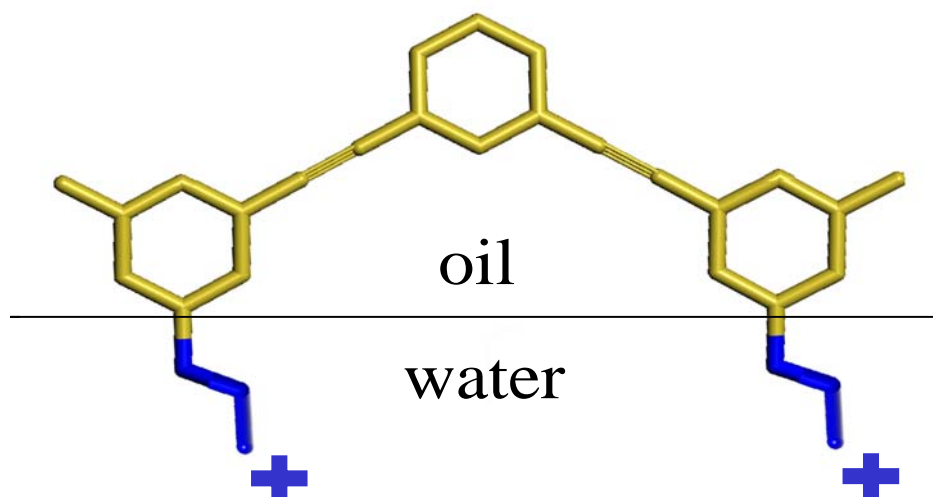


Figure 8: Schematic picture of the peptidomimetic LA-03-149. The amphiphilic nature and the cationic charges of the substance are indicated (modified after Arnt, L. et al. J. Polym. Sci. A: Polym. Chem. 2004).

The powder of LA-03-149 was dissolved in dimethyl sulfoxide (DMSO) and then diluted in double distilled water to a final concentration of 1mM. In order to test the influence of the solvent DMSO all antibacterial tests and the hemolysis were done with the respective concentrations of DMSO as reference measurements.

3.5. Lipids

The phospholipids POPC, POPG and POPE (the structures in figure 9 were taken from Avanti Polar Lipids Inc.) were purchased from Sigma-Aldrich (Deisenhofen, Germany). The lipids DPPC, DOPE-trans and DiPOPE (figure 9) used for the preparation of liposomes were purchased from Avanti Polar Lipids Inc. (Alabaster, USA). All lipids were stored airtight in the freezer at -20°C. In table 4 an overview of the biophysical properties important for this work, of all lipids is given. Depending on the headgroups and the acyl chain composition the phospholipids form different phases, having different phase transition temperatures and also different molecular shapes (see also the chapter within the introduction part about lipids). Furthermore, the phase transition temperatures of the lipids are also strongly depending on the solvents in which the measurements are made.

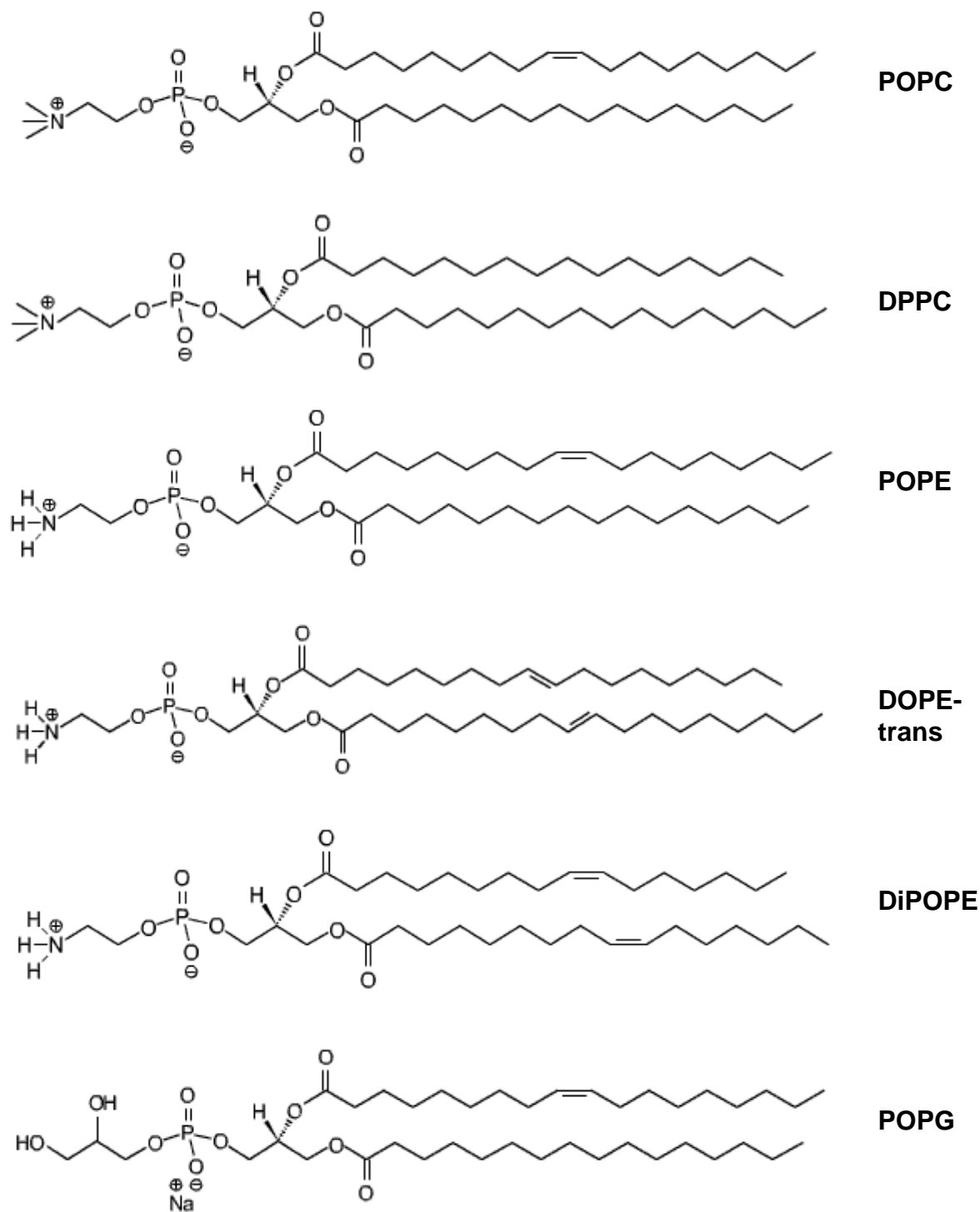


Figure 9: Schematic picture of the used lipids. The structures were taken from the data sheets of the company Avanti Polar Lipids Inc. The degree of saturation is indicated by the black bars in the acyl chains of the lipids.

Table 4: Important characteristics of the used phospholipids. Gel is gel state phase, l.c. is liquid crystalline phase and H_{II} is the inverse hexagonal phase.

Lipid	Synonym	MW (Da)	Transitions	Temperature [°C]	Buffer	Reference
POPC	1-palmitoyl-2-oleoyl-phosphatidylcholine	760,1	gel – l.c.	11	10mM KPO ₄ pH7,4	Lee, T. et al, 1980
			gel – l.c.	-3	H ₂ O	Curatolo, W. et al, 1985
DPPC	1,2-dipalmitoyl-phosphatidylcholine	734,05	gel – l.c.	35	NaPO ₄ pH7,4	Boyd, P. et al, 1980
			gel – l.c.	42,6	H ₂ O	Rudolph, A. et al, 1986
POPG	1-palmitoyl-2-oleoyl-phosphatidylglycerin	766,1	gel – l.c.	-2	1mM NaCl + 40mM Tris-acetate pH7	Fleming, B. et al, 1983
			gel – l.c.	-5	10mM Pipes + 2mM EDTA pH7,1	Borle, F. et al, 1985
POPE	1-palmitoyl-2-oleoyl-phosphatidylethanolamine	716,99	gel – l.c.	25,3	H ₂ O	Jaworsky, M. et al, 1985
			gel – l.c.	6	50mM KPO ₄ pH7,2	Rujanavech, C. et al, 1986
			l.c. - H _{II}	71	H ₂ O	Sanderson, P. et al, 1991
			l.c. - H _{II}	68	150mM Na + 10mM Tes + 1mM EDTA pH 7.4	Leventis, R. et al, 1991

DOPE-trans	1,2-dielaidoyl-phosphatidylethanolamine	744,05	gel – l.c.	35	40mM Tris-acetate / EG 1:1 v/v, 0.1M NaCl pH7	van Dijck, P. et al, 1976
			gel – l.c.	36,1	10mM HEPES pH7,4	Nosedá, A. et al, 1988
			l.c. - H _{II}	57	0.1M NaCl + 25mM Tris-acetate + 0.2mM EDTA pH7	van Echteld, C. et al, 1981
			l.c. - H _{II}	61,8	10mM HEPES pH7,4	Nosedá, A. et al, 1988
DiPOPE	1,2-dipalmitoleoyl-phosphatidylethanolamine	687,93	gel – l.c.	-33,5	40mM Tris-acetate/EG 1 :1 v/v, 0,1M NaCl pH7	van Dijck, P. et al, 1977
			l.c. - H _{II}	38,3	20mM PIPES, 1mM EDTA, 150mM NaCl, 0,02mg/ml Na-azide pH7,4 [D ₂ O]	Eband, R.M. et al, 1990
			l.c. - H _{II}	43,2	20mM PIPES, 1mM EDTA, 150mM NaCl, 0,02mg/ml Na-azide pH7,4 [H ₂ O]	Eband, R.M. et al, 1990

3.6. Bacterial culture

All antimicrobial substances were tested against the Gram negative *Escherichia coli* strain K-12 (ATCC 23716), which was purchased by Dr. J. Andrä (Research Center Borstel, Germany). The bacteria were cultured in the following medium and agar plates:

Luria-Bertani medium (LB-medium):	10g NaCl	
	10g Bacto tryptone	
	5g Yeast extract	ad 1000ml ddH ₂ O
LB- culture plates:	15g Bacto Agar	ad 1000ml LB-medium

Selected peptides were also tested against the Gram positive bacteria *Staphylococcus carnosus* (ATCC 51365) and *Bacillus subtilis* (ATCC 6051). Both strains were purchased from the German Collection of Microorganisms and cell cultures (DSZM, Braunschweig, Germany). The *S. carnosus* bacteria were cultured in:

Corynebacterium medium (CM):	10g Casein peptone	
	5g Yeast extract	
	5g Glucose	
	5g NaCl	ad 1000ml ddH ₂ O
Agar plates:	15g Bacto Agar	ad 1000ml CM

The *B. subtilis* strain was cultured in:

Nutrient medium (NM):	5g Peptone	
	3g Meat extract	ad 1000ml ddH ₂ O
Agar plates:	15g Bacto Agar	ad 1000ml NM

Before use all media were autoclaved for 20 minutes at 120 degrees. When the medium with agar cooled down to approximately 40 degrees, it was rapidly poured into the Petri plates (10cm diameter, Nunc, Wiesbaden, Germany) and kept for two hours at room temperature.

3.6.1. Overnight and growth cultures

Exemplarily a brief description of the culturing of bacteria will be given for the K12 strain of *E. coli*. All other strains were treated similar. The bacteria were cultivated on LB-agar plates at 37°C for 24 h. Then one colony was picked from the plate with an inoculating loop and suspended in LB-medium to grow overnight at 37°C. The bacteria were then inoculated again in LB-medium and kept growing shaking at 37°C to reach the log-phase. Within 2 to 4 hours the extinction at 600nm

wavelength was photometrically measured to determine the density of bacteria. At an OD₆₀₀ of 0.1 to 0.2 the bacteria are in the log-phase. The absolute number of cells, respectively the number of colony forming units (CFU), was acquired by making a dilution series of the bacteria suspension at a fixed optical density. Every dilution step (100µl) was plated again on LB- plates and incubated at 37°C overnight. Every visible colony was counted manually by using a bacteria counter. From these experiments the direct linear coherence between the number of CFU and the extinction at 600nm wavelength was deduced; i.e. for *E. coli* K12 (ATCC 23716) an optical density of 0.1 measured at 600nm wavelength is equivalent to 2.5×10^7 CFU per millilitre

3.6.2. Microsusceptibility assay

The peptides were dissolved in double distilled H₂O and twofold serial diluted again in double distilled H₂O to final concentration of 10µM, 5µM, 2,5µM, 1,25µM, 0,63µM, 0,31µM, 0,16µM and 0,08µM. 10µL of the log-phase bacteria suspension containing 100 CFU were added to 90µL of the peptide solution to measure the antibacterial activity by a microdilution susceptibility test. The peptide plus bacteria solution was incubated in a 96 multiwell plate (Greiner bio-one, Frickenhausen, Germany) at 37°C for overnight and subsequently measured photometrically at 620nm wavelength with a micro plate reader (Tecan). Values of the minimal inhibitory concentration (MIC) were defined as the concentration of the highest dilution of the peptides at which the bacteria growth was completely suppressed. For a better presentation (in case of the peptide NK-2, NK-CS and NKCS-[AA]) the control values (bacteria without peptide) was set as 100 percent, while the different peptide concentrations were related to this value.

3.7. Hemolysis

To measure the haemolytic activity of the peptides, human blood (group 0 rhesus positive), that was stored for two days longest, was centrifuged for three minutes at 2000rpm. The supernatant was discarded and the pellet washed with phosphate buffered saline (PBS) at pH7.4. This procedure was repeated until the supernatant was clear after centrifugation. The originated erythrocytes pellet was than diluted with MES buffer until 20µl of this suspension added to 980µL water had an optical density of 1.4 at a wavelength of 412nm. The wavelength is optimized for absorption by haemoglobin, and an extinction of 1.4 is equivalent to approximately 5×10^8 cells per mL. The peptides were diluted in MES buffer to concentrations of 10, 3, 1, 0.3 and 0.1µM. Then 20µL of the erythrocyte suspension were added to 80µL peptide solution. As control 20µL erythrocyte suspension were mixed with 80µL water, expecting 100% lysis of the erythrocytes. The negative control was made by mixing 20µL erythrocyte suspension and 80µL MES buffer, here the lysis is zero. After mixing all samples carefully, the suspensions were incubated for 30 minutes at 37°C. Directly after incubation the samples were stored on ice and 900µL MES buffer were added. All suspensions were centrifuged for ten minutes at 2000rpm to sediment all intact erythrocytes. Finally, the optical density was measured with a spectrometer (Tecan) at 412nm wavelength.

3.8. Mass spectroscopy

Mass spectrometry (MS) is an analytical tool used for measuring the molecular mass of a sample. The accuracy of this method is sufficient to allow minor mass changes to be detected, e.g. the substitution of one amino acid for another; or a post-translational modification. Mass spectrometers can be divided into three fundamental parts, namely the ionisation source, the analyser and the detector. The sample has to be introduced first into the ionisation source of the instrument. Once inside the ionisation source, the sample molecules are ionised, because ions are easier to manipulate than neutral molecules. These ions are extracted into the analyser region of the mass spectrometer where they are separated according to their mass(*m*)-to-charge(*z*) ratios (*m/z*). The separated ions are detected and this signal sent to a data system where the *m/z* ratios are stored together with their relative abundance for presentation in the format of a *m/z* spectrum. The analyser and detector of the mass spectrometer, and often also the ionisation source, are maintained under high vacuum to give the ions a reasonable chance of travelling from one end of the instrument to the other without any hindrance from air molecules.

The method of sample introduction to the ionisation source often depends on the ionisation method being used, as well as the type and complexity of the sample. The sample can be inserted directly into the ionisation source, or can undergo some type of chromatography to the ionisation source. This latter method of sample introduction usually involves the mass spectrometer being coupled directly to a high pressure liquid chromatography (HPLC), gas chromatography (GC) or capillary electrophoresis (CE) separation column, and hence the sample is separated into a series of components which then enter the mass spectrometer sequentially for individual analysis (Ashcroft, A.E. In: Ionization Methods in Organic Mass Spectrometry, 1997).

In this work the technique of ESI (Yamashita, M. and Fenn, J.B., J. Phys. Chem. 1984) was used. In ESI samples (*M*) with molecular masses up to ca. 1200 Da give rise to singly charged molecular-related ions, usually protonated molecular ions of the formula (*M+H*)⁺ in positive ionisation mode, and deprotonated molecular ions of the formula (*M-H*)⁻ in negative ionisation mode. Samples (*M*) with molecular weights greater than ca. 1200 Da give rise to multiply charged molecular-related ions such as (*M+nH*)ⁿ⁺ in positive ionisation mode and (*M-nH*)ⁿ⁻ in negative ionisation mode.

The experiment was prepared by diluting the peptides NK-2 and NK-CS in double distilled water to a concentration of 100pmol/μl. Before the mass spectroscopy the solution was given onto a capillary-liquid chromatography (LC) system (Agilent 1100 series, Waldbronn, Germany) coupled with a reversed-phase column (Zorbax SB C18 150 mm x 0.5 mm, Agilent). The LC system was operated at ambient column temperature, the flow rate was adjusted to 10 μL per minute and the injection volume for the measurement was 1 μL.

Solvent A: Purified water / 0.1% trifluoroacetic acid v/v.

Solvent B: Acetonitrile / 0.1% trifluoroacetic acid v/v.

The LC was isocratic with 5% solvent B for 5 minutes and then followed immediately by a 5-95% linear gradient of solvent B.

To determine the molecular mass of the peptides, a quadropole time-of-flight mass spectrometer (positive TOF MS) with a TOF mass range of 200 to 2000 amu (atomic mass units) (Qstar pulsar I, Applied Biosystems, Darmstadt, Germany) was used. The MS was equipped with an Ion Spray source linked to the LC system. Here the ion spray voltage constituted 5000 V, the nebuliser gas flow was 1.16 L per minute and the curtain gas flow was adjusted to 1.82 L per minute with a declustering potential of 80 V (Applied Biosystems). The data acquisition time was 1 second and analyzed with the provided Analyst & BioAnalyst software packages (Applied Biosystems).

3.9. Circular Dichroism Spectroscopy

Circular dichroism (CD) is a special variation of absorption spectroscopy at the UV and VIS spectrum of light. The basic principle of this method is the interaction of polarized light with optically active substances in order to measure the chirality of the molecule. Chiral or asymmetric molecules produce a CD spectrum because they absorb left and right handed polarised light to a different extent, thus being considered as "optically active". Biological macromolecules such as proteins and DNA are composed of optically active elements and because they can adopt different three-dimensional structures, such as unordered random coil, alpha-helical or beta-sheet structures, where each structure produces a distinct CD spectrum.

The principle of a CD measurement will be described very briefly, a more detailed description can be found in Greenfield, N. and Fasman, G., 1969: If linearly polarized light passes through an optically active substance, it is possible that not only the phases of the two circularly polarized components are different, but also the absorption coefficients, ϵ_L and ϵ_R . The difference in the absorption coefficient (ellipticity) is the parameter that will be measured. Since the absorptions of the left circular polarized light and the right circular polarized light are different, elliptically polarized light emerges from the sample. In practice, the ellipticity is determined from the difference of the absorption coefficients:

$$\Theta_\lambda = \text{const} \cdot (\epsilon_L - \epsilon_R) \cdot c \cdot d \quad (1)$$

where d is the thickness and c the concentration of the sample. The const is given by:

$$\text{const} = 180 \cdot \ln(10) \cdot 4\pi^{-1} \approx 33 \quad (2)$$

The molar ellipticity is given by:

$$[\theta]_\lambda = M_\gamma \cdot \Theta_\lambda \cdot (10 \cdot d \cdot c)^{-1} \quad (3)$$

where M_γ is the molar mass in $\text{g} \cdot \text{mol}^{-1}$. If the molar extinction coefficients of both circularly polarized waves are known, the term of the molar ellipticity can be expressed as:

$$[\theta]_\lambda = 3300 \cdot \Delta\epsilon \quad (4)$$

The dependence of the ellipticity on the wavelength of the incident light defines the CD spectrum. The CD spectrum has the form of an absorption band and a positive and a negative circular dichroism is observed as a function of the wavelength, depending on which of the two circularly polarized components is absorbed stronger.

Figure 10 shows an exemplary CD measurement of poly-L-lysine with indicated secondary structures of this protein.

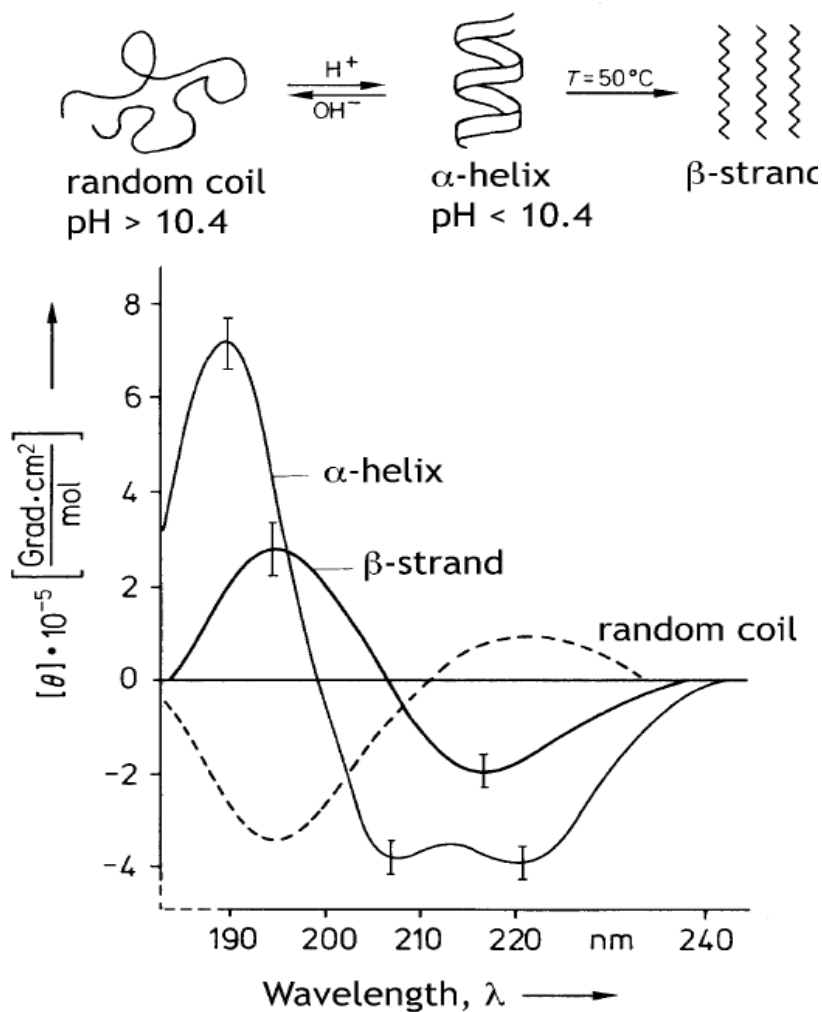


Figure 10: CD spectra of poly-L-lysine in aqueous solution. Taken from Greenfield, N. and Fasman, G. Biochem, 1969.

CD data for this work were acquired with a CD spectrophotometer using quartz cuvettes with an optical path length of 0.1 cm. The response was measured between 190 to 300 nm with a 0.2 nm step resolution and a 1 nm bandwidth. The counting rate was 50 nm per minute with a 2 second response time. Each spectrum is a sum of at least four scans to improve the signal-to-noise ratio. All spectra are reported in terms of mean residue molar ellipticity $[\theta]_R \text{ deg cm}^2 \text{ d mol}^{-1}$.

The detergent sodium dodecyl sulphate (SDS) was added to the cuvette with final concentrations of 1mM, 10mM, 50mM and 100mM. It was chosen in this experiment to investigate the possible interaction of the cationic peptides and the negatively

charged detergent; SDS is often taken to study the secondary structure of peptides and proteins. Furthermore it was also necessary to investigate the interaction of the peptides with liposomes, but in case of lipids the data analysis is more difficult due to the bad signal to noise ratio of the spectra resulting from the multiple signals of the multilayers. As references the spectra of water, buffer, SDS at the respective concentrations and spectra of the liposomes were subtracted from the measurements with peptides. All spectra were collected for a concentration of 60 μ M peptide in double distilled water. The molar ratio of peptide to lipid during the liposome measurements was 1 to 100; the molar ratio of peptide to SDS was 1 to 17 (for 1mM SDS), 1 to 167 (10mM SDS), 1 to 834 (50mM SDS) and 1 to 1667 (100mM SDS).

3.10. Preparation of liposomes for SAXS experiments

The preparation was done in due time before measurements (usually two or three days before the experiments) with stainless steel or glass equipment. The phospholipids were weighted into thoroughly cleaned glass vials (Wheaton, Millville, USA), which were closed with a Teflon lid covered with parafilm (American National Can, Greenwich, USA) and stored at -20°C before dissolving them in a methanol/chloroform (1/2, by volume or respectively 1/1, by volume) solution. This solvent was then slowly removed by a constant stream of nitrogen. The resulting lipid film was dried in a vacuum oven at 40°C over night. Just before the experiments the lipid films were hydrated in water or buffer (with a final concentration of 25mg/ml). The buffer was 10mM sodium phosphate buffer (pH7,4) in order to simulate physiological conditions and for some measurements sodium chloride was added in final concentrations of 90mM and 130mM, here also the pH value was adjusted to physiological conditions around a value of 7. According to the specific protocol for each lipid the liposomes were formed.

Multilamellar vesicles

POPE, DOPE-trans and DiPOPE: The buffer was added at room temperature (RT) to the lipid films (and also additionally the peptides were added) and a small amount of glass balls was put into the vials. After vortexing for 1 minute the solution was heated for 2 hours at 28°C, while every 30 minutes the sample was vortexed again. Then the solution was cooled down to RT and was left for 30 minutes at RT.

POPC and DPPC: After mixing lipid, buffer and peptide the solution was vortexed for 1 minute and afterwards heated at 50°C for 4 hours with repeated vortexing (1 min) every 30 min of incubation time. Before the measurements the samples were stored at RT for 30 minutes.

Unilamellar vesicles

POPG: The preparation of POPG liposomes is slightly different, here the sample is heated two times for 5 min at 65°C, two times for 10 min at 65°C and once for 30 min at 65°C (also with repeated 1 min vortexing in between). Before the measurements the samples were also stored for 30 minutes at RT.

For the measurements the samples (30 μ l) were filled into glass capillaries (Hilgenberg GmbH, Malsfeld, Germany, wall thickness 0.1 mm) and were put into the sampler holder at the beamline A2.

3.11. Small Angle X-ray Scattering (SAXS)

Small Angle X-ray Scattering (SAXS) is usually used to determine the low resolution structure of dissolved macromolecules such as surfactants, polymers or biological molecules like proteins. The molecules are randomly oriented and the scattering pattern is caused by a spacial and temporal average of the scattering events. In this work, a special application of SAXS on *partially ordered systems* like multilamellar vesicles was used. Therefore in the following sections emphasis is put on X-ray diffraction on dissolved multilamellar structures rather than the more commonly used SAXS.

X-rays are electromagnetic waves with wavelengths (λ) between 0,01 nm and 1 nm, which is equivalent to a photon energy between 1 keV and 100 keV. For the investigation of macromolecules in solution, monochromatic X-ray radiation is used; this radiation can be provided by an X-ray tube (λ from a Cu-K α tube is 0,154 nm) or a synchrotron. The X-rays interact with the electrons of the atoms in the studied molecule respectively sample, and Electron density inhomogeneities within the observed sample give rise to coherent, angle dependent scattering which can be correlated to the molecular structure. The scattering angle ranges from $\theta = 0,02^\circ - 8^\circ$ what equals a scattering vector of $q = 0,02 \text{ nm}^{-1}$ to 6 nm^{-1} . This angular range or pattern is analyzed using the inverse relationship between particle size and scattering angle to distinguish characteristic shape and size features within a given sample. The relationship between the scattering vector and Bragg's Law (for an explanation see below and figure 11) results in a description of the particle's dimension: $D=2\pi \cdot \theta$ (Guinier and Fournet, 1955). The measurable dimensions of the samples are therefore between 2 nm to 200 nm. Later, the method became more and more important in the study of biological macromolecules in solution as it allowed one to get low-resolution structural information on the overall shape and internal structure in the absence of crystals (Svergun, D.I. and Koch, M.H.J. Rep. Prog. Phys. 2003). A breakthrough in small angle X-ray scattering experiments came in the late 1970s, by introducing the powerful synchrotron radiation. It was soon realized that scattering studies on solutions provide, for a minimal investment in time and effort, useful insights into the structure of non-crystalline biochemical systems. Moreover, the technique also made it possible to investigate intermolecular interactions including assembly and large-scale conformational changes, on which biological function often relies, in real time. An exact description of the scattering theory and the scattering of biological samples can for example be found in within the review of Svergun, D.I. and Koch, M.H.J. 2003.

Bragg's Law

Bragg's Law refers to the simple equation:

$$n\lambda = 2d \sin\theta \quad (1)$$

The variable d is the distance between atomic layers in a crystal, and the variable λ is the wavelength of the incident X-ray beam; n is an integer.

The Braggs were awarded the Nobel Prize in physics in 1915 for their work in determining crystal structures beginning with sodium chloride, zinc sulphide and

diamonds. Although Bragg's law was used to explain the interference pattern of X-rays scattered by crystals, diffraction has been developed to study the structure of all states of matter with any beam, e.g., ions, electrons, neutrons, and protons, with a wavelength similar to the distance between the atomic or molecular structures of interest. Bragg's Law is applied for ordered atoms or molecules (like in a crystal) and describes the condition leading to interference of diffracted waves. A specific, simple relation must be obeyed to achieve constructive interference between an incoming and diffracted beam.

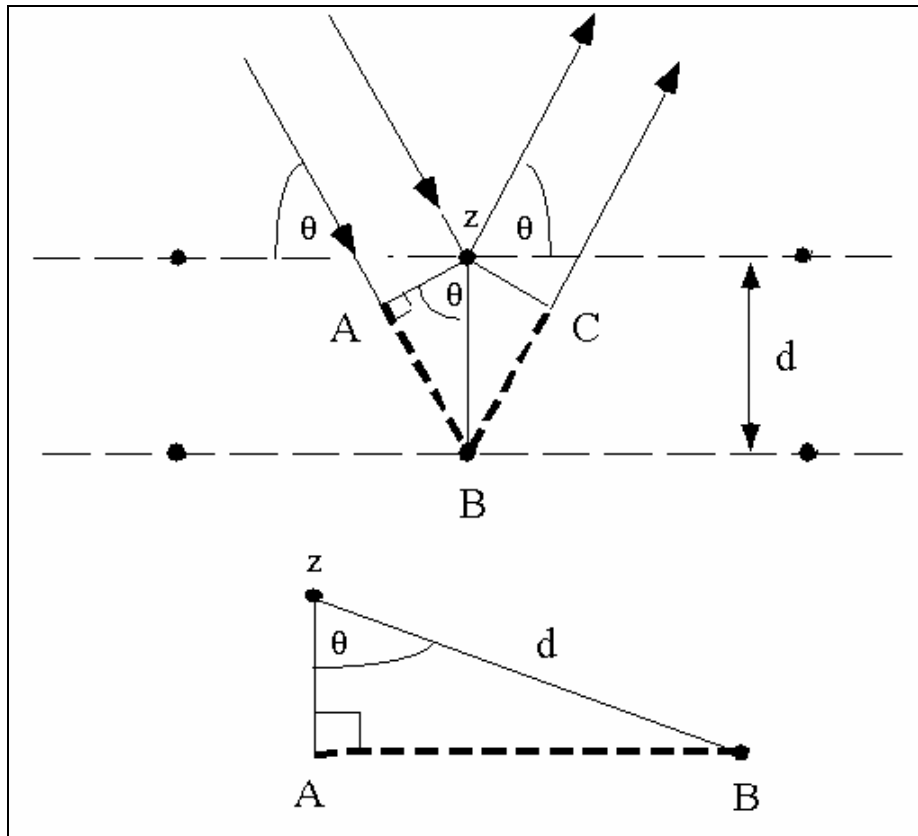


Figure 11: Schematic picture of the trigonometry of Bragg' Law.

The interpretation of Bragg's Law says that there is a diffraction of the x-ray radiation with the scattering angle θ . This diffraction comes from the net planes of a crystal, where d is the distance between the planes and n determines the order of the reflections. Only for a single crystal there is exact defined Reflection, in case of biological samples the crystalline areas within the sample are rare, so the reflections are not sharp and interpreted as a Debye-Scherrer scattering pattern. From these patterns the structural arrangement of the sample is derived. In this work the interest of the scattering experiments was put on lipids and model membranes and therefore an explanation of the typical structures of these systems will follow (figure 12 and 13).

Sub Gel phase (L_c)



Gel phase (L_β)



Gel phase with tilted chains ($L_{\beta'}$)



Ripple phase (P_β)



Liquid crystalline phase (L_α)

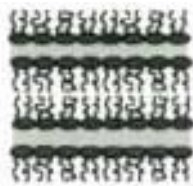


Figure 12: Schematic picture of the lamellar phases of a phospholipid.

Reflections of ordered lamellar structures (figure 12) can be described with the term d , $d/2$, $d/3$, $d/3$ etc. In case of unilamellar structures (e.g. observed for POPG) the reflections are not sharp but extremely broad; here it is very hard to detect higher orders of the reflection and the analysis is difficult.

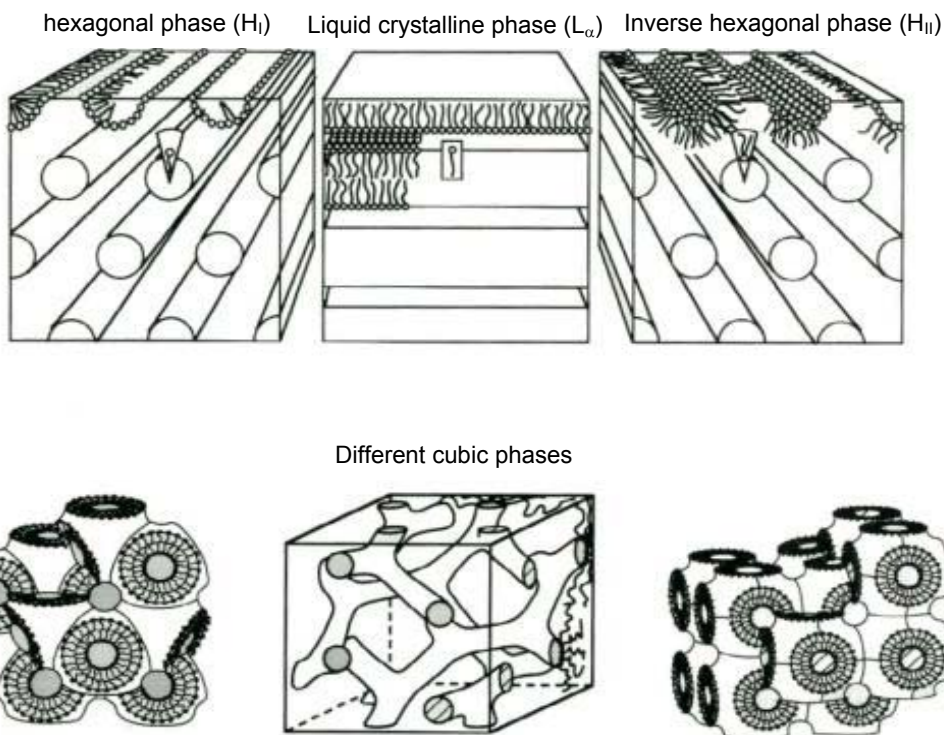


Figure 13: Non-lamellar lipid phases.

The dependency of the position of reflections for hexagonal phases is expressed by: 1, $\sqrt{3}$, $\sqrt{4}$, $\sqrt{7}$, $\sqrt{9}$, $\sqrt{12}$ etc. The calculation of cubic phases is more difficult, because it is depending on the different space groups of the crystal (an excellent and detailed overview of this topic is given in Lindblom, G. and Rilfors, L., 1992).

X-ray diffraction is a convenient way to study the structure of lipid systems. Phospholipids form aggregates with a certain type of local symmetry that can be classified as lamellar, hexagonal, or cubic structures. This symmetry is depending on the nature of the lipid and the physicochemical state of the system (like concentration or the addition of salts).

The SAXS experiment A2 at HASYLAB, DESY, Hamburg

The A2 beamline (figure 14) runs with a wavelength $\lambda = 0.15$ nm and covers a scattering vector $s = 1/d = (2\sin\theta)/\lambda$ ($2\theta =$ scattering angle, $d =$ lattice spacing) from 1×10^{-2} to 0.5 nm^{-1} .

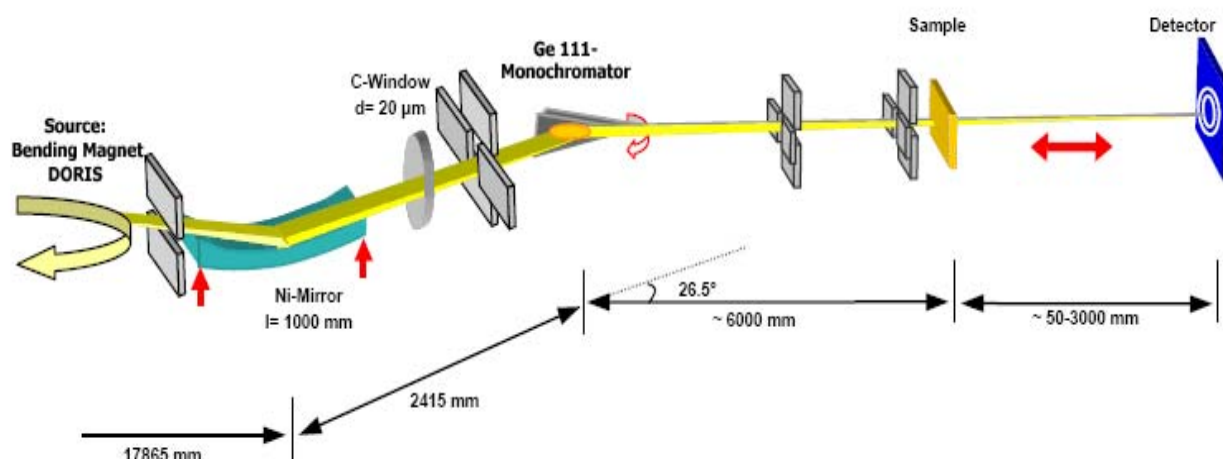


Figure 14: A2 set-up at HASYLAB/DESY

The calibration for the SAXS pattern was done by measuring rat tail tendon (repeat distance 65 nm, standard at beamline A2) in addition to silver-behenate ($[\text{CH}_3(\text{CH}_2)_2\text{OCOO-Ag}]$, repeat distance 5.838 nm, made available at beamline A2). The samples were measured in a temperature-controlled sample holder, where the temperature was varied in different ranges chosen for the lipids with an increase of $2^\circ\text{C}/\text{min}$ and the data were collected for every 10 seconds per measurement (except for DPPC; here the data were collected every 5°C).

Data treatment:

The data were normalized with respect to the primary beam and the background (buffer measurement) subtracted with a program supplied at the beamline by A. Meyer. The positions of the diffraction peaks were determined using the OTOKO software (Boulin, C. et al. Nucl. Instrum. Methods. 1986) and the Software ScatA written by Dipl.-Wi.-Ing. Boris Goltzsch. The repeat distances were calculated from the peak positions based on rat tail tendon and silver-behenate calibration. The corresponding temperature was calculated from resistance values stored for each measurement.

4. Description of the peptides

4.1. NK-2

All peptides studied in this work are derived from the peptide NK-2 (sequence see table 5 and figure 15). The structure of NK-2, as it will be displayed for clarity reasons in this work, was taken from the NMR structure of NK-lysin assuming that the substitution of three amino acids (labeled in red within figure 15) and the depletion of the rest of the NK-lysin molecules did not affect the secondary structure of the peptide. Thus, the peptide consists of two alpha-helices (indicated as H3 and H4) which are connected by a rather unstructured region formed by phenylalanine (F) at position 14 and lysine (L) at position 15.

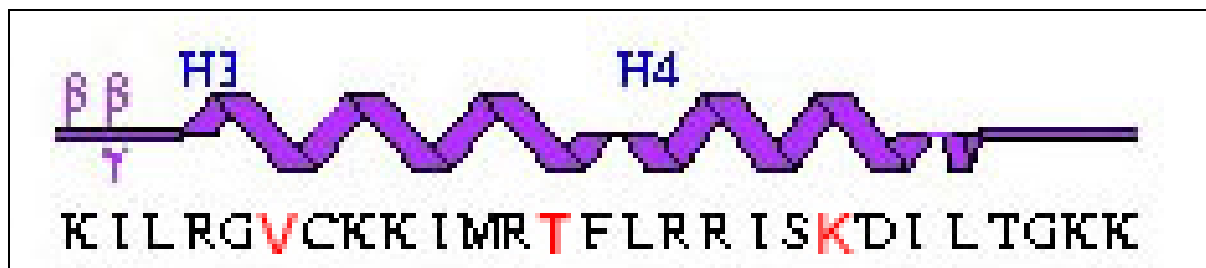


Figure 15: Amino acid sequence and assumed structure of NK-2 (the two α -helices (H3 and H4) are taken from the structure of NK-lysin (see figures 3 and 4); the three exchanged amino acids in NK-2 are labeled in red).

The alpha-helical structure of NK-2 was confirmed by circular dichroism (CD) and Fourier transformed infrared spectroscopy (FTIR- spectroscopy) measurements (Andrä, J. et al. Med. Microbiol. Immunol. 1999 and Schröder-Borm, H. et al. BBA. 2003).

Table 5: Comparison of the amino acid sequences of all tested peptides (NK-2 and 11 derivatives; plus 2 'standard' peptides). The changed amino acids of the modifications are highlighted in red and the unstructured region of NK-2 and its derivatives is marked with bold letters.

K	I	L	R	G	V	C	K	K	I	M	R	T	F	L	R	R	I	S	K	D	I	L	T	G	K	K	NK-2		
K	I	L	R	G	V	S	K	K	I	M	R	T	F	L	R	R	I	S	K	D	I	L	T	G	K	K	NK-CS		
K	I	L	R	G	V	S	K	K	I	S	R	T	F	L	R	R	I	S	K	D	I	L	T	G	K	K	NKCS-[MS]		
K	I	L	R	G	V	S	K	K	I	M	R	T	F	L	R	R											NKCS-[17]		
K	I	L	R	G	V	S	K	K	I	M	R	T	F														NKCS-[14]		
														L	R	R	I	S	K	D	I	L	T	G	K	K	NKCS-[15-27]		
K	I	L	R	G	V	S	K	K	I	M	R	T	F	L	R	R	I	S	K	K							NKCS-[20K]		
			R	G	V	S	K	K	I	M	R	T	F	L	R	R	I	S	K	K							NKCS-[RKK]		
K	I	L	R	G	V	S	K	K	I	M	R	T	F	P	R	R	I	S	K	D	I	L	T	G	K	K	NKCS-[LP]		
K	I	L	R	G	V	S	K	K	I	M	R	T	P	R	R	I	S	K	D	I	L	T	G	K	K		NKCS-[LP26]		
K	I	L	R	G	V	S	K	K	I	M	R	T	A	A	F	L	R	R	I	S	K	D	I	L	T	G	K	K	NKCS-[AA]
K	I	L	R	G	V	S	K	K	I	M	R	T	R	L	R	R	I	S	K	D	I	L	T	G	K	K		NKCS-[FR]	
G	I	G	K	F	L	H	S	A	K	K	F	G	K	A	F	V	G	E	I	M	N	S						Magainin-II	
G	L	G	A	V	L	K	V	L	T	T	G	L	P	A	L	I	S	W	I	K	R	K	R	Q	Q			Melittin	
1	2	3	4	5	6	7	8	9	10	11	12	13	14	15	16	17	18	19	20	21	22	23	24	25	26	27	28	29	

4.2. Substitutions of reactive amino acids

4.2.1. NK-CS

The first modification of NK-2 was a single amino acid substitution to inhibit the dimerisation of NK-2 by disulfide bridges: for the new peptide NK-CS the amino acid cysteine at position 6 (cys⁶) was replaced by a serine (figure 16). Serine was chosen to minimize the overall alteration in the sequence, and this amino acid is very similar to cysteine (the sulphur atom in cysteine is replaced by oxygen). This decision was based on the finding that, after approximately six months of storage, NK-2 forms dimers most likely by disulfide-bridges (see results of mass spectroscopy experiments). A similar dimerisation was not detected for NK-CS.

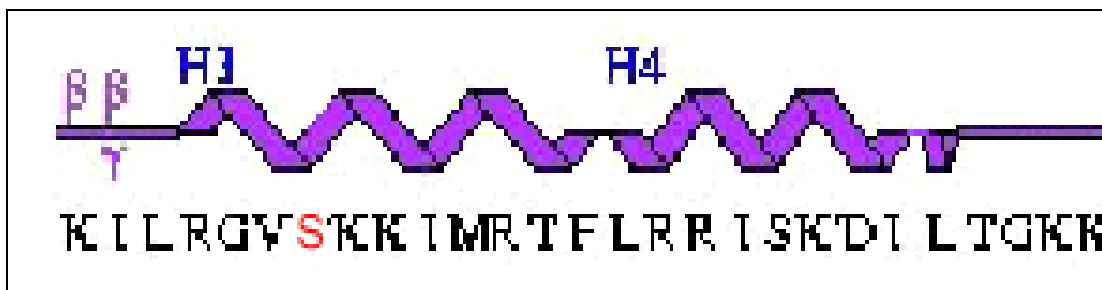


Figure 16: Amino acid sequence and the probable structure of NK-CS. The exchanged amino acid is marked in red.

Since NK-CS was found to be more potent than NK-2 (see chapter 5) all further modifications were then based on the sequence of NK-CS.

4.2.2. NKCS-[MS]

For the peptide NKCS-[MS] the amino acid met¹¹ was replaced in the first helix by serine (ser¹¹) (figure 17) for the same reasons described for the peptide NK-CS above. Methionine is also an amino acid with sulfur in its sequence and therefore it is a reactive site for interactions. Like for the cysteine in NK-CS this amino acid was cut out to avoid these possible interactions; in case of methionine the methyl group of the side chain can be transferred to other molecules by a thioether group.

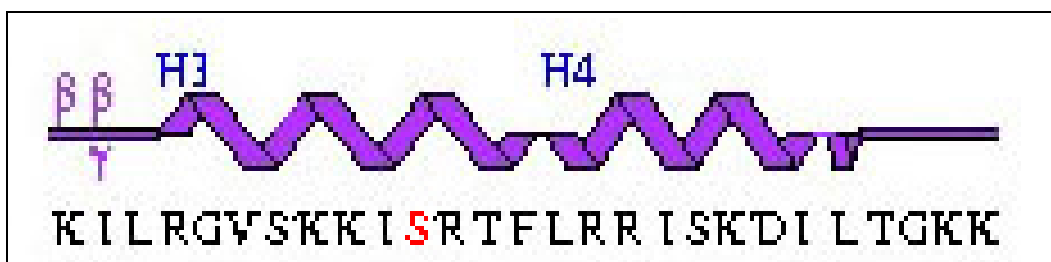


Fig. 17: Amino acid sequence and assumed structure of NKCS-[MS].

4.3. Shortened analogues of NK-CS

To study the partial activity of the NK-CS peptide and to determine the function and the importance of different sections of the peptide, three short derivatives were synthesized: NKCS-[14], NKCS-[17] and NKCS-[15-27]. NKCS-[14] and NKCS-[15-27] are the two halves of the original peptide (figure 18), which was cut in the middle of the unstructured region. Both peptides have a net charge of +5, but the second half of the original peptide, NKCS-[15-27], has a significant lower hydrophobicity than NKCS-[14] (see table 6). The third short peptide is NKCS-[17]. It corresponds to the first helix, but is prolonged over the unstructured middle region to the amino acid lys¹⁷ (fig. 18). By the prolongation of the peptide NKCS-[14] by three amino acids the net charge was increased by +3 but the overall hydrophobicity was decreased (table 6).

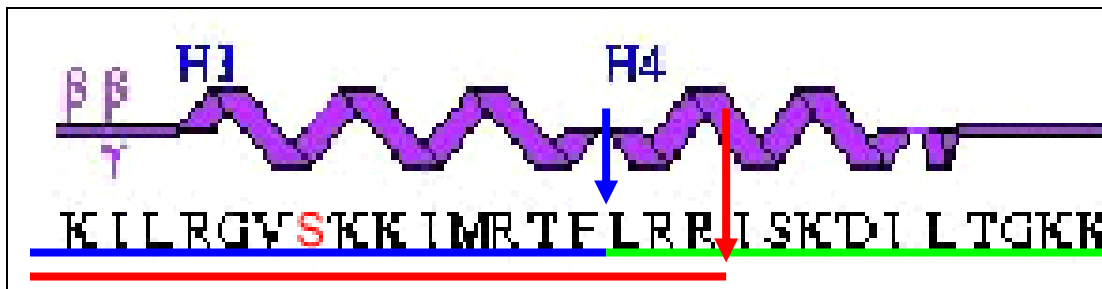


Figure 18: Schematic picture of the shortened analogues. The blue arrow points to the cut in the middle of the unstructured region and the resulting peptides NKCS-[14] (underlined in blue) and NKCS-[15-27] (underlined in green). The red arrow marks the cutting position for the peptide NKCS-[17] (underlined in red).

Two more shortened analogs are called NKCS-[20K] and NKCS-[RKK]. NKCS-[20K] (figure 19) was cut at lys²⁰, while another lys²¹ was added to have the same ending of the sequence as in the original peptide and to gain a higher positive net charge of the new peptide by introducing the charged lysine (table 6). Compared with NKCS-[17] this peptide is prolonged again by three amino acids of the original sequence (plus an additional lysine) and beside the net charge (+4 compared to NKCS-[17]), the hydrophobicity for NKCS-[20K] is decreased.

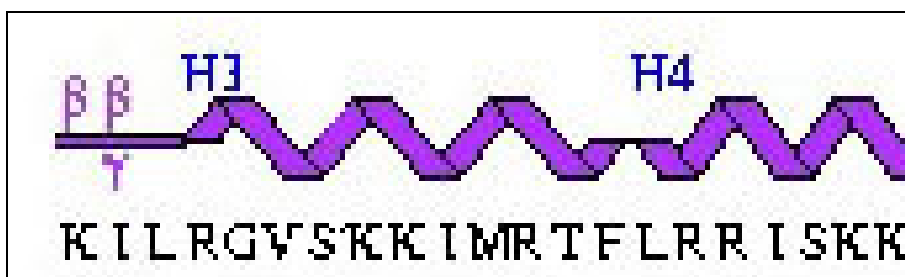


Figure 19: Amino acid sequence and assumed structure of NKCS-[20K].

The same concept led to the synthesis of NKCS-[RKK] (figure 20), but here the first three amino acids of NK-CS were also cut out, in order to test the importance of the beginning sequence of NK-CS. Furthermore the amino acids ile² and leu³ from the original sequence are both hydrophobic, that means the peptide NKCS-[RKK] has a higher hydrophilic property compared to NKCS-[14] and NKCS-[17] (table 6).

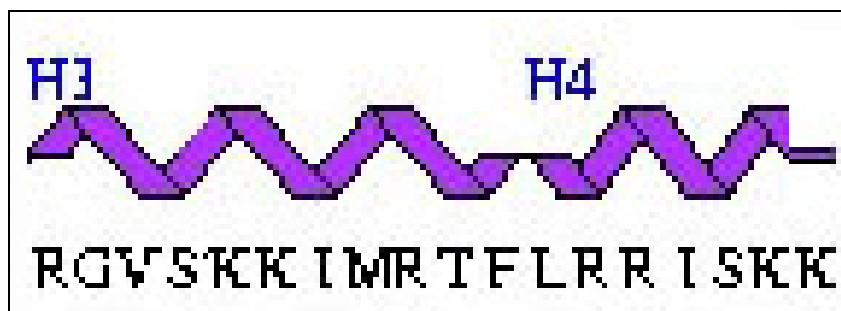


Figure 20: Amino acid sequence and assumed structure of NKCS-[RKK].

4.4. Amino acid substitutions within the unstructured region of NK-CS

The structure displayed for NK-2 or NK-CS is an assumption based on the structure of NK-lysin. From this picture the molecule should have an unstructured region in the middle. To investigate if this assumption is correct and if that might explain the good selectivity and activity of the peptides in comparison for example with magainin, which is a rod-like peptide, the importance of the middle region of NK-CS was investigated.

Therefore three modifications were synthesized by changing the overall charge, the hydrophobicity and the flexibility within this region. For NKCS-[FR] the phe¹⁴ was exchanged with an arginine (figure 21). Arginine is a positive charged amino acid and replaces in this modification the strong hydrophobic amino acid phenylalanine. The peptide NKCS-[FR] has the highest positive net charge of all tested peptides (table 6) and a decreased hydrophobicity compared to NK-CS.

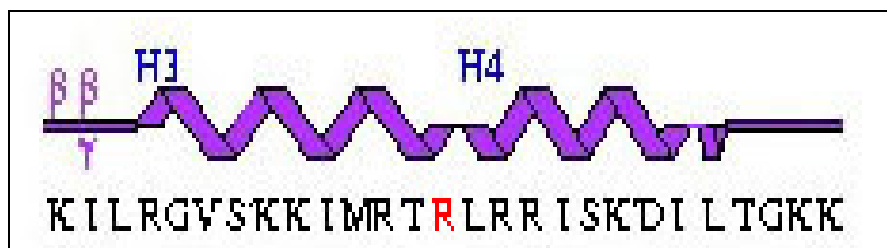


Figure 21: Amino acid sequence and assumed structure of NKCS-[FR].

The leu¹⁵ in the middle region was replaced by a proline (NKCS-[LP]) (figure 22)). Proline is a cyclic amino acid and can interrupt structures of proteins and peptides. In case for NK-CS, the assumed orientation of the amino acids sequence can be changed or interrupted by proline.

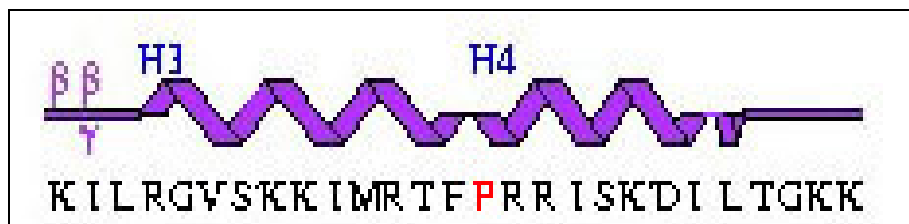


Figure 22: Amino acid sequence and assumed structure of NKCS-[LP].

Based on the peptide NKCS-[LP] additionally the phe¹⁴ of the unstructured middle region was cut out, so the whole region was changed in the peptide called NKCS-[LP26] (figure 23). The loss of phenylalanine means, as mentioned above, also a lower hydrophobicity of the peptide (as indicated by a higher value in table 6).

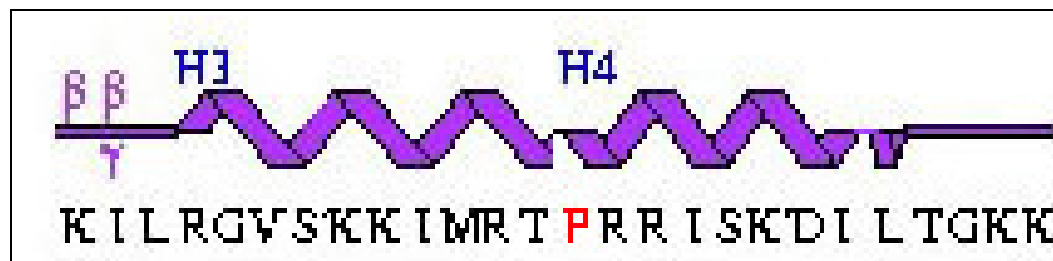


Figure 23: Amino acid sequence and assumed structure of NKCS-[LP26].

4.5. A modification predicted by computational modelling

From modelling the interaction of the peptides NK-2 and NK-CS with model membranes the amino acid sequence of NKCS-[AA] was calculated by Dalith Bechor in the group of Prof. Nir Ben-Tal, Tel-Aviv University. Computer simulations confirmed a helical structure for the peptide NK-CS with an unstructured region in the sequence. A better interaction of the peptide with model membranes was found in calculations in which two alanine were added at positions 14 and 15 prolonging the first helix of NK-CS. The addition of the two alanine residues also results in a higher amphipacity and in an increase of the membrane binding free energy for the new peptide NKCS-[AA].

4.6. Summary of important peptide parameters

Table 6: Calculated mass, net charge and hydrophobicity of all peptides. The net charge was calculated by counting the N-terminus, lys, his and arg as positive charges and counting the C-terminus, asp and gln as negative charges. The hydrophobicity is the sum of all amino acids hydrophobicity values (the lower the calculated values the higher the hydrophobicity and vice versa).

Peptide	Mass (Da)	Net charge	Hydrophobicity
NK-2	3203	+10	6,39
NK-CS	3186	+10	6,76
NKCS-[MS]	3142	+10	7,12
NKCS-[17]	2103	+7	3,46
NKCS-[14]	1676	+5	2,4
NKCS-[15-27]	1528	+5	4,36
NKCS-[20K]	2559	+9	5,26
NKCS-[RKK]	2203	+8	5,14
NKCS-[LP]	3170	+10	7,77
NKCS-[LP26]	3023	+10	8,9
NKCS-[AA]	3329	+10	7,1
NKCS-[FR]	3196	+11	8,88
Magainin-II-amide	2466	+5	3,27
Melittin	2846	+3	1,77

5. Results

The development of new antibacterial peptides was based on the observations found for the peptide NK-2. The most active peptide was found to be NK-CS, which was investigated comprehensively in order to understand the mechanism of membrane selection and membrane disruption.

All peptides were tested against the Gram negative bacteria *Escherichia coli* (K-12), the resulting minimal inhibitory concentrations (MICs) are listed in table 10. Selected peptides were also tested against the Gram positive bacteria *Staphylococcus carnosus* and *Bacillus subtilis*.

In order to explain the mechanism of selectivity and bacteria killing the influence of the peptides on the phase behaviour of different phospholipids was investigated by small angle x-ray scattering (SAXS) experiments. Phospholipids with a **phosphatidylcholine** headgroup were chosen because they are one of the major compounds of the human erythrocyte membrane (table 2), and they are not abundant in the *E. coli* membrane. The investigated **phosphatidylglycerin** lipid represents the main compound of the cytoplasmic membrane of bacteria (i.e. *E. coli*). In addition, the introduction of a charged head group offers the possibility to investigate electrostatic interactions with the positively charged peptides. Furthermore, the zwitterionic **phosphatidylethanolamine** lipids can be found in both bacterial and human cell membranes, but the amount of phosphatidylethanolamine is significantly higher in bacterial membranes (table 2).

5.1. Structure-Function correlation for the peptide NK-2

Antibacterial and hemolytic activity

NK-2 was found to be a potent antimicrobial peptide with a MIC against *E. coli* bacteria of 2,5µM, and a higher MIC against *S. carnosus* and *B. subtilis* of (10µM and 5µM). The MIC is defined as the concentration for which no bacteria growth was observed (figure 24). Interestingly, a threshold concentration seems to be necessary for Gram negative bacteria, while for Gram positive bacteria a weak concentration dependent effect was found.

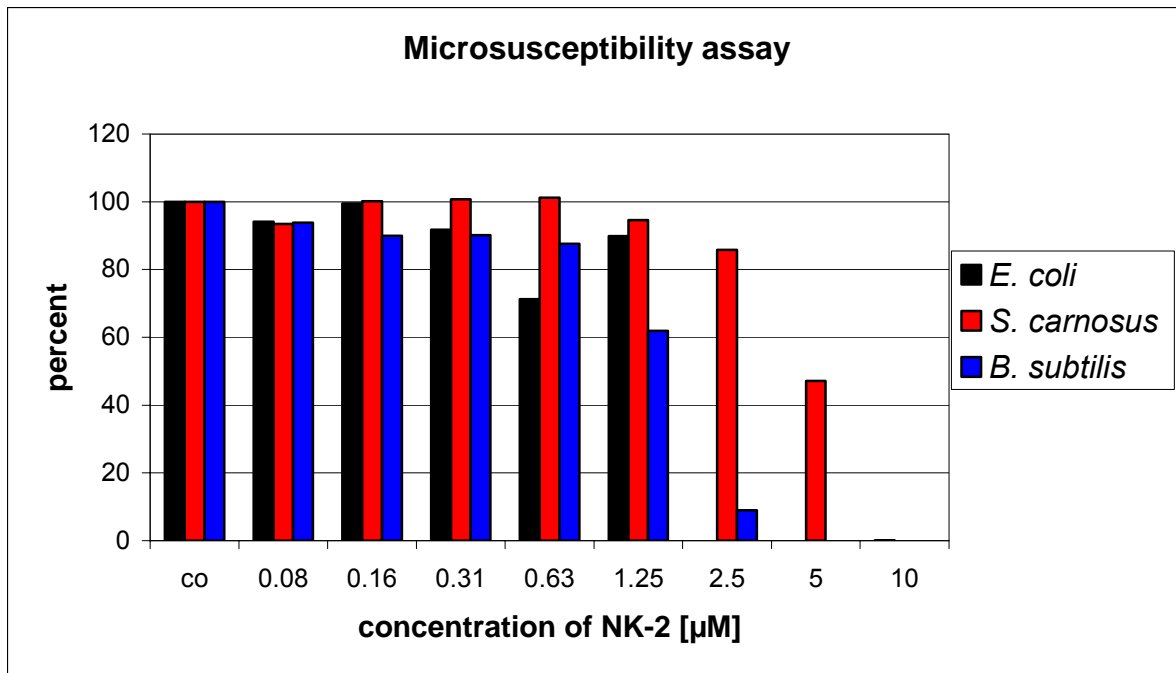


Figure 24: Antibacterial activity of NK-2 against *E. coli*, *S. carnosus* and *B. subtilis*.

NK-2 has only a weak hemolytic activity against human red blood cells (RBC) (figure 25), which is comparable to the hemolysis of magainin-II-amide. Up to a concentration of 10µM NK-2 lyses less than 10 percent of the erythrocytes. Compared with melittin, that lyses more than 20 percent RBCs at 3µM and all 100 percent at 10µM, the activity of NK-2 is negligible.

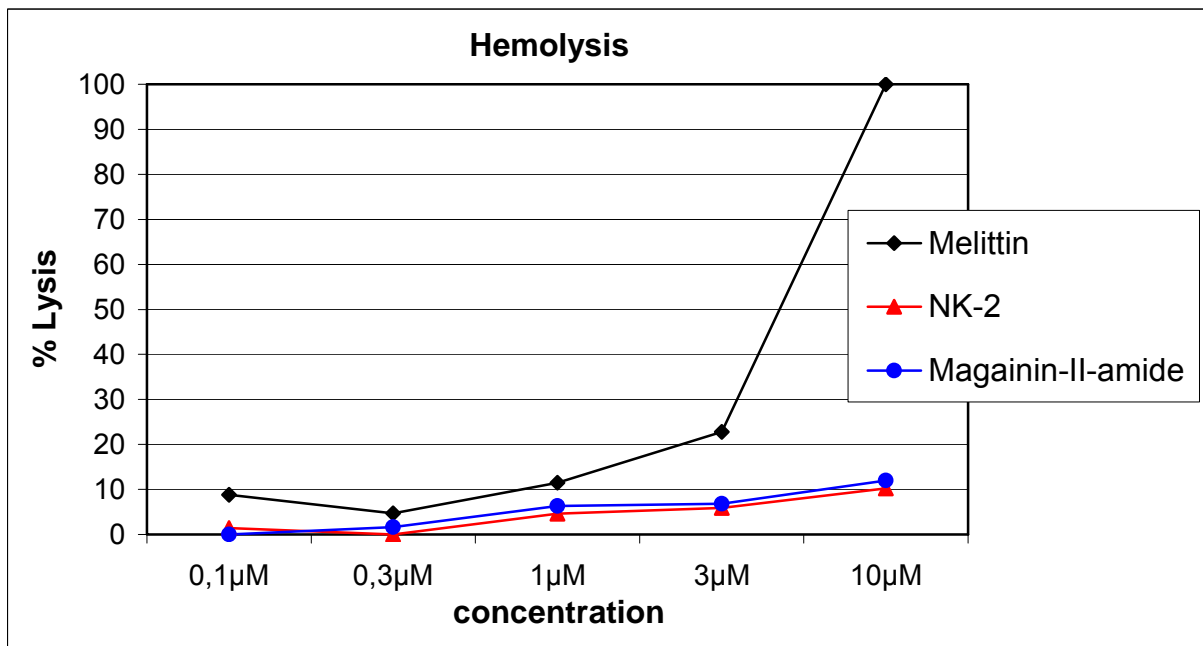


Figure 25: Hemolytic activity of NK-2 against human erythrocytes in comparison with melittin and magainin-II-amide.

SAXS measurements for phosphatidylcholine lipids

POPC

Experiments with phosphatidylcholine lipids (and also with the following phosphatidylglycerin lipid) were published before in Willumeit, R., Kumpugdee, M., Funari, S.S., Lohner, K., Pozo Navas, B., Brandenburg, K., **Linsler, S.** and Andrä, J., BBA 2005.

In summary the following results were obtained:

The top line in figure 26 shows the diffraction pattern of **1-palmitoyl-2-oleoyl-phosphatidylcholine (POPC)** liposomes. The pattern shows the first and second order diffraction peaks of the lamellar liquid crystalline phase (L_{α}) of POPC. The second order peak disappears at a temperature of 40°C and also the first order peaks loses intensity with increasing temperature. The highlighted area in this figure represents the values for temperatures higher than 60°C, here the peak position is hard to determine, which is due to the melting of the vesicles with increasing temperature. Beside the determination of the lipid phase which can be done by the evaluation of the peak positions (see materials chapter), the repeat distance (RD) of the multilayer is an important parameter for the description of the peptide's influence. At the bottom line of figure 26 the influence of NK-2 at different concentrations on the RD is summarized. The SAXS experiment showed no significant effects of different concentrations (even up to a molar ratio of 300:1 [peptide:lipid]) of NK-2 up to a temperature of 60°C; above this temperature the lipid vesicles start to decompose giving rise to a very small scattering intensity which can only be analysed with high errors. The visible increase of the RD from 6,5 to 7,5 nm for the increase of temperature can be explained by the enlargement of the water layer, which implies the swelling of the POPC vesicles before melting.

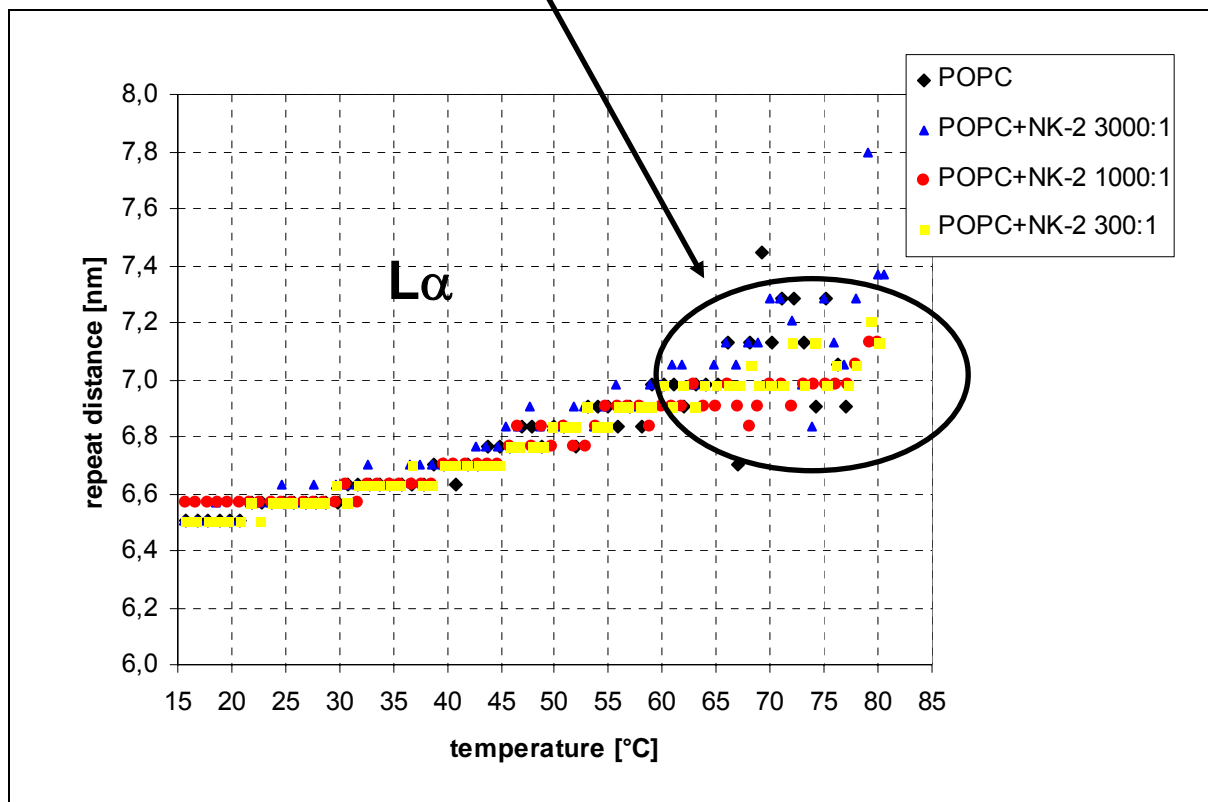
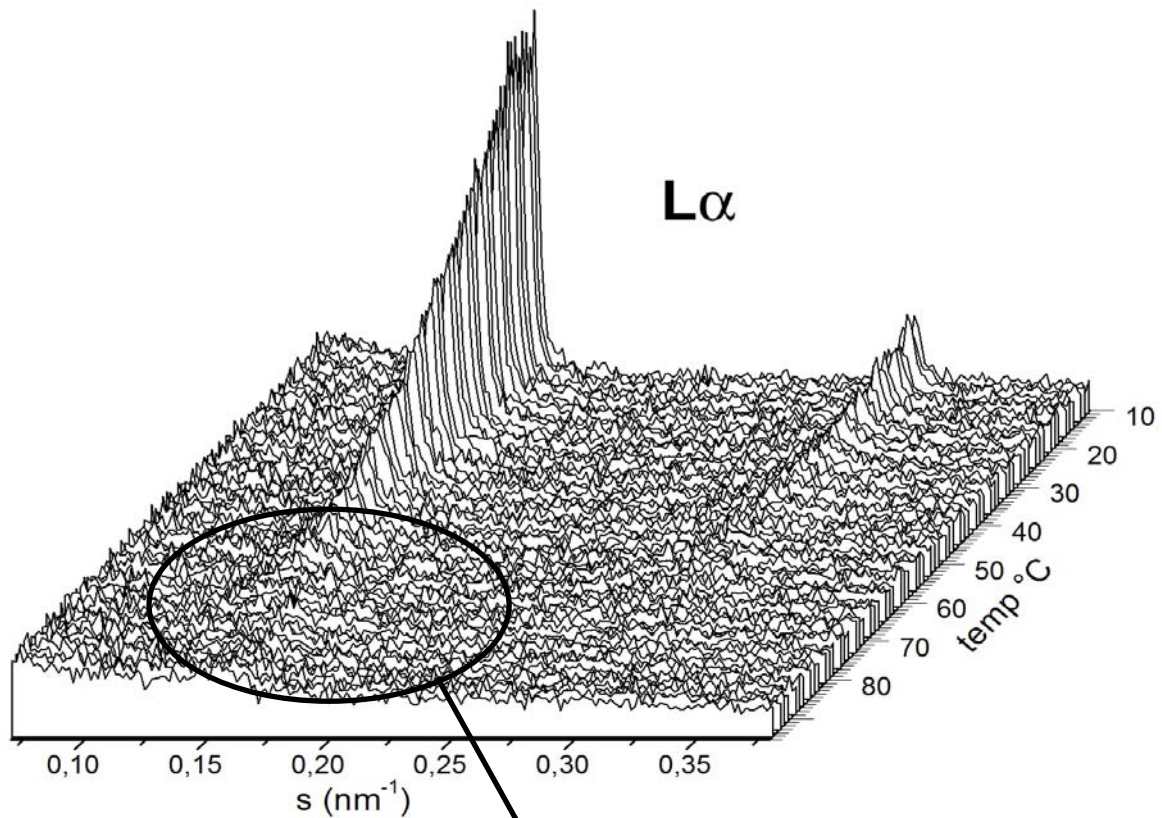


Figure 26: Top: SAXS pattern for POPC liposomes measured at a temperature range from 10 to 90°C with normalized intensity. $s=1/d=2\sin(\theta)/\lambda$, where λ is the wavelength of the X-ray beam and 2θ is the scattering angle. Bottom: The repeat distance of POPC and after addition of NK-2 in a temperature range from 15 to 80°C.

DPPC

DPPC (1,2-dipalmitoyl-phosphatidylcholine) (figure 27) was chosen because this lipid has the same headgroup (PC) as POPC, but a different acyl chain composition (see also the description in the materials chapter). Instead of the oleoyl chain (with a double bond), in the lipid DPPC two saturated acyl chains (palmitoyl) are crucial for the parallel alignment of the chains.

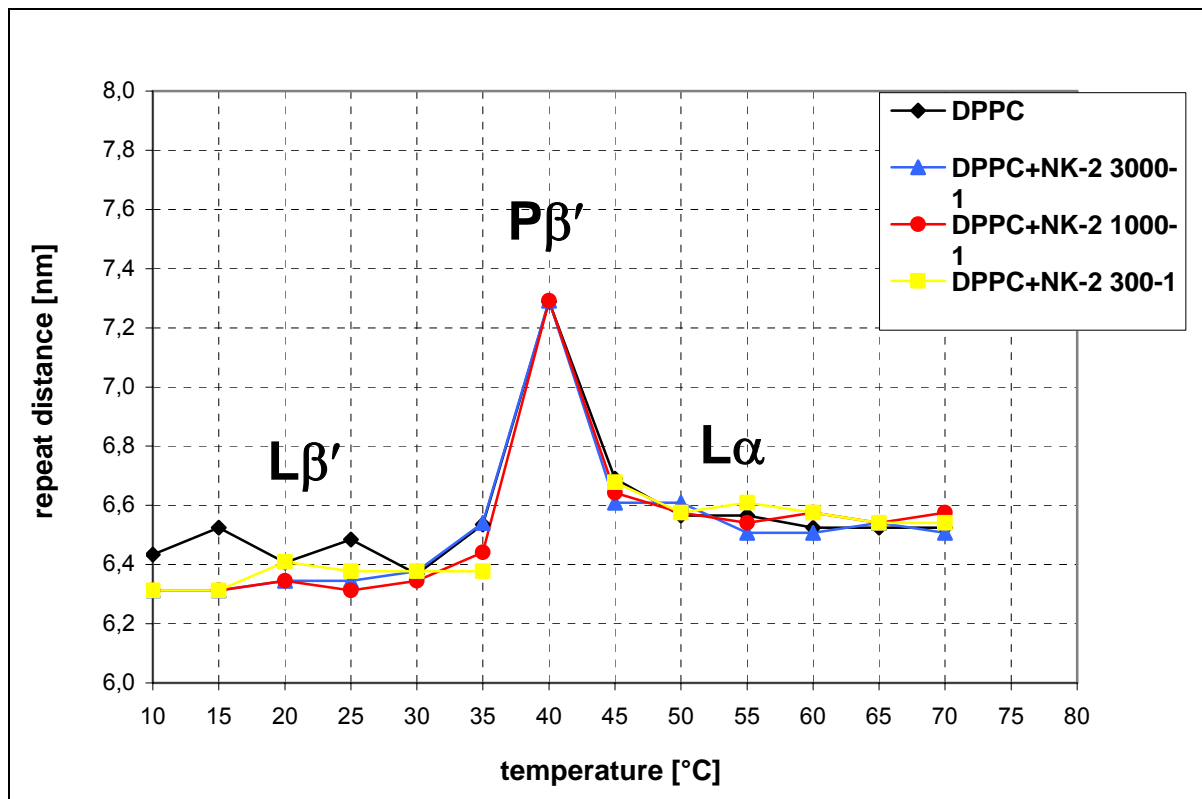


Figure 27: The repeat distance of DPPC and after addition of NK-2 in a temperature range from 10 to 70°C. In this experiment data were collected every 5 degrees.

In figure 27 the repeat distance as determined from the first order peak of DPPC is plotted. At 35°C the phase transition from the gel phase ($L\beta'$) to the ripple phase ($P\beta'$) is observable. The second transition from the ripple to the liquid crystalline phase ($L\alpha$) occurs between 40°C and 45°C and ends in a slightly increased RD for DPPC liposomes. The addition of NK-2 does not influence the repeat distance up to concentration of 300:1 [lipid:peptide]. Any statement about a change in the phase transition temperature is very difficult because the step width of the temperature ramp was 5°C per minute. Still, the comparison to POPC and the missing influence on the RD justify the assumption that NK-2 does not alter the Phase transition

SAXS measurements for phosphatidylglycerin lipids

POPG

The scattering of **POPG (1-palmitoyl-2-oleoyl-phosphatidylglycerin)** (measured in H_2O) is shown in figure 28. In contrast to POPC, the scattering signal of POPG does not show well defined diffraction peaks, but to a broad maximum which is typical for unilamellar vesicles formed by charged amphiphiles (Hauser, H., BBA, 1984 and Deme, B., et al, Langmuir, 2002). The data of POPG scattering are difficult to

analyze, because in this case the calculation of a repeat distance is not possible, the scattering angle at the maximum of the peaks indicates rather a value for the membrane thickness. The influence of NK-2 on the POPG vesicles is very small (at 55°C the bilayer is decreased at most by 0,4 nm), but the peptide tends to decrease the POPG bilayer thickness (figure 29).

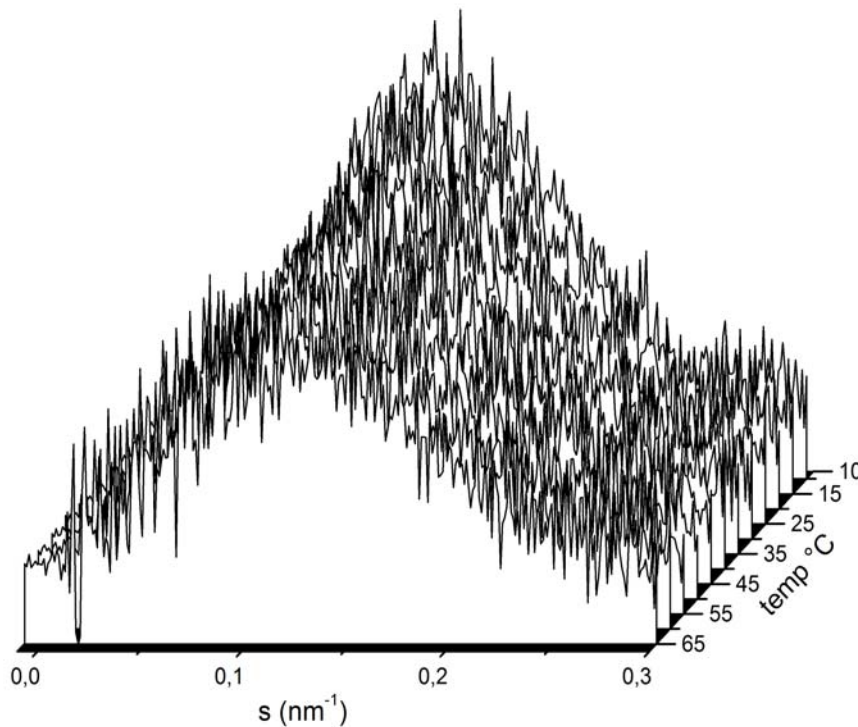


Figure 28: Scattering pattern of POPG liposomes measured in 10mM sodium phosphate buffer (pH7,4) at a temperature range from 10 to 65°C with normalized intensity. $s=1/d=2\sin(\theta)/\lambda$, where λ is the wavelength of the X-ray beam and 2θ is the scattering angle.

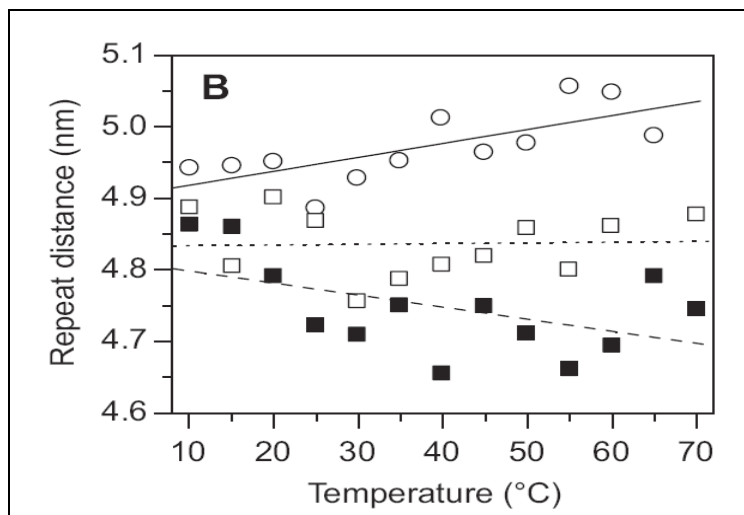


Figure 29: Influence of NK-2 on POPG vesicles within a temperature range from 10 to 70°C: Circles stand for pure POPG, transparent squares for POPG plus NK-2 at a concentration of 300:1 (lipid:peptide) and filled squares for a concentration of 100:1. Lines represent a linear fit of the respective data series. Taken from Willumeit, R. et al, BBA, 2005.

SAXS measurements for phosphatidylethanolamine lipids

The analyses of the SAXS experiments of the influence of NK-2 on phosphatidylethanolamine lipids was often difficult, because of the above described problems with the melting of vesicles at higher temperatures and also due to the very fast aggregation of the samples after the addition of the peptide already at low peptide concentrations.

POPE

In figure 30 a typical diffraction pattern of **POPE (1-palmitoyl-2-oleoyl-phosphatidylethanolamine)** is shown; the phases (gel phase ($L\beta$), liquid crystalline phase ($L\alpha$) and the inverse hexagonal phase (H_{II})) are indicated in the figure. The head group of PE is relatively small leading to a rather conical shape of the lipid, which allows the lipids to form an inverted hexagonal phase. The transition from the gel to the liquid crystalline phase takes place at 25°C for pure POPE and is not changed after addition of NK-2 up to a concentration of 100:1 [lipid:peptide] (figure 31). These findings were also confirmed by DSC (differential scanning calorimetry) measurements (see Willumeit, R. et al, BBA, 2005), although here at very high concentrations of NK-2 (up to 30:1) a slightly decrease of the transition temperature is observable. The highest concentration of NK-2 (100:1) shows a slightly influence on the lamellar phase of POPE (fig. 34). The RD is increased after addition of the peptide by 0,1 to 0,2 nm due to a probable inclusion of the peptide between the lipid bilayers. Interestingly, the transition temperature from the lamellar liquid crystalline phase to the inverse hexagonal phase is remarkably influenced by the peptide. The transition temperature of 71°C for pure POPE is decreased in a concentration dependent manner; down to 67°C for 300:1 [lipid:peptide] and down to 66°C for 100:1 [lipid:peptide]. This effect was even more pronounced in former SAXS measurements (what could be due to the storage dependent loss of activity of NK-2) and also approved in DSC measurements (Willumeit, R. et al, BBA, 2005).

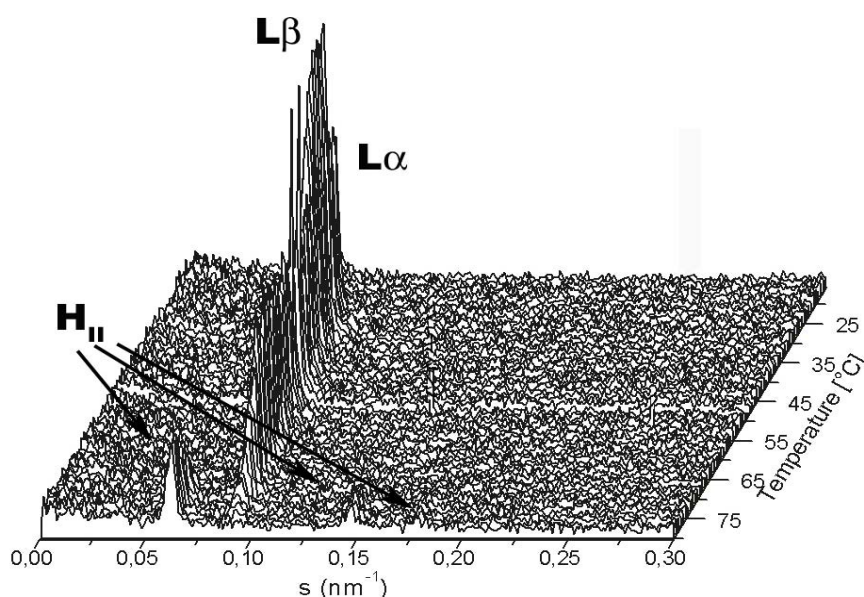


Figure 30: Diffraction pattern of POPE liposomes measured in 10mM sodium phosphate buffer (pH7,4) at a temperature range from 15 to 80°C with normalized intensity and background subtracted. Phases are indicated. $s=1/d=2\sin(\theta)/\lambda$, where λ is the wavelength of the X-ray beam and 2θ is the scattering angle.

Furthermore, the coexistence of the lamellar and the inverse hexagonal phase is more pronounced after addition of the peptide. For pure POPE the lamellar phase disappears at 75°C (figure 30 and 31), but NK-2 conserves the liquid crystalline phase up to 80°C (figure 31).

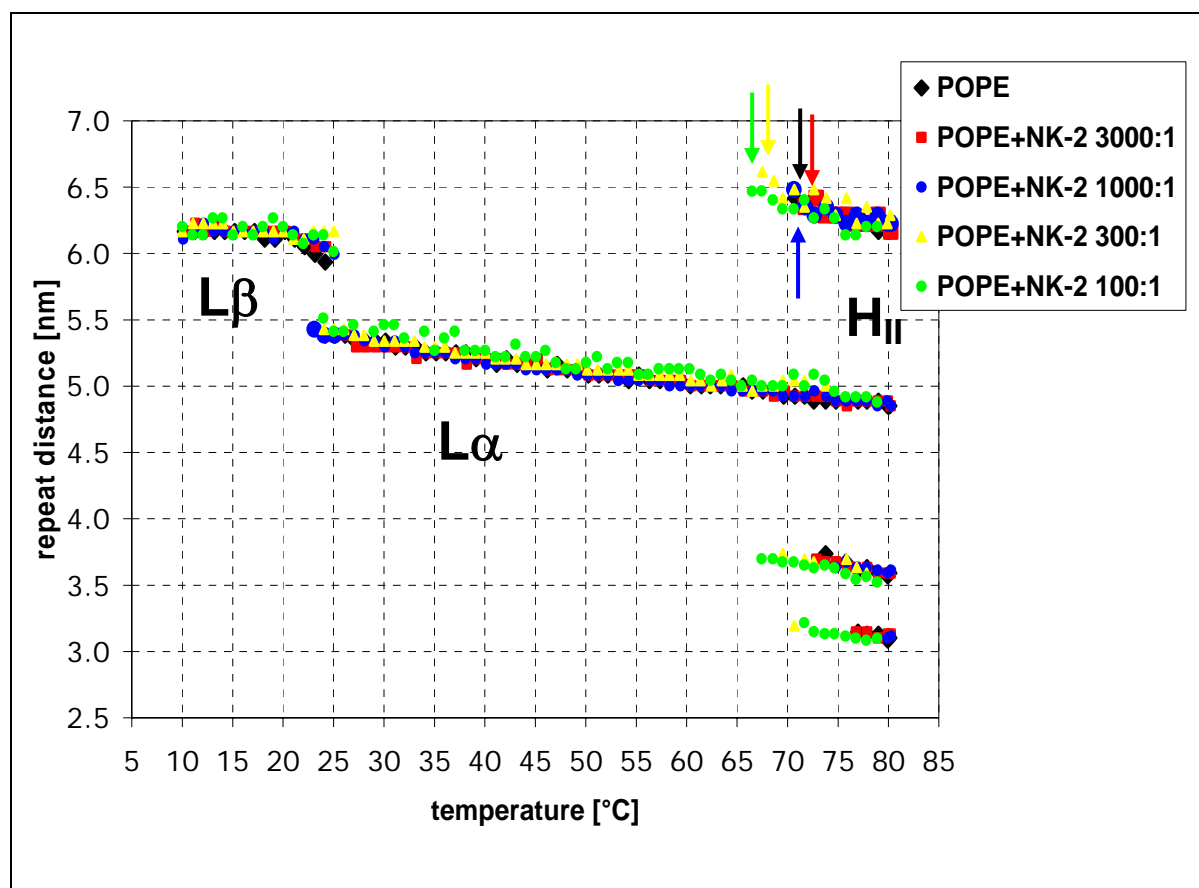


Figure 31: The repeat distance of POPE measured in 10mM sodium phosphate buffer (pH7,4) in a temperature range from 10 to 80°C. Phases and transition temperatures are indicated.

Summary

The results of this section show that NK-2 is a potent antibacterial peptide (against Gram positive and Gram negative bacteria) with a good selectivity for bacterial over mammalian cells. The analysis of the SAXS experiments resulted in a negligible influence of the peptide on phosphatidylcholine and phosphatidylglycerin lipids. The most significant effect of the peptide was found during the interaction of NK-2 with phosphatidylethanolamine lipids. Here the lamellar phases were again not effected, but a strong influence of NK-2 on the inverse hexagonal phase transition was obvious. In a concentration dependent manner the addition of NK-2 decreased the transition temperature of the PE liposomes.

5.2. Results for NK-CS

The SAXS measurements for NK-CS were focussed on phosphatidylcholine and phosphatidylethanolamine lipids. This choice was based on the results found for NK-2; the influence of NK-CS on the lamellar phases of POPC was investigated in order to compare the data with the results for NK-2, and the main concentration was put on PE lipids, because of the significant influence of NK-2 on the inverse hexagonal phase transition of POPE.

The peptide NK-CS was developed to inhibit possible molecular interactions by the sulfides of the amino acids cysteine; with the replacement of the cysteine by the amino acid serine the formation of disulfide bridges should be prevented and ageing effects as they were found for NK-2 should be omitted.

Electrospray ionisation mass spectroscopy

To determine the effect of ageing the peptides NK-CS and NK-2 were investigated by mass spectroscopy (figure 32-34 and 35-36) after a storage period of six month and the results were compared with the mass spectroscopy data provided by the companies that delivered the peptides (data not shown).

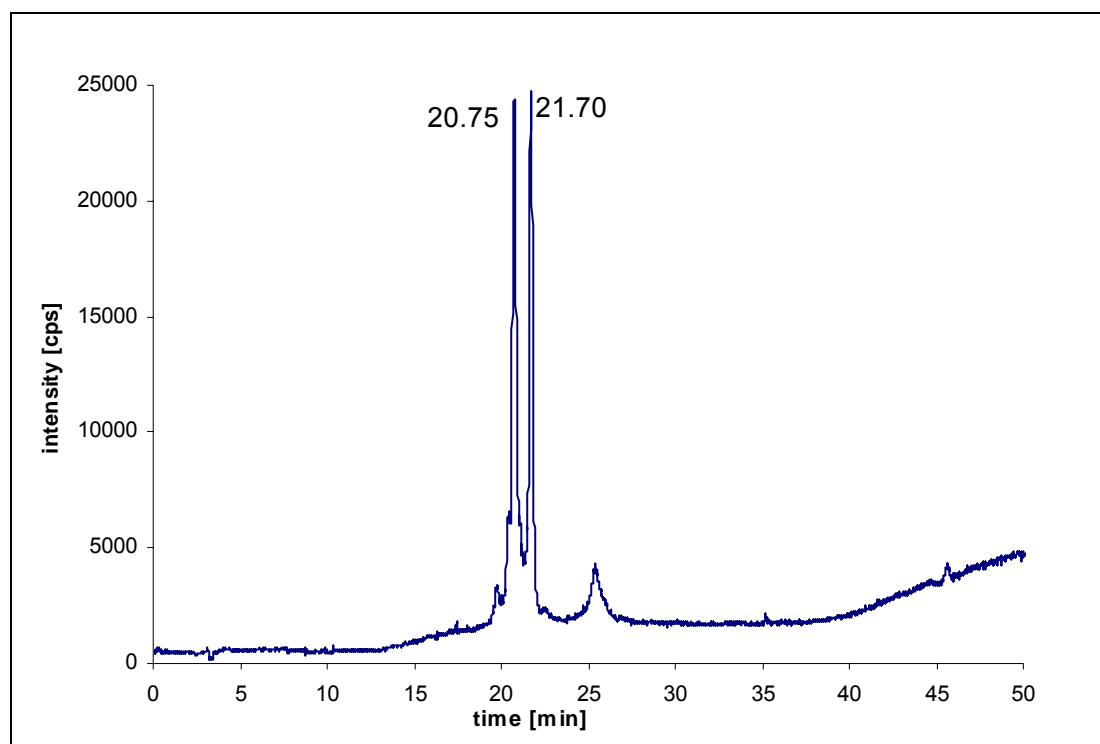


Figure 32: ESI-MS chromatogram of NK-2, the elution positions of the monomer and the dimer are indicated at 20.75 min, res. 21.70 min.

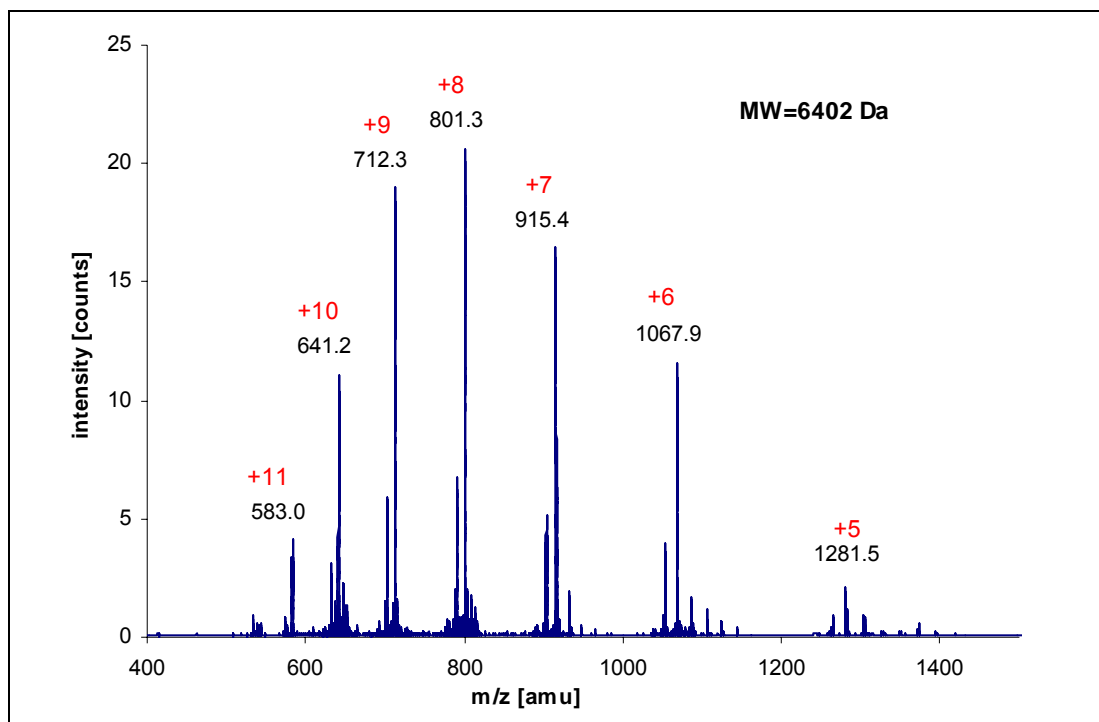


Figure 33: Mass spectrum (m/z 400-1500) of the NK-2 dimer eluting at 20.75 min (fig. 32). The charged ion gives a mass of 6402 Da indicated in the picture.

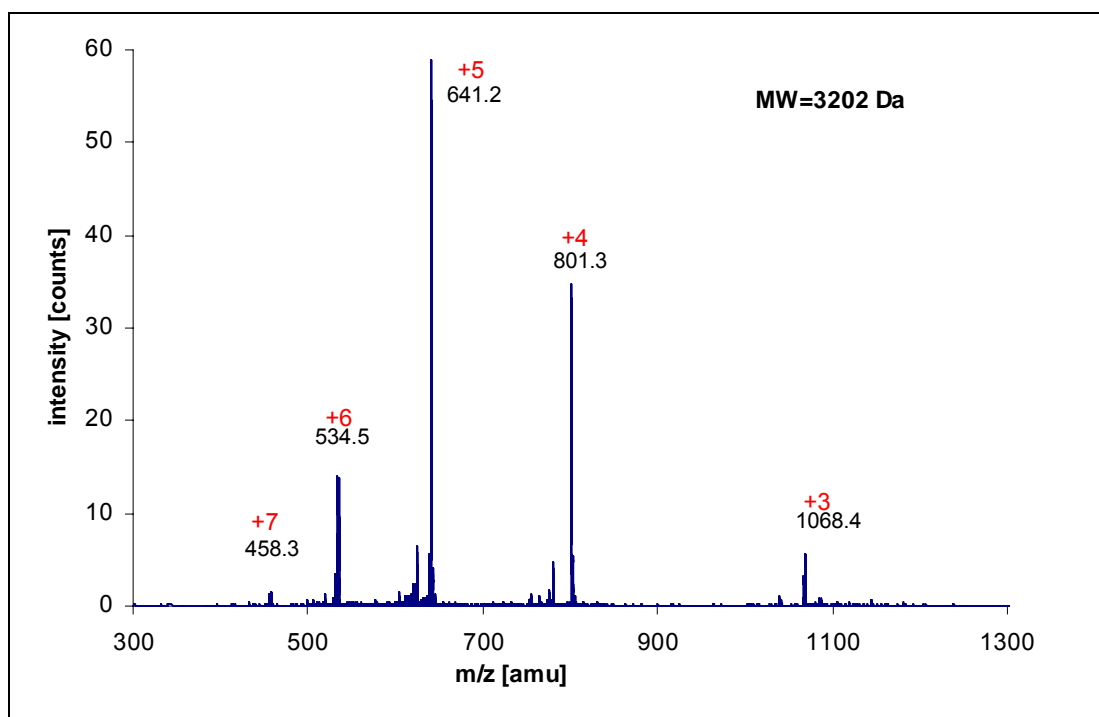


Figure 34: Mass spectrum (m/z 300-1300) of the NK-2 monomer eluting at 20.70 min (fig. 32). The mass of 3202 Da is indicated in the picture.

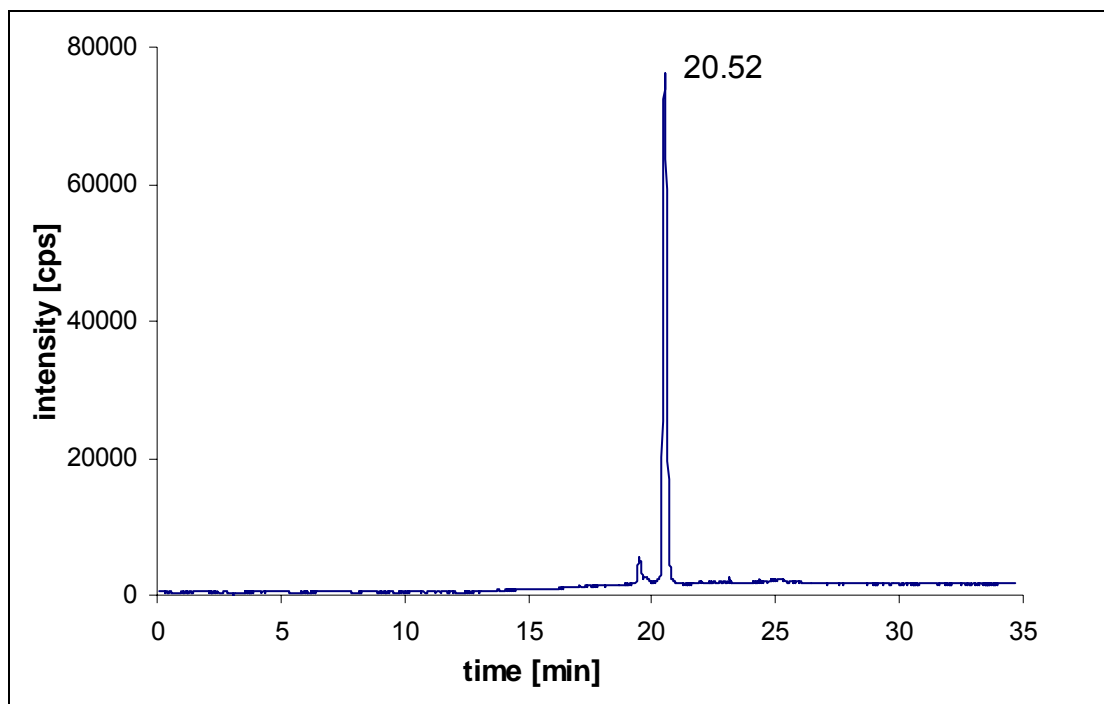


Figure 35: ESI-MS chromatogram of NK-CS, the elution position of the peptide is indicated at 20.52 min.

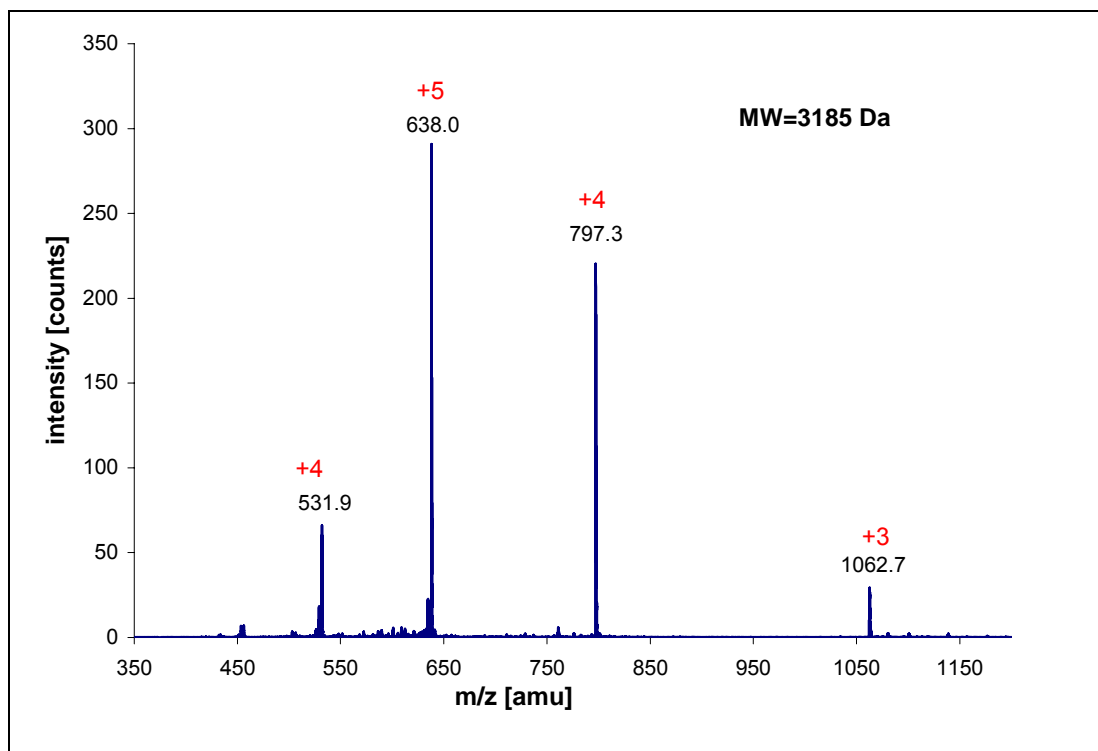


Figure 36: Mass spectrum (m/z 350-1200) of the NK-CS monomer eluting at 20.52 min (fig. 35). The mass of 3185 Da is indicated in the picture.

The mass spectroscopy experiment with NK-2 showed two remarkable peaks in the chromatogram (figure 32); the elution peaks were calculated with molecular weights of 3202 Da (fig. 34) and 6402 Da (fig. 33). These values correspond to the MW of the NK-2 monomer (with a calculated MW of 3203 Da – the difference of 1 Da is probably due to the technique of analysis of the measurement and is negligible), respectively to the dimer without two protons due to the building of a disulfide bridge. This finding

demonstrates a time-dependent dimerisation of the peptide, because in the MS data sheet of the company Wita GmbH no peak that corresponds to the dimer of NK-2 occurs. The chromatogram of NK-CS showed only one pronounced peak (fig. 35), that corresponds to a MW of 3185 Da (fig. 36). The calculated MW of NK-CS is 3186 Da and fits very well to the experimental value (again with a negligible difference of one proton) and also to the data provided by the company Biosyntan. That proves a good stability of the peptide after a storage time of six month. These findings justified the substitution of the amino acid cysteine by serine; in the modified peptide NK-CS the time-dependent dimerisation is inhibited.

Antibacterial and hemolytic activity

In figure 37 the minimal inhibitory concentrations of NK-CS against *E. coli*, *S. carnosus* and *B. subtilis* bacteria are shown. The MIC of 0,63 μ M measured for NK-CS against *E. coli* is four times better than the MIC observed for NK-2 (2,5 μ M). The same factor of 4 is found for the MICs against *S. carnosus* (2,5 μ M) and against *B. subtilis* (1,25 μ M).

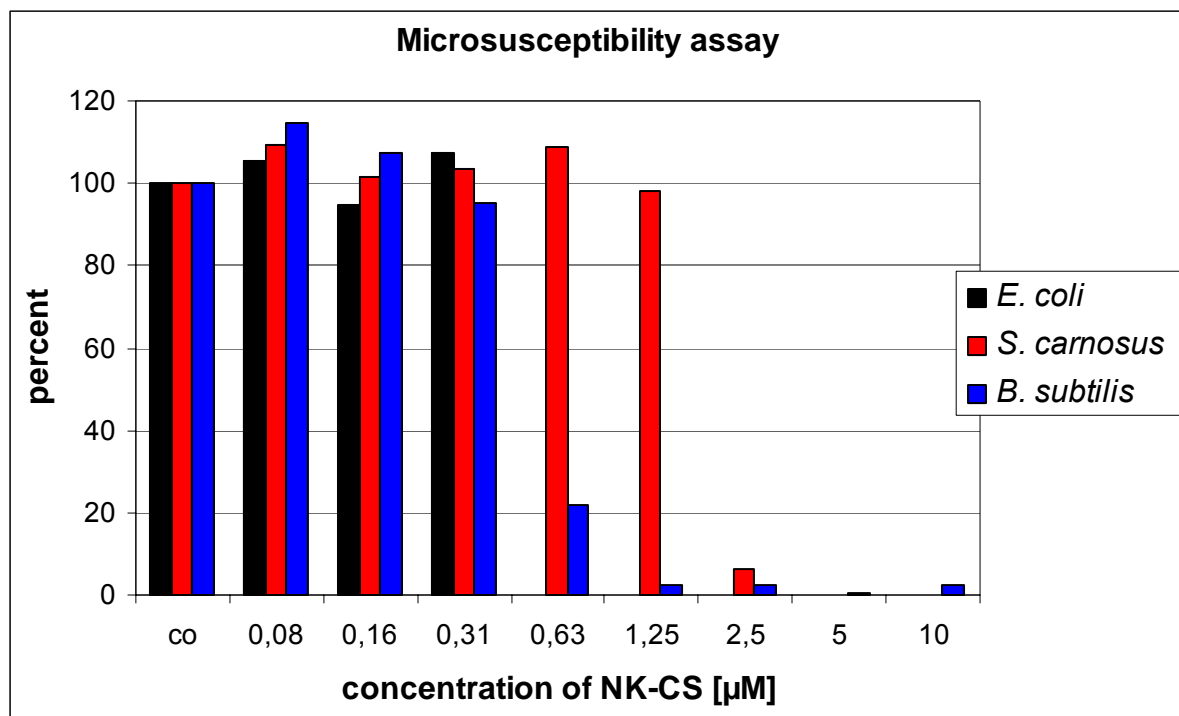


Figure 37: Antibacterial activity of NK-CS against *E. coli*, *S. carnosus* and *B. subtilis*.

The selectivity of NK-CS for bacteria over mammalian cells was comparable to the results for NK-2 (figure 38). At the highest concentration of 100 μ M, NK-CS lyses only 25 percent of the erythrocytes. Melittin lyses all blood cells already at a concentration of 10 μ M.

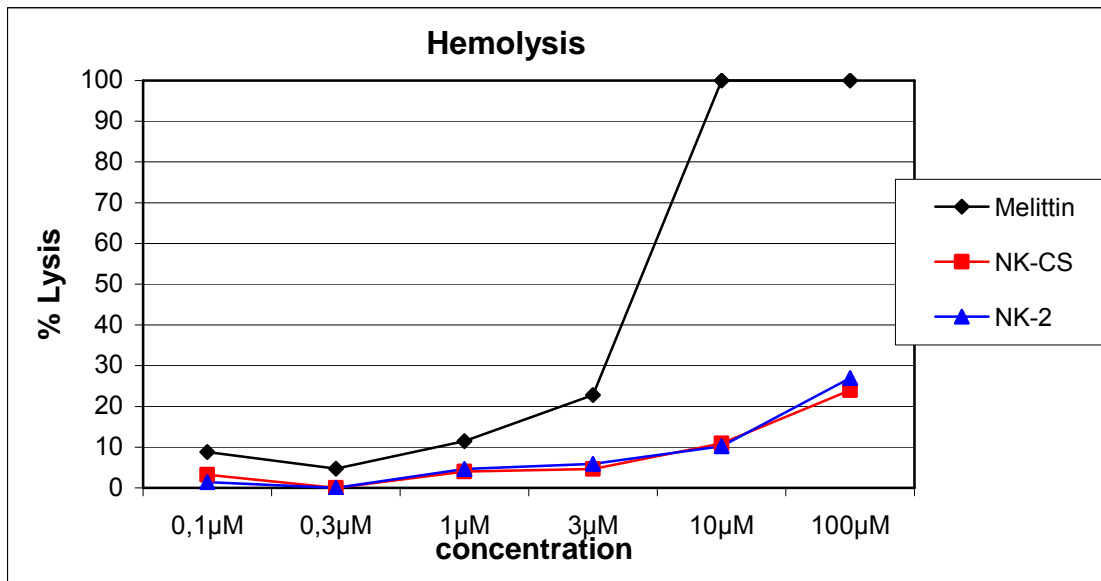


Figure 38: Hemolytic activity of NK-CS against human erythrocytes in comparison with NK-2 and melittin.

SAXS measurements for PC lipids

POPC

In order to test the influence on the lamellar phase of phosphatidylcholine lipids, POPC vesicles were investigated after addition of NK-CS. The repeat distance increases during the heating cycle up to 60°C by 0,4 nm (figure 39) which is comparable to data found for NK-2. Furthermore, NK-CS shows an effect on the RD of POPC. The RD is slightly increased (by 0,2 nm) at the starting temperature of 20°C (fig. 39), what indicates an inclusion of the peptide between the lipid bilayers. But at higher temperatures NK-CS decreases the RD by 0,1 to 0,2 nm, e.g. the amount of water floating between the bilayers is decreased.

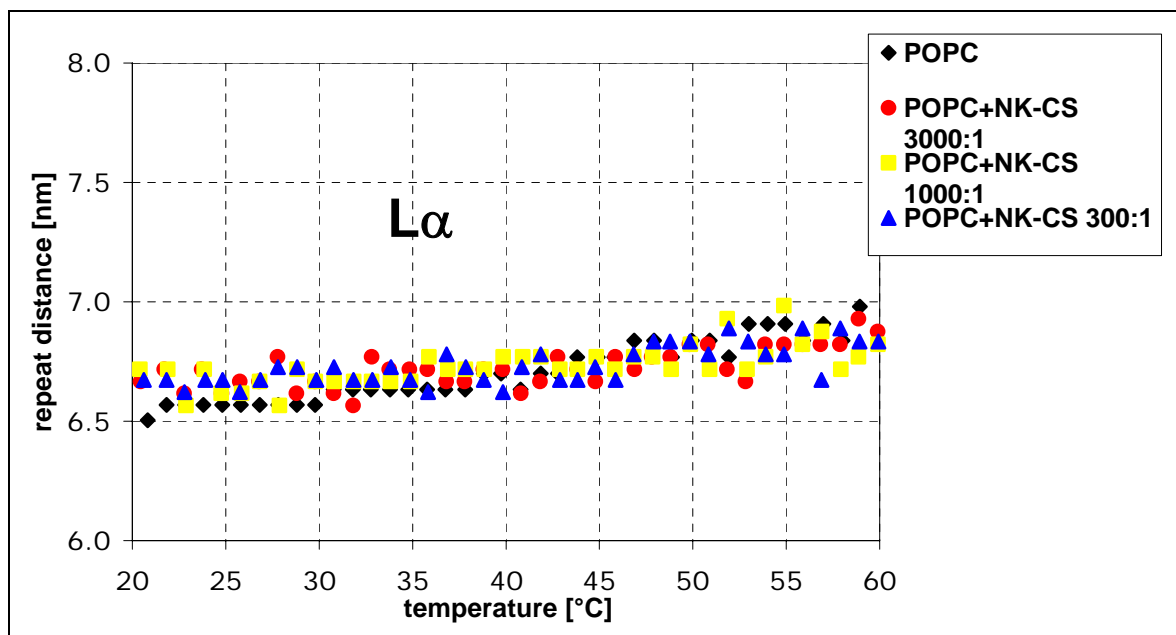


Figure 39: The repeat distance of POPC measured in 10mM sodium phosphate buffer (pH7,4) in a temperature range from 20 to 60°C.

The lamellar phase behaviour was tested for NK-CS with POPC. Again no influence of the peptide was found; for that reason the lamellar phase transitions and lipids with only lamellar phases will not be in the point of interest anymore.

SAXS measurements for PE lipids

POPE

As it was observed for NK-2 before, no influence of the peptide on the phase transition from the gel to the liquid crystalline phase of POPE was found for NK-CS (data not shown). But a significant impact was observed when the influence of NK-CS on the non-lamellar phase behaviour of POPE liposomes was measured.

The hexagonal phase transition of POPE is significantly changed after the addition of NK-CS (figures 40 and 41). Contrary to the findings for NK-2, here the phase transition temperature is **increased**. At a molar ratio of 1000:1 [lipid:peptide] the temperature is shifted by 4°C (figure 41). In a concentration dependent manner this influence is even more pronounced at a molar ratio of 300:1 [lipid:peptide] (figures 40 and 41), here the temperature is increased by 10°C up to 77°C.

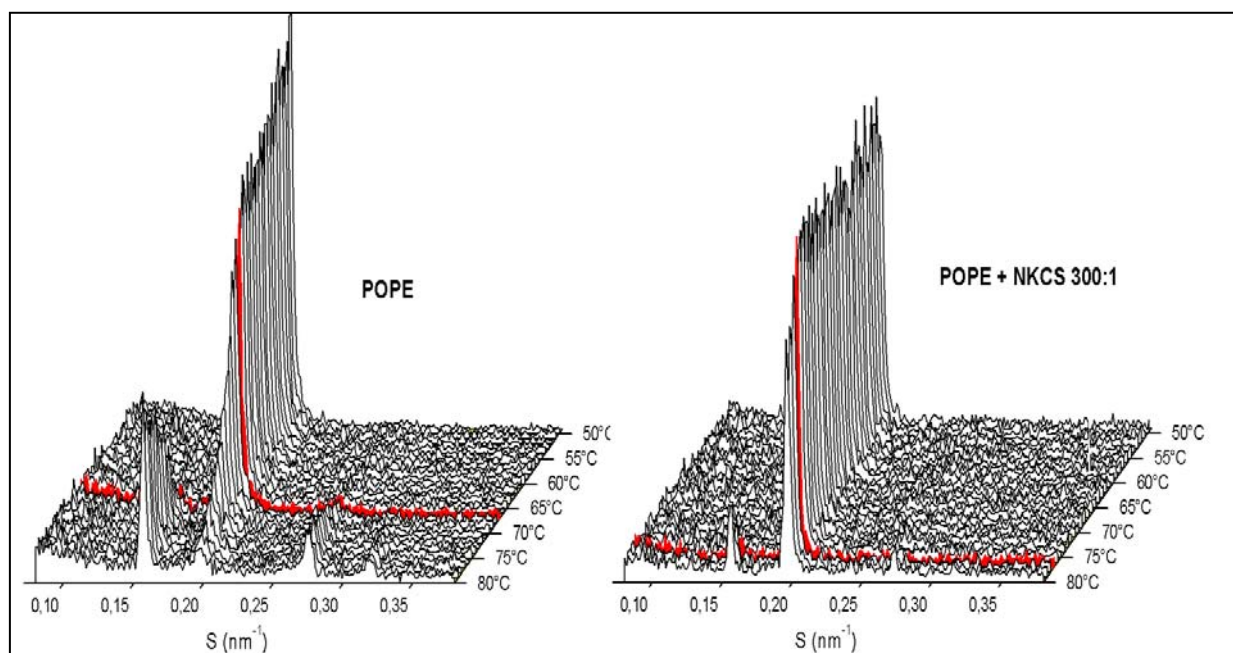


Figure 40: Diffraction pattern of pure POPE (left) and POPE after addition of NK-CS at a concentration of 300:1 [lipid:peptide] (right) measured in 10mM sodium phosphate buffer (pH7,4). The phase transition temperatures are marked in red.

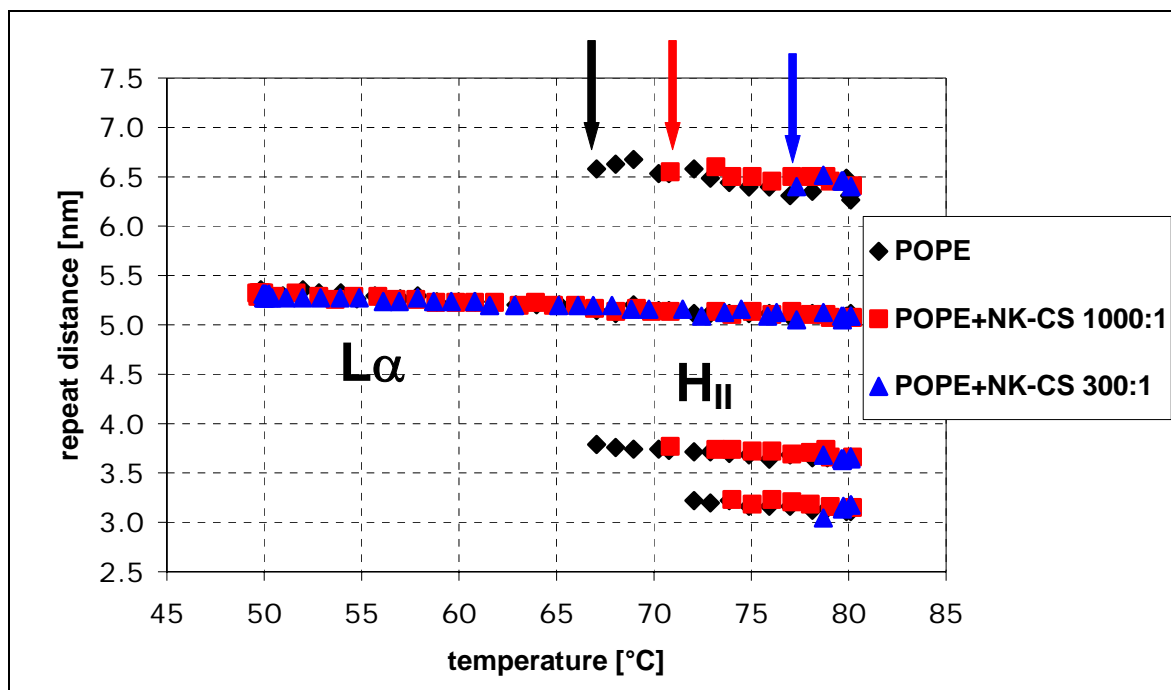


Figure 41: The repeat distance and the inverse hexagonal phase transition of POPE measured in 10mM sodium phosphate buffer (pH7,4) in a temperature range from 50 to 80°C.

The co-existence of liquid crystalline and inverse hexagonal phase ($L\alpha$ and H_{II}) is significantly prolonged after addition of NK-CS; here the peptide shows the same effect as it was reported for NK-2.

DOPE-trans

The influence of the acyl chain composition of phosphatidylethanolamine lipids on the interaction with NK-CS, as the most active peptide so far, was studied with **DOPE-trans (1,2-dielaidoyl-phosphatidylethanolamine)** liposomes (figure 42). Again, an increase of the H_{II} phase transition temperature was detected though it was not as pronounced as it was for POPE. An increase of the H_{II} transition temperature from 56°C for pure DOPE-trans to 58°C (at a molar ratio of 300:1 [lipid:peptide]) was found. This equals an increase of 4%, which is more than 3-fold smaller than for POPE where the effect for the same concentration of peptide (300:1) was 15%. At higher concentrations of NK-CS (100:1) this effect is even more pronounced (the temperature is increased by 11%).

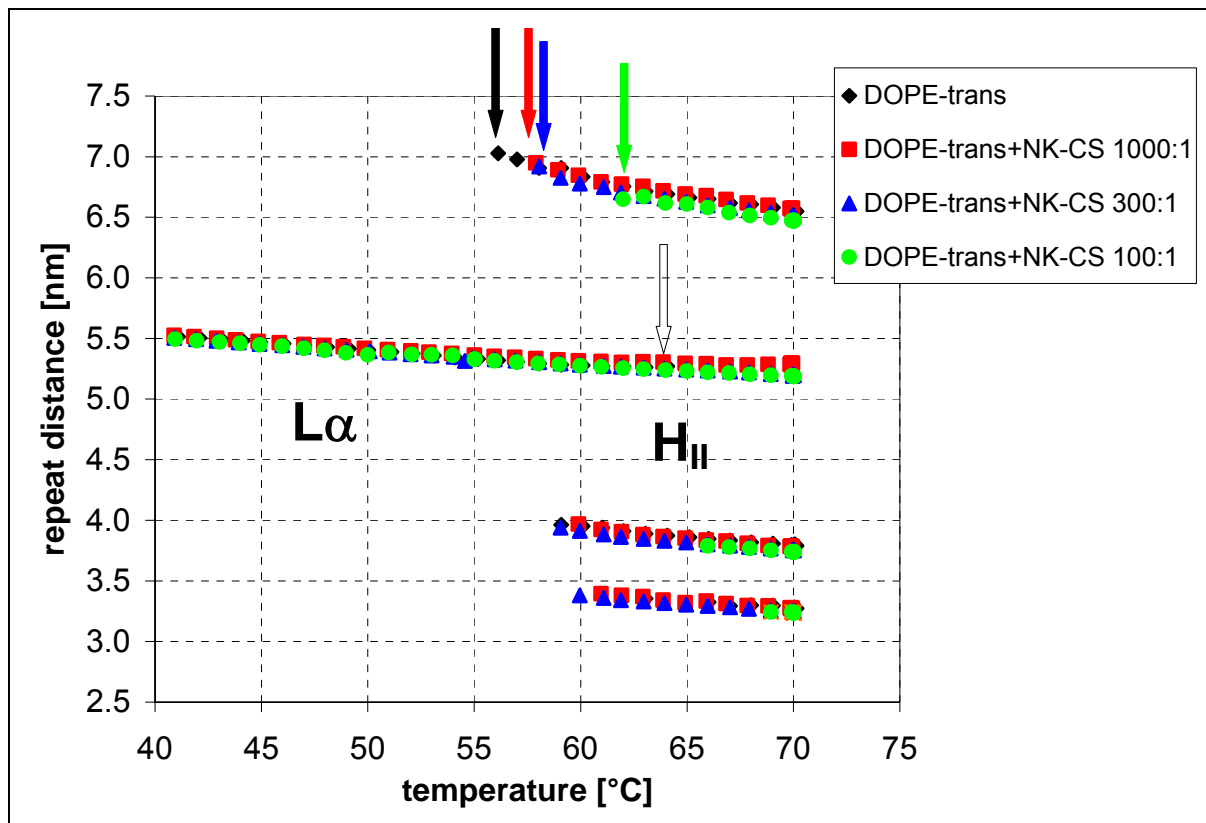


Figure 42: The repeat distance and the inverse hexagonal phase transition of DOPE-trans and after addition of NK-CS measured in 10mM sodium phosphate buffer (pH7,4) in a temperature range from 40 to 70°C. The phases are indicated and the phase transitions are marked by the coloured arrows. The transparent arrow indicates the end of the lamellar phase of pure DOPE-trans.

The addition of NK-CS to DOPE-trans liposomes had also the effect of the prolongation of the lamellar phase of the lipid (figure 42). At the lowest concentration of NK-CS (1000:1) the lamellar phase was still observable up to the final temperature of 70°C, which indicates, like for POPE, a co-existence of the $L\alpha$ and H_{II} phases.

DiPOPE

In order to prove, if the effect of NK-CS is also repeatable for a third PE lipid, the influence of the peptide on **DiPOPE (1,2-dipalmitoleoyl-phosphatidylethanolamine)** liposomes was investigated (figure 43). This lipid has two identical, unsaturated acyl chains, which are shorter (16:1/16:1) than the acyl chains of DOPE-trans.

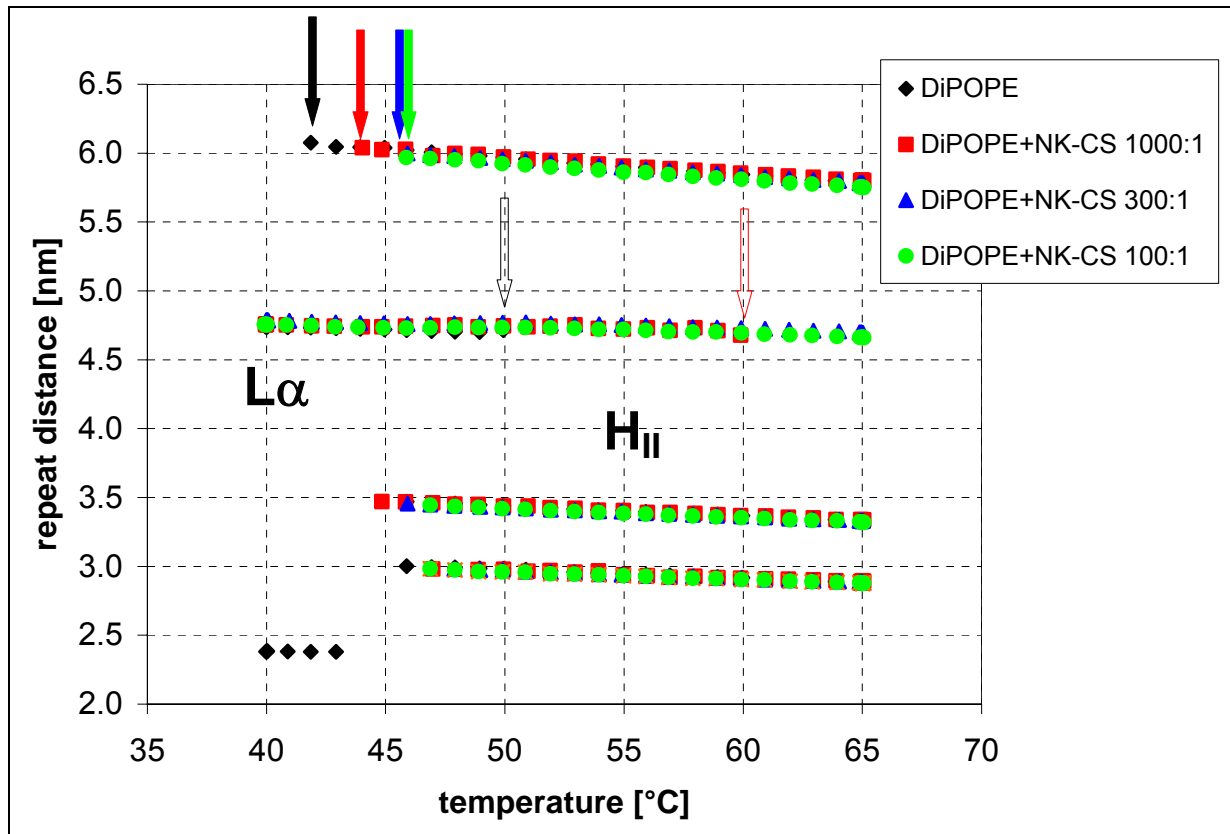


Figure 43: The repeat distance and the inverse hexagonal phase transition of pure DiPOPE and after addition of NK-CS measured in 10mM sodium phosphate buffer (pH7,4) in a temperature range from 40 to 65°C. The phases are indicated and the phase transitions are marked by the coloured arrows. The transparent arrows indicate the end of the lamellar phase.

Also for DiPOPE an increase of the H_{II} phase transition temperature was observed. Here an increase of the transition temperature of 42°C for pure DiPOPE-trans to 46°C (at a molar ratio of 300:1 [lipid:peptide]) was found. This is an increase of 10%, which is a value between the effect of NK-CS on POPE and DOPE-trans. Contrarily to the data for DOPE-trans, this impact on DiPOPE liposomes is not more pronounced at the highest concentration of NK-CS (100:1).

The addition of NK-CS to DOPE-trans liposomes had two more visible effects: The lamellar phase is also prolonged (figure 43) as it was found for POPE and DOPE-trans. But after addition of the lowest concentration of NK-CS (1000:1) the lamellar phase disappears at 60°C, while for higher concentrations the lamellar phase was still observable up to the final temperature of 65°C. Another effect of NK-CS is the disappearance of the second order peak of the lamellar phase. For pure DiPOPE this peak is observable with a RD of 2,4 nm.

Structural investigations with Circular Dichroism

Beside the structural impact of the peptides on the lipids also some structural information about the peptides was obtained. As mentioned earlier NK-2 is mainly α -helical (Andr , J. et al. Med. Microbiol. Immunol. 1999) with the assumption of a flexible region in the middle of the amino acid chain. One method giving low resolution structural information is circular dichroism (CD). The measurements were performed with the help of Claudia Olak from the Max-Planck-Institute of Colloids and

Interfaces in Golm. In aqueous environment (double distilled water and potassium phosphate buffer (PPB) at pH7) NK-CS has a random coil conformation (fig. 44), although the addition of PPB leads to a shift in the CD spectra and indicates a slight tendency of the peptide to build a structure.

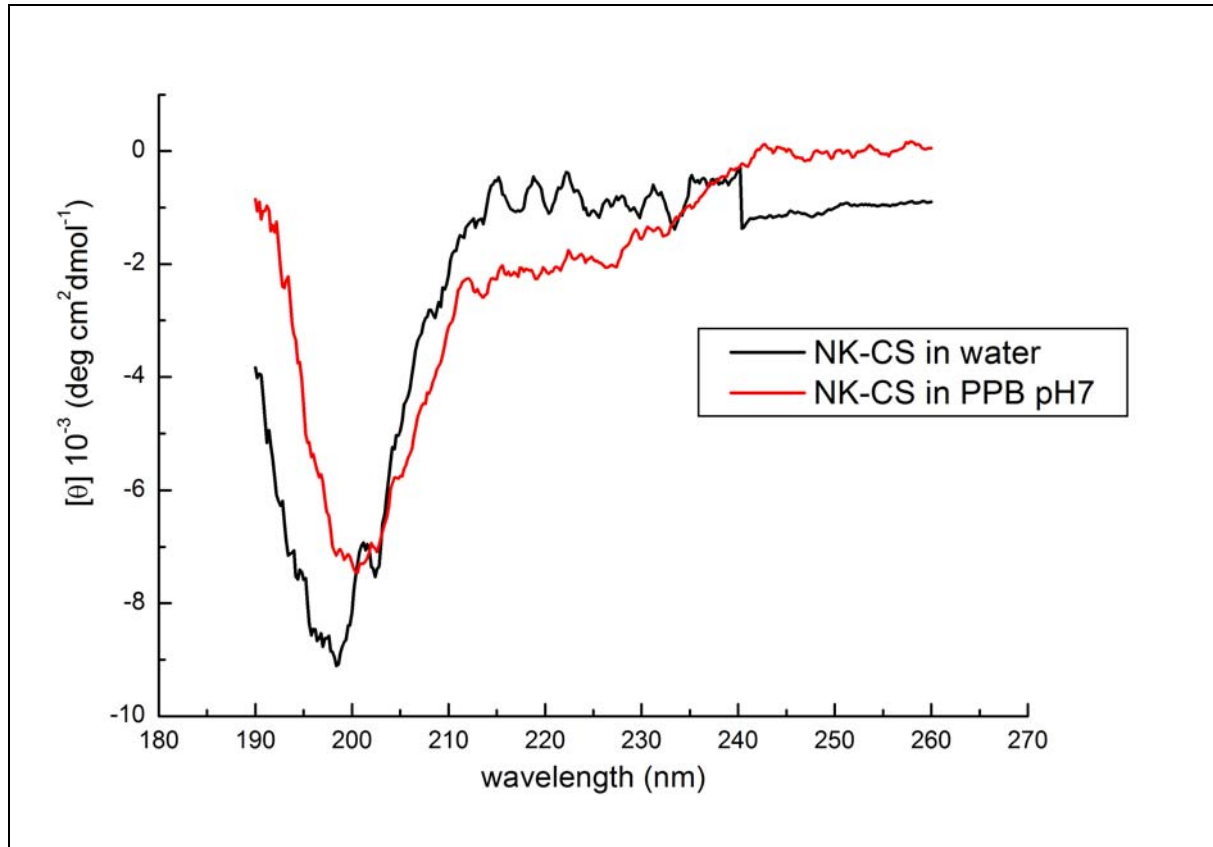


Figure 44: Circular dichroism (CD) measurements of NK-CS in water and in potassium phosphate buffer (PPB).

The random coil structure of NK-CS changes after addition of SDS (dissolved in double distilled water) (see figure 45). SDS is a negatively charged detergent that aggregates into micelles at a critical micelle concentration (CMC) of 8mM and is often used to induce alpha-helical or beta-sheet structures in peptides (Waterhous, D.V. and Johnson, W.C. jr, Biochem. 1994). At a SDS concentration of 1mM NK-CS seems to fold into a mixture of beta-sheet and alpha-helix, which is caused by the interaction of the peptide and the SDS monomers. By increasing the SDS concentration the peptide folds more clearly into an alpha-helix; here the peptide interacts with the spherical micelles of SDS. This interaction leads finally into the folding of an alpha-helix.

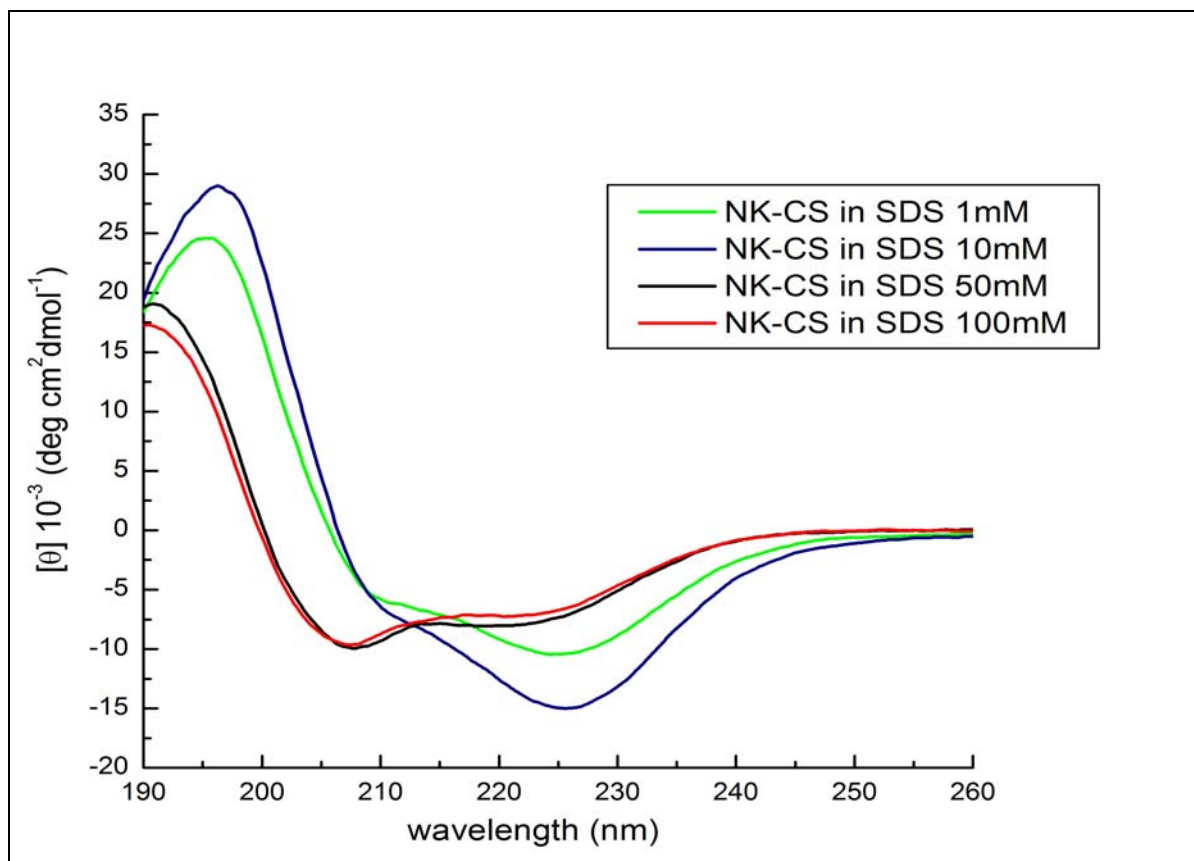


Figure 45: Circular dichroism (CD) measurements of NK-CS in a mixture with SDS in different concentrations.

Summary

To summarize, the replacement of the amino acid cysteine by serine inhibited the dimerisation of NK-2 and lead to a significant increase of the antibacterial activity of the peptide NK-CS against both Gram negative and Gram positive bacteria. The hemolytic activity of NK-CS is also very weak, compared with NK-2 even lower, and the influence of the peptide on PC lipids is again negligible. Like it was discussed for NK-2 before a significant influence on the inverse hexagonal phase transition of PE lipids was found. But contrarily to the previous findings, the addition of NK-CS increased the transition temperature of the lipid in a concentration dependent manner. Finally, CD measurements proved a random coil structure of NK-CS in aqueous conditions, but an alpha-helix was observable during the interaction of the peptide with negatively charged SDS micelles.

5.2.1. NKCS-[MS]

Due to the excellent antimicrobial activity, all further modifications were based on the peptide NK-CS. The first modification of NK-CS was to replace the amino acid methionine also by a serine (NKCS-[MS]). This exchange was thought to inhibit further interactions of the peptide by the reactive amino acid methionine and serine

was chosen to keep the overall changes in charge, size and hydrophobicity as marginal as possible.

Antibacterial and hemolytic activity

The additional replacement of methionine by serine for the peptide NKCS-[MS] results in a decreased activity compared to NK-CS, here a MIC of 2,5 μ M was found, which is equivalent to the MIC of NK-2. Therefore the activity of NKCS-[MS] against Gram positive bacteria was not tested. The hemolytic activity of NKCS-[MS] is comparable to the activity of NK-2 and NK-CS (figure 46).

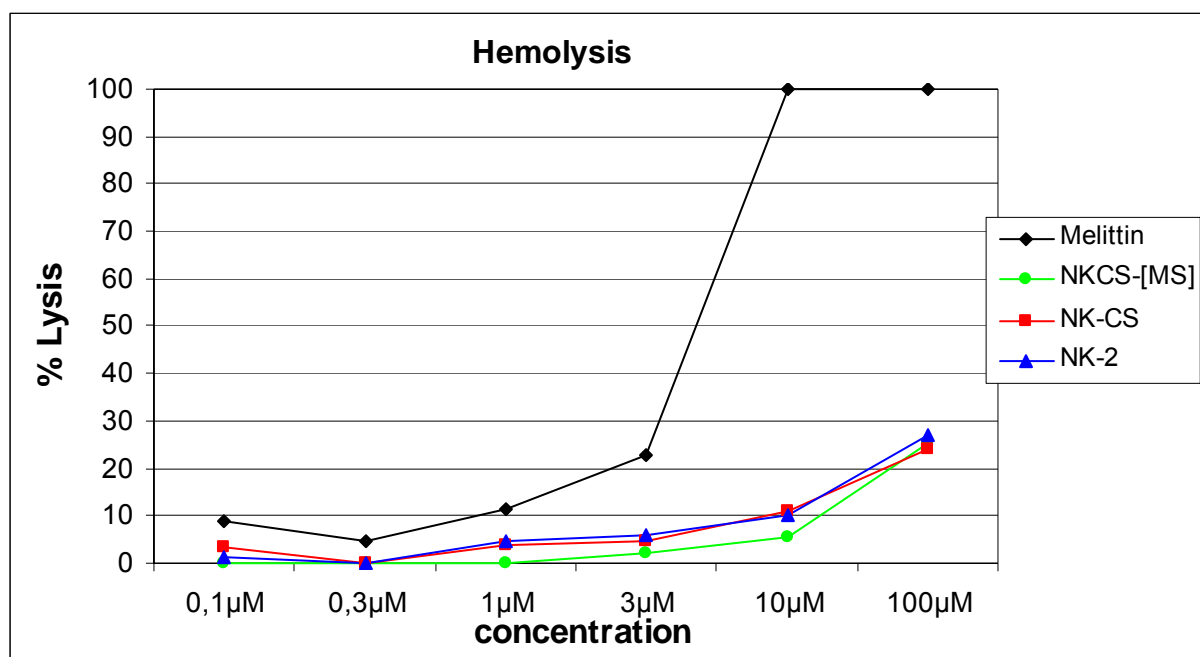


Figure 46: Hemolytic activity of NKCS-[MS] against human erythrocytes in comparison with NK-CS, NK-2 and melittin.

Thus, the met¹¹ in the sequence of NK-CS plays a crucial role in the antimicrobial activity and the replacement reduces the potent antibacterial effect of NK-CS. Therefore the investigation by SAXS of the peptide NKCS-[MS] was reduced to the phosphatidylethanolamine lipid POPE.

SAXS measurements with PE lipids

The same effect on the phase transition temperature of POPE as described above for NK-CS was observed for NKCS-[MS] (figure 47) and also the lamellar phase of POPE is prolonged after addition of NKCS-[MS] up to 80°C. Here the influence of the peptide is not as strong as reported for NK-CS (the temperature is only shifted by 3°C). At a concentration of 300:1 the increase of the phase transition temperature is 5%, which is 3-times smaller than the effect of NK-CS (15%) at this concentration. That seems to indicate a correlation between the antibacterial activity and the effect on the inverse hexagonal phase of PE lipids.

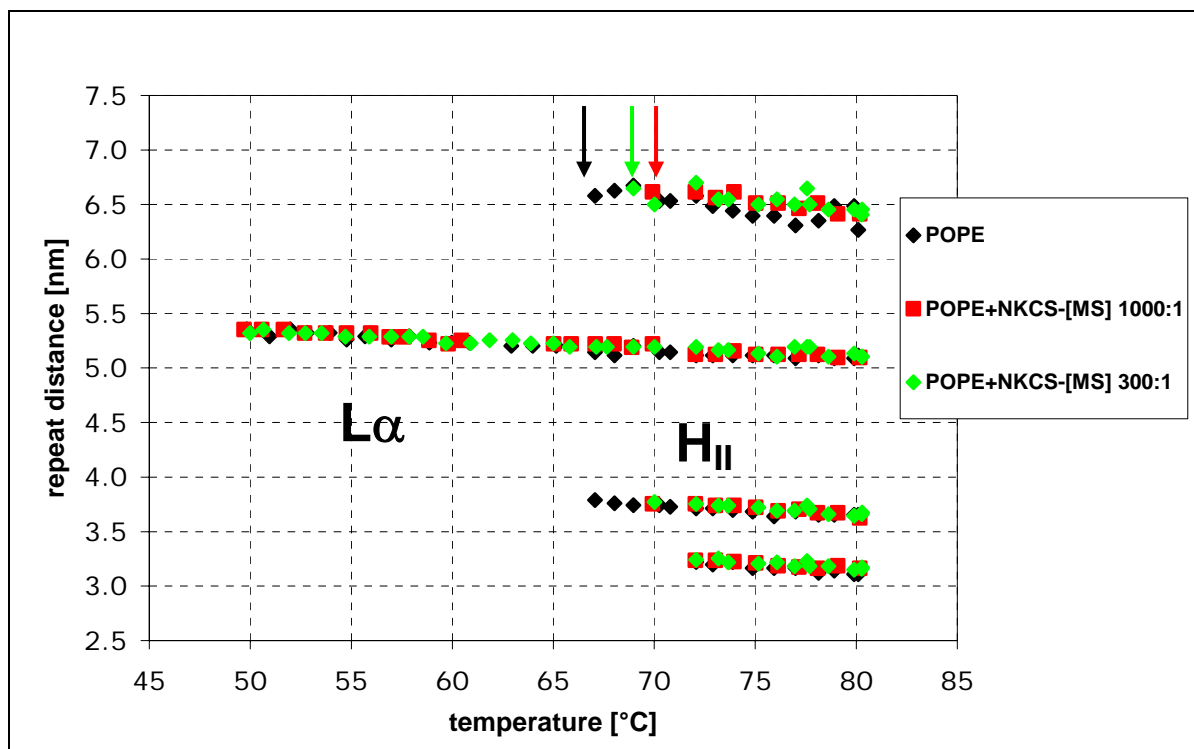


Figure 47: The repeat distance and the inverse hexagonal phase transition of POPE and after addition of NKCS-[MS] measured in 10mM sodium phosphate buffer (pH7,4) in a temperature range from 50 to 80°C.

Summary

With the replacement of the amino acid methionine by serine the antibacterial activity of NK-CS was not improved, and the hemolytic activity of NKCS-[MS] is comparable to the activity of NK-2 and NK-CS. The influence of the peptide on the inverse hexagonal phase transition of POPE was repeatable and the same effect as observed for NK-CS was detected. But after the addition of NKCS-[MS] to the liposomes the increase of the transition temperature was not as pronounced as it was for NK-CS.

5.2.2. Investigation of shortened analogues of NK-CS

Short fragments of NK-CS were synthesized to get information about the importance of different sections of the amino acid sequence (see table 5). NKCS-[14] equals the first half of the amino acid sequence of NK-CS, NKCS-[15-27] the second half and NKCS-[17] includes the first seventeen amino acids of the original sequence. For the peptide NKCS-[20K] the sequence includes the first twenty amino acids and an additional lysine was inserted, while NKCS-[RKK] is identical to NKCS-[20K] except for the first three amino acids, that are missing in the sequence of the peptide NKCS-[RKK]. A more detailed description of the peptides was given in chapter four.

Antibacterial and hemolytic activity

The short NK-CS fragments NKCS-[14], NKCS-[17], NKCS-[15-27], NKCS-[20K] and NKCS-[RKK] were tested for antimicrobial activity against *E. coli* and hemolytic activity. The resulting MICs are listed in table 7. NKCS-[14] exhibits a MIC of 2,5µM, which is equivalent to the MIC of NK-2. If the sequence is then prolonged by three

amino acids (NKCS-[17]) the activity stays at the same level, and shows that the first amino acids are important for the antibacterial activity. For NKCS-[20K] the activity is increased to a MIC of 1,25 μ M, and thus a better activity as shown for NK-2 was obtained. Compared to NKCS-[14] and NKCS-[17], the net charge of the peptide NKCS-[20K] was increased (see table 6). This shows how important the positive charge of the peptide is to enable a potent interaction between the peptide and the bacteria. In contrast, the activity of NKCS-[RKK] is very weak (it shows a MIC of 10 μ M) compared to NK-CS, respectively to NK-2. The sequence was only altered by cutting out the first three amino acids (compared to NKCS-[20K]), but the antimicrobial activity dropped drastically. This stresses again the importance of the first amino acids and the positive net charge. In case of the second half of the amino acid sequence (NKCS-[15-27]) no MIC up to a peptide concentration of 10 μ M was observable (table 7 and figure 48). This underlines the importance of the beginning part of the sequence.

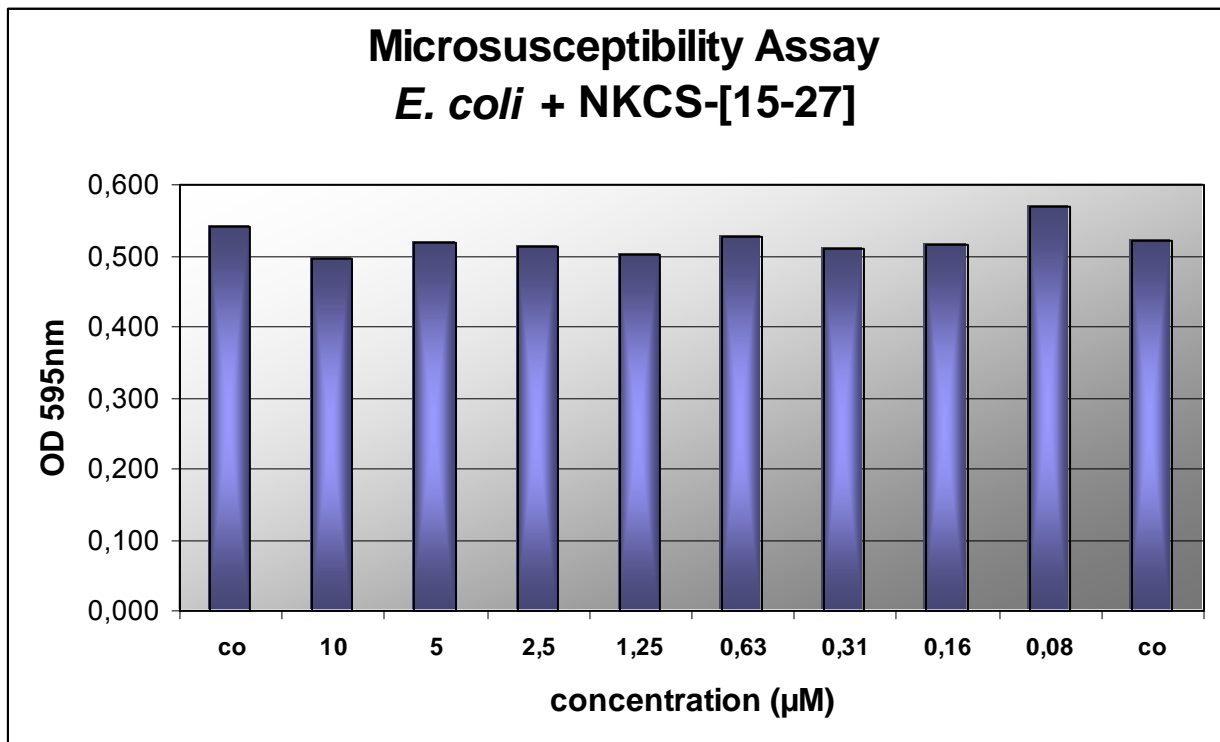


Figure 48: Antibacterial activity of NKCS-[15-27] against *Escherichia coli*.

The hemolytic activity of all tested peptides is small, at a peptide concentration of 100 μ M the lysis is still below 30 percent (figure 49). The activity at the highest concentration of the fragments NKCS-[14], NKCS-[17] and also NKCS-[RKK], with respective values of 10%, 16% and 11% lysis, stays even below the determined values for NK-CS (25% lysis) and NK-2 (27% lysis) (table 7).

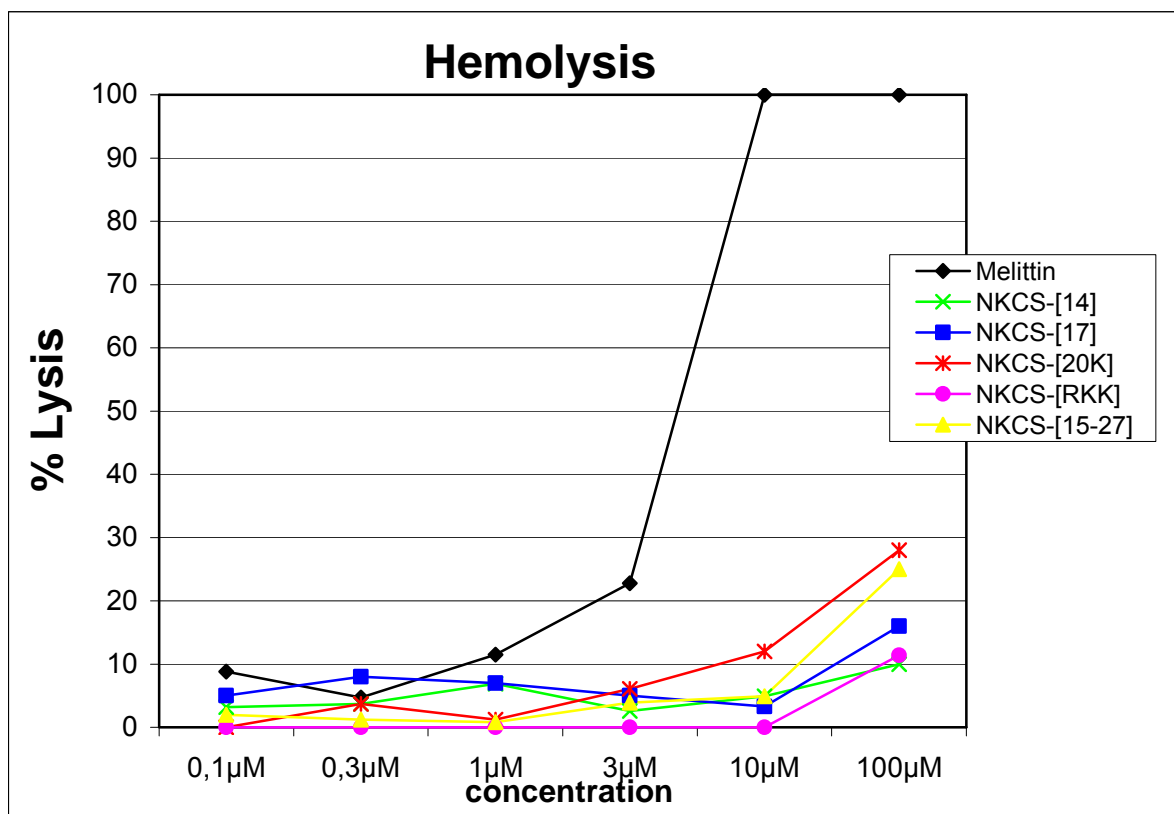


Figure 49: Hemolytic activity of NKCS-[14], NKCS-[17], NKCS-[20K], NKCS-[RKK] and NKCS-[15-27] against human erythrocytes in comparison with melittin.

Table 7: Minimal inhibitory concentrations (MICs) of NKCS fragments tested against *E. coli* and the hemolytic activity of the peptides at a concentration of 100μM.

Peptide	MIC	Lysis [%]
NKCS-[14]	2,5μM	10
NKCS-[17]	2,5μM	16
NKCS-[20K]	1,25μM	28
NKCS-[RKK]	10μM	11
NKCS-[15-27]	>10μM	25
NK-CS	0,63μM	24
NK-2	2,5μM	27

SAXS measurements for PE lipids

Except for the antibacterial inactive peptide NKCS-[15-27] and for NKCS-[RKK], which exhibited only a weak activity, the tests of the antimicrobial and hemolytic activity showed that also short NK-CS fragments are potent and selective. Since previous systematic studies showed that the influence of the peptides on the lamellar phases of phosphatidylcholine lipids and the interaction with phosphatidylglycerin lipids is negligible, only POPE – and only the inverse hexagonal phase transition – was chosen to study the structural impact of the derivatives.

POPE

The three most potent peptides NKCS-[14], NKCS-[17] and NKCS-[20K] were chosen to elucidate a possible relationship between activity and selectivity and influence on the lipid bilayer structure (figure 50). The three tested peptides (all in a molar ratio of 1000:1, respectively 300:1 for NKCS-[20K], [lipid:peptide]) exhibited a strong influence on the phase transition of POPE. Like observed for NK-CS before, the transition temperature is increased after addition of the peptides. NKCS-[14] and NKCS-[17] shift the temperature by 2°C and the longer fragment NKCS-[20K] even by 5°C (but at a higher concentration).

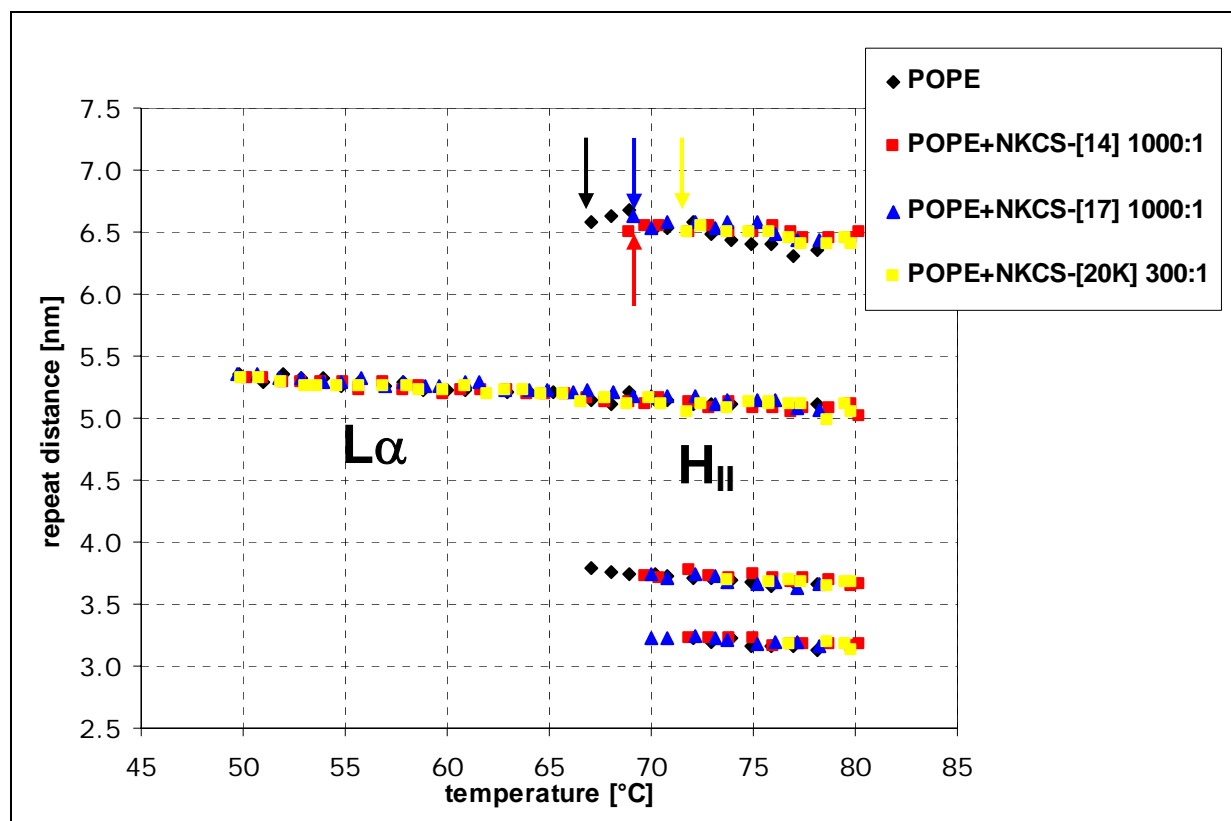


Figure 50: The repeat distance and the inverse hexagonal phase transition of POPE and after addition of the peptides measured in 10mM sodium phosphate buffer (pH7,4) in a temperature range from 50 to 80°C. The phases are indicated.

Structural investigations with Circular Dichroism

The structure of NK-2 is assumed to be equivalent to two alpha-helices of the protein NK-Lysine, which are connected by an unstructured region. CD and FTIR measurements of NK-2 proved the assumption of still resembling a α -helical structure to be right. Since the amino acid sequence of NK-CS is derived from NK-2, it was assumed, that the substitution of a single amino acid did not alter the structure and that NK-CS also still resembles a α -helix, what was proved with CD spectroscopy in the previous chapter. The CD measurements with SDS showed a more complex picture with folding intermediates. But for the two extreme conditions NK-CS behaves like NK-2: It is random coil in aqueous solutions and folds into an alpha-helix by interacting with SDS micelles.

In order to prove that also the two halves of the amino acid sequence of NK-CS, NKCS-[14] and NKCS-[15-27], fold either into a beta-sheet structure or a α -helical structure, the peptides were also investigated by circular dichroism. The peptide NKCS-[14] exhibited a random coil structure in water and in 10mM sodium phosphate buffer at different pH values (figure 51). Below the CMC value (8mM) of SDS the random coil structure of NKCS-[14] disappears and the peptide tends to fold into a beta-sheet. Above the CMC (10mM and 50mM of SDS) the interaction of the positively charged peptide with the detergent leads to the folding into an alpha-helix. The full alpha-helical structure is achieved at lower SDS concentrations as determined for NK-CS which is correlated with the number of amino acids to be folded.

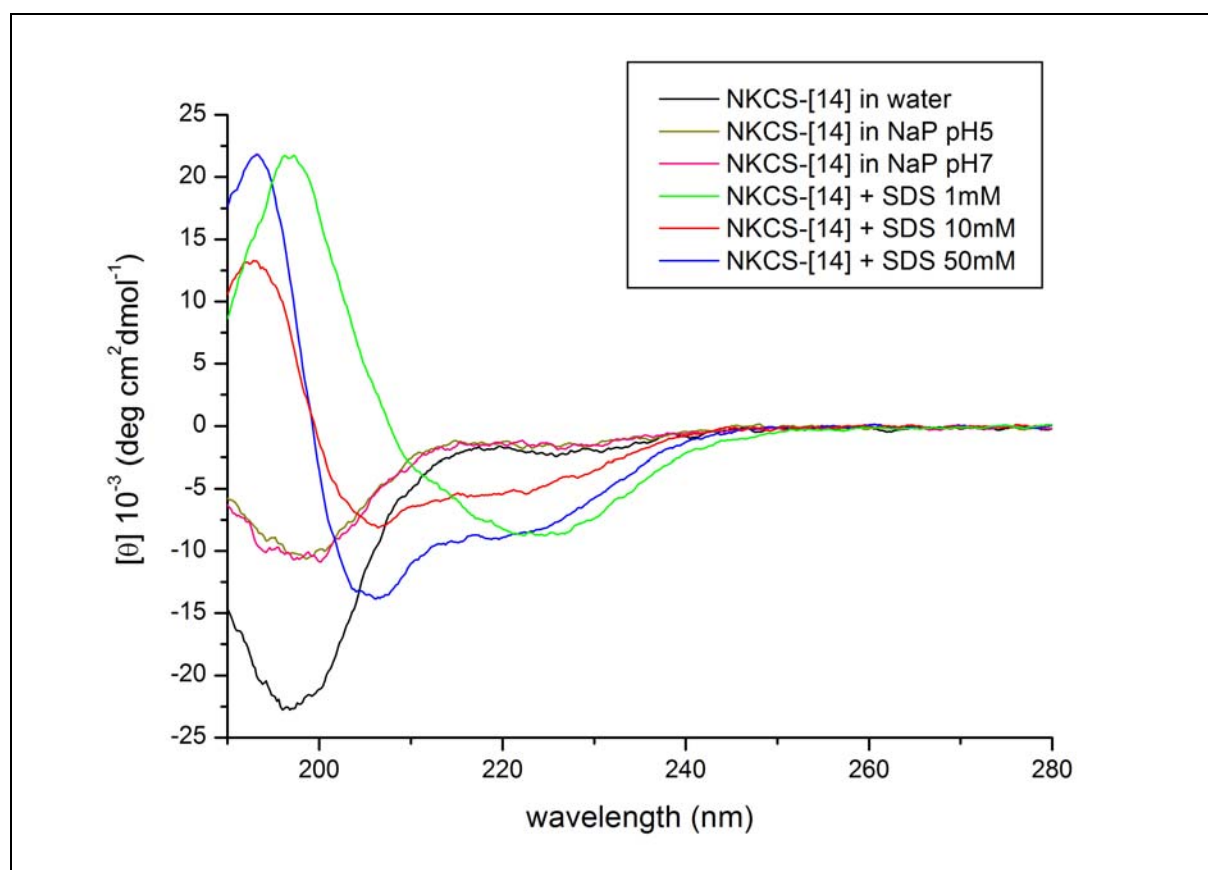


Figure 51: Circular dichroism (CD) measurements of NKCS-[14] in different aqueous solutions and after addition of SDS.

SDS is a standard surfactant for CD measurements, but still a more realistic picture is only obtained working with liposomes, although the analysis of the CD spectra is more difficult due to the bad signal to noise ratio. Therefore NKCS-[14] was mixed with POPE and POPG liposomes (figure 52). The random coil structure of the peptide is not changed in contact with zwitterionic POPE liposomes (neither if the liposomes are prepared in water nor in buffer). The interaction of the peptide with negatively charged POPG liposomes leads to a beta-sheet-like structure of the peptide. Since the signal to noise ratio is decreased significantly due to the scattering of the light by the multilamellar vesicles, especially the interpretation of the POPE interaction remains subject of future studies.

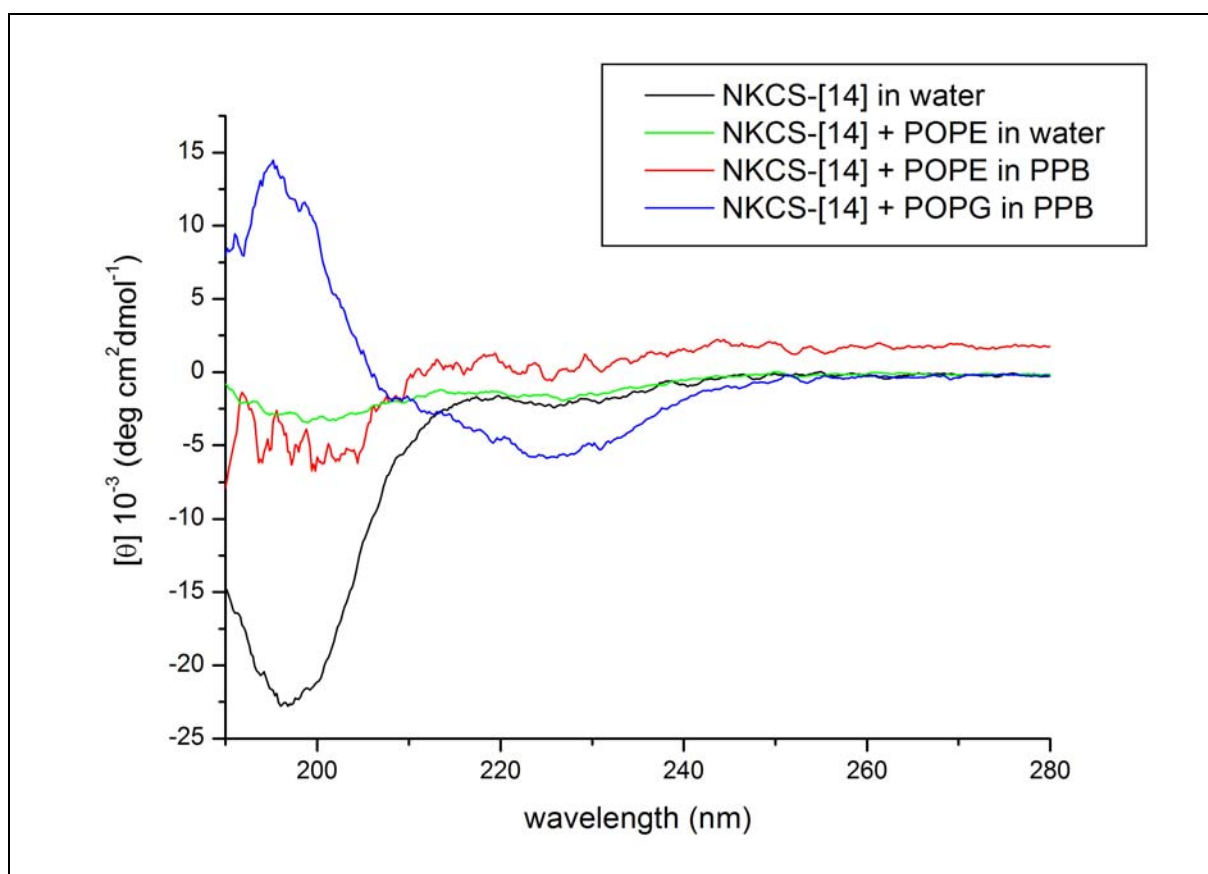


Figure 52: Circular dichroism (CD) measurements of NKCS-[14] after addition of POPE and POPG liposomes. The liposomes were prepared in water and potassium phosphate buffer pH7 (PPB).

CD measurements for NKCS-[15-27], the second helix of NKCS, showed an unfolded random coil structure in aqueous solutions (like NKCS-[14]) (figure 53). After addition of SDS below the CMC, the structure changes and tends again to fold into a beta-sheet. The structure changes again after addition of SDS above the CMC. In a mixture with higher concentration of SDS (10mM and 50mM) the peptide tends to fold into an alpha-helix, but the structure is not very well defined. As observed for the previous investigated peptides, also here the electrostatically driven interaction of the peptide with SDS micelles leads to the arrangement of a helical-like folding. As described above for NKCS-[14], the random coil structure of NKCS-[15-27] does not change in contact to POPE liposomes (figure 54). But interestingly, NKCS-[15-27] tends to fold into an alpha-helix by interacting with the charged liposomes of POPG.

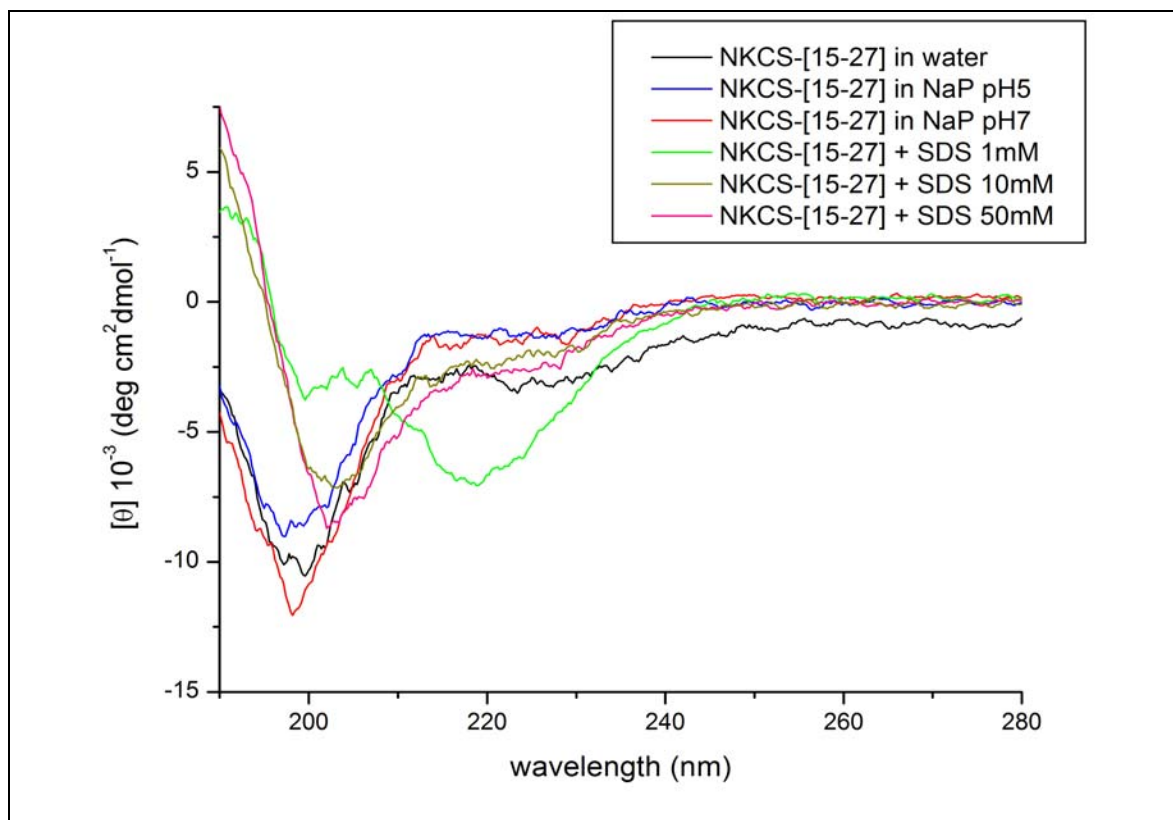


Figure 53: Circular dichroism (CD) measurements of NKCS-[15-27] in different aqueous solutions and after addition of SDS.

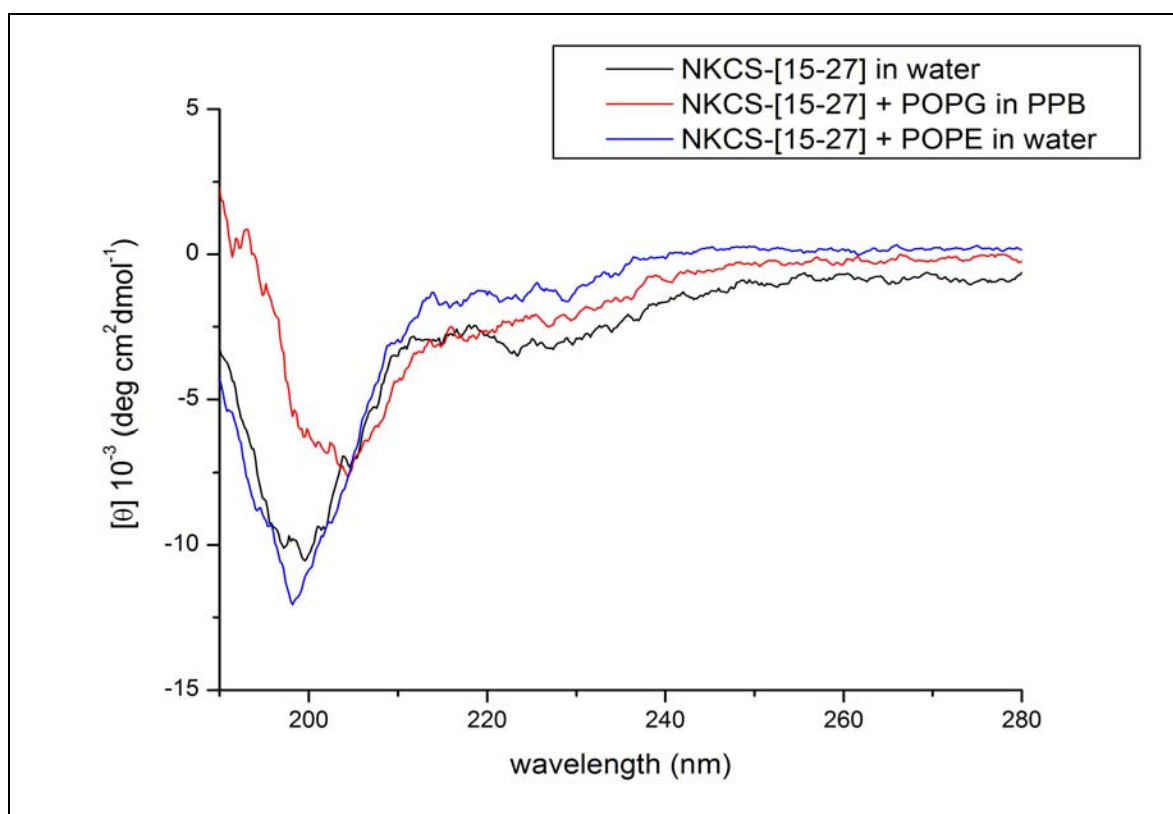


Figure 54: Circular dichroism (CD) measurements of NKCS-[15-27] after addition of POPE and POPG liposomes. The liposomes were prepared in water and kalium phosphate buffer pH7 (KBP).

The structures of NKCS-[14] and NKCS-[15-27] are both random coil in aqueous solutions and after addition of the zwitterionic POPE. The structure changes by interacting with negatively charged SDS and POPG, below the CMC of SDS the folding into a beta-sheet is promoted, above the CMC alpha-helical structure is the favorite folding. A comparison of the data found for NKCS-[14] and NKCS-[15-27] with the data for NK-CS is given in table 9.

Summary

The five shortened analogues of NK-CS were synthesized to investigate the importance of distinct parts of the original sequence of NK-CS. The antibacterial activity was not improved by cutting the sequence, but it is obvious that the first amino acids of the NK-CS sequence play a pivotal role in the killing of *E. coli* bacteria. The second half of NK-CS showed no activity within the range of the test and also the peptide NKCS-[RKK] exhibit only a weak antibacterial activity. From the structural aspect, the two halves of NK-CS, NKCS-[14] and NKCS-[15-27], were found to fold with an intermediate beta-sheet into an alpha-helical structure when interacting with negatively charged SDS, as it was also observed for NK-CS. The interaction of three shortened analogues showed the same effect on the phase transition of POPE. Again the inverse hexagonal phase transition temperature was increased, but not as pronounced as it was for NK-CS.

5.2.3. Results for peptides with modifications in the possible unstructured region

Assuming that NK-CS is structured in two alpha helices with a short unstructured linker region, this hypothesis was tested by inducing modifications within the unstructured region. This region could play a pivotal role in the alignment of the peptide and was therefore changed by substituting one amino acid (phe¹⁴ by arginine for NKCS-[FR] and lys¹⁵ by proline for NKCS-[LP]), and by an additional excision in this region of the amino acids phenylalanine (NKCS-[LP26]). For NKCS-[FR] the amino acid phenylalanine was also factored out to investigate the influence of the highly hydrophobic amino acid on the function of the peptide. The introduced amino acid proline (in NKCS-[LP] and NKCS-[LP26]) is known to disturb the structure of proteins due to its cyclic and very rigid conformation.

Antibacterial and hemolytic activity

The results for the antimicrobial assays are listed in table 8. For NKCS-[FR] a high activity (MIC of 1,25µM) against *Escherichia coli* was found, but the substitution of proline leads to weaker activities. A MIC of 2,5µM for NKCS-[LP] and of 5µM for NKCS-[LP26] was observed. The three peptides were also tested against human red blood cells (figure 55), to control the selectivity observed for NK-2, NK-CS and the former modifications of NK-CS. The hemolytic activity of NKCS-[FR] is comparable to the activity of NK-CS. For NKCS-[LP26] the rate of hemolysis is even weaker and stays below 10 percent of lysis at a concentration of 100µM. Contrary, the peptide NKCS-[LP] exhibits the strongest hemolytic activity of all tested peptides so far and lysis 45 percent of the erythrocytes at 100µM. The amino acid composition of a phenylalanine and a proline within the unstructured region leads to higher activity

against human blood cells, or decreases the ability to distinguish between different cell types. A summary of the determined MICs and hemolytic activities of the three peptides is given in table 8.

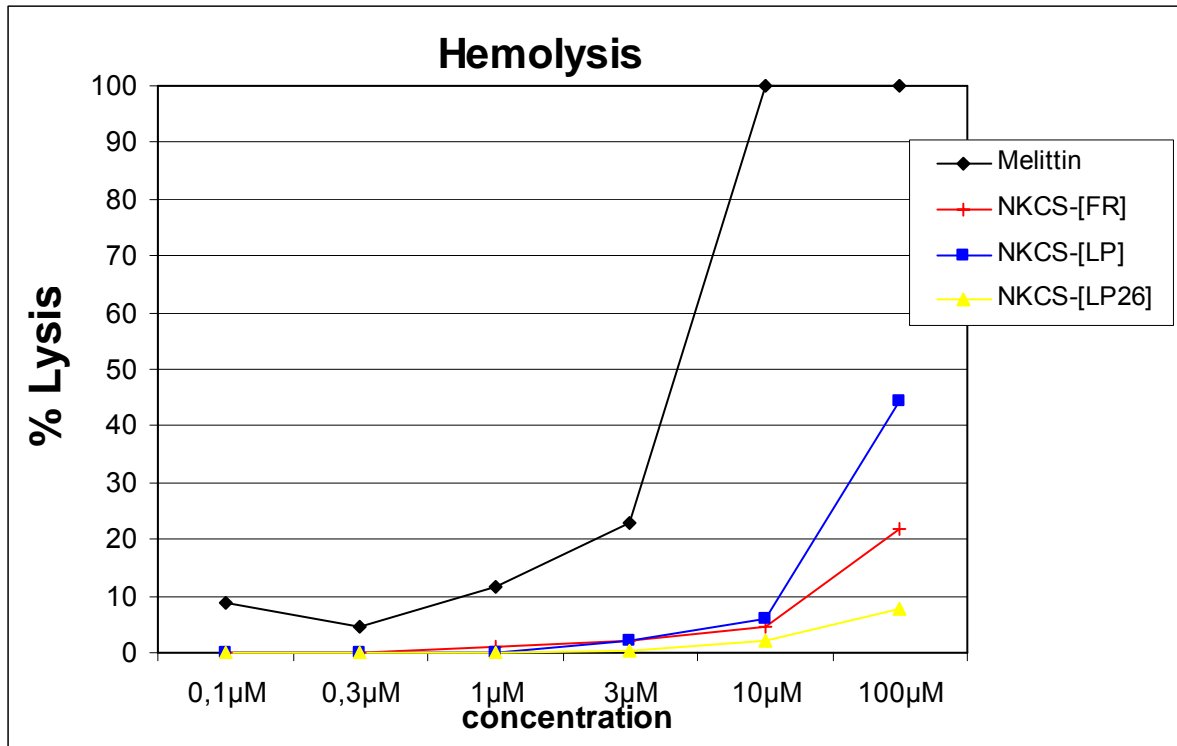


Figure 55: Hemolytic activity of NKCS-[FR], NKCS-[LP] and NKCS-[LP26] against human erythrocytes in comparison with melittin.

Table 8: Minimal inhibitory concentrations (MICs) of the peptides tested against *E. coli* and the hemolytic activity at a concentration of 100µM.

Peptide	MIC	Lysis [%]
NKCS-[FR]	1,25µM	22
NKCS-[LP]	2,5µM	45
NKCS-[LP26]	5µM	8
NK-CS	0,63µM	24
NK-2	2,5µM	27

SAXS measurements for PE lipids

POPE

The influence of the two more active peptides of this section NKCS-[FR] and NKCS-[LP] on the phase transition of POPE liposomes was investigated (figure 56). Again, the influence of the peptides on the pre-transition from the gel to the liquid crystalline phase is negligible (data not shown). The repeat distance of the lamellar phase of POPE is also not altered after addition of the peptides. But furthermore, the SAXS measurements showed the same effect as described for NK-CS and all other modifications thereof. NKCS-[FR] and NKCS-[LP] both increased the phase transition temperature of POPE by 5%, respectively 6% and also the lamellar phase of POPE is prolonged after addition of the peptides up to the final temperature of 80°C.

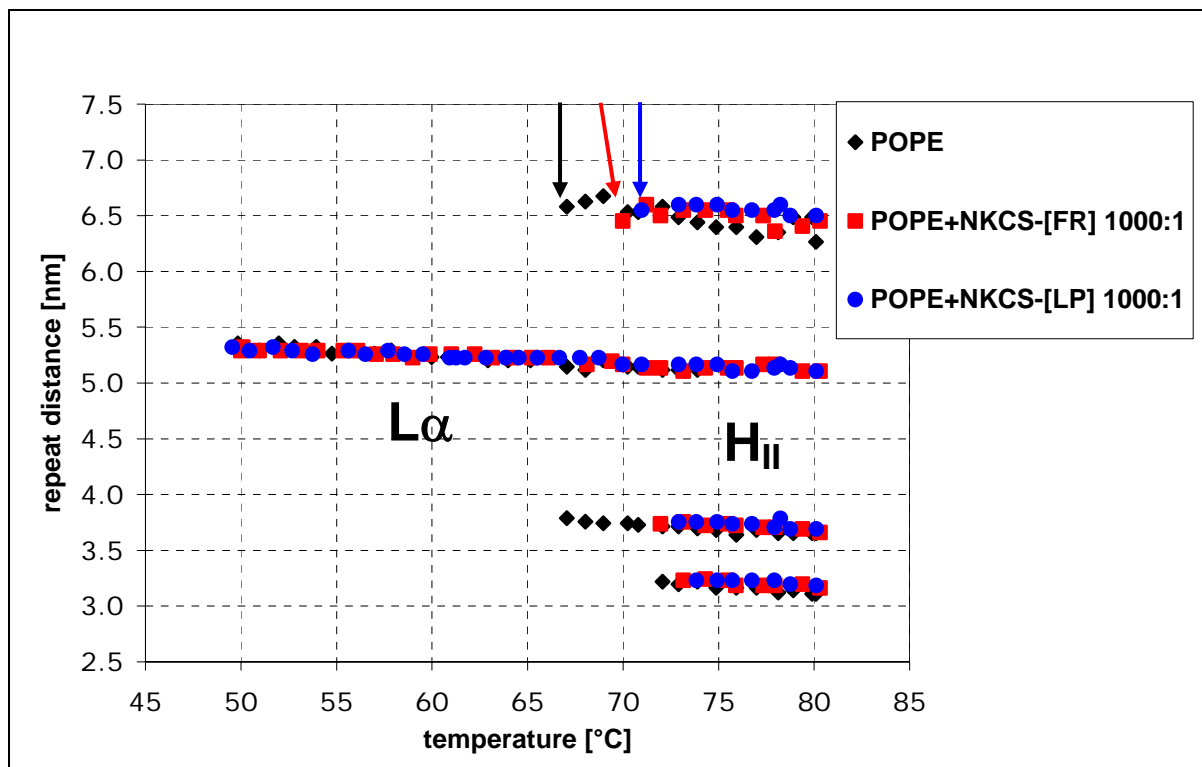


Figure 56: The repeat distance and the inverse hexagonal phase transition of POPE and after addition of NKCS-[FR] and NKCS-[LP] measured in 10mM sodium phosphate buffer (pH7,4) in a temperature range from 50 to 80°C. The phases and transition temperatures are indicated.

Summary

In this section the results for three modifications of NK-CS were presented. By replacing the strong hydrophobic amino acid phenylalanine by an arginine within the unstructured middle region of NK-CS, the antibacterial activity of the peptide dropped just one concentration step and is until now the second best value (also found for NKCS-[20K], and the hemolytic activity is comparable to the hemolysis found for NK-CS. The replacement of the second amino acid leucine in the middle region by proline, the MIC against *E. coli* dropped by two concentration steps compared to NK-CS, and interestingly the hemolytic activity increased by more than 100% compared with NKCS-[FR]. Hemolysis was decreased significantly when the amino acid phenylalanine was additionally excised for the peptide NKCS-[LP26], here the weakest interaction with erythrocytes for all tested peptides was found; but the antibacterial activity dropped even more (the MIC was found at 2,5µM). Finally, the

peptides NKCS-[FR] and NKCS-[LP] increased both the phase transition temperature of POPE liposomes again. Still the peptide NK-CS showed the strongest effect on the transition temperature of all peptides.

5.3. NKCS-[AA] – predicted by computational biology

For the peptide NKCS-[AA] the addition of two alanine amino acids into the sequence of NK-CS was suggested by modelling. This should increase the amphipathicity of the peptide to gain a better antimicrobial activity.

Antibacterial and hemolytic activity

The antimicrobial activity of the peptide was tested against *Escherichia coli*, and due to the good activity of the new peptide also against the Gram positive *Staphylococcus carnosus* and *Bacillus subtilis* (figure 57). The minimal inhibitory concentration against *E. coli* bacteria is reached for NKCS-[AA] at 1,25 μ M, which equals an activity between NK-2 and NK-CS. The same finding is true for the MIC against *S. carnosus*; here a concentration of 2,5 μ M of NKCS-[AA] is sufficient to destroy the bacteria. In case of *B. subtilis* a concentration dependent effect is found, leading to a drastic decrease in bacteria viability at 5 μ M, but 100% cell death is only achieved for a concentration of 10 μ M of the peptide (figure 57).

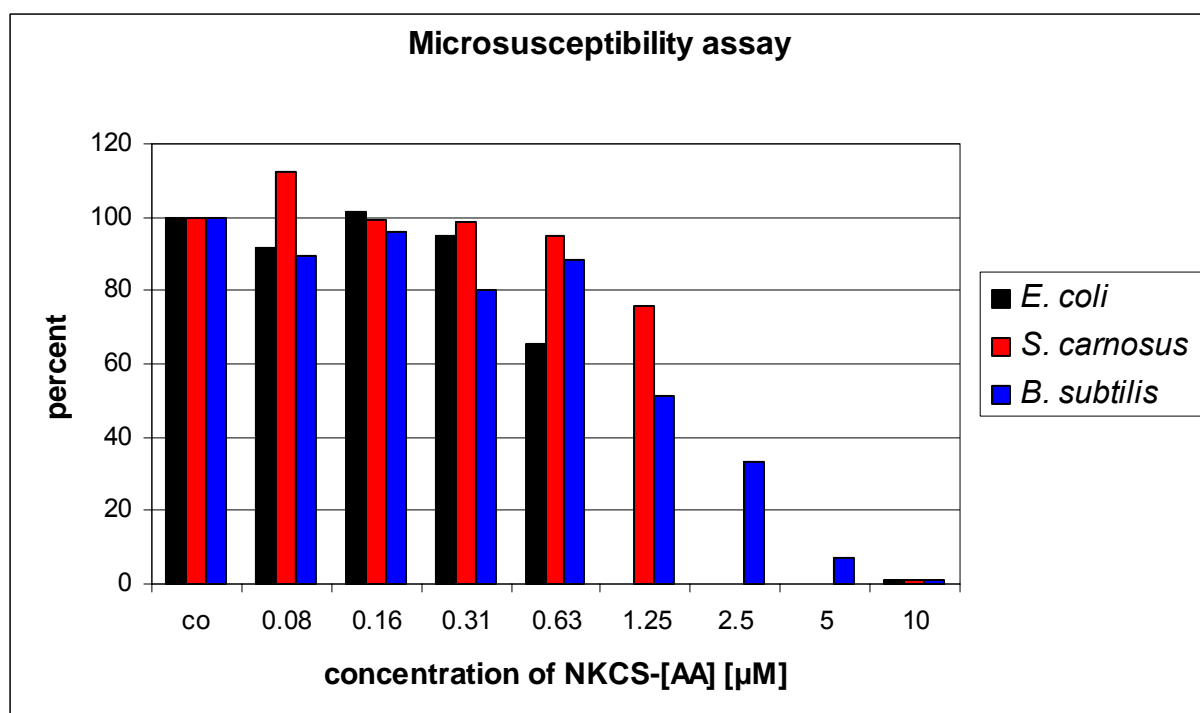


Figure 57: Antibacterial activity of NKCS-[AA] against *E. coli*, *S. carnosus* and *B. subtilis*.

The hemolysis of NKCS-[AA] is significant: 38.9% of the erythrocytes at 100 μ M, which is a higher value than observed for NK-CS and the modifications thereof (except for NKCS-[LP]) (figure 58).

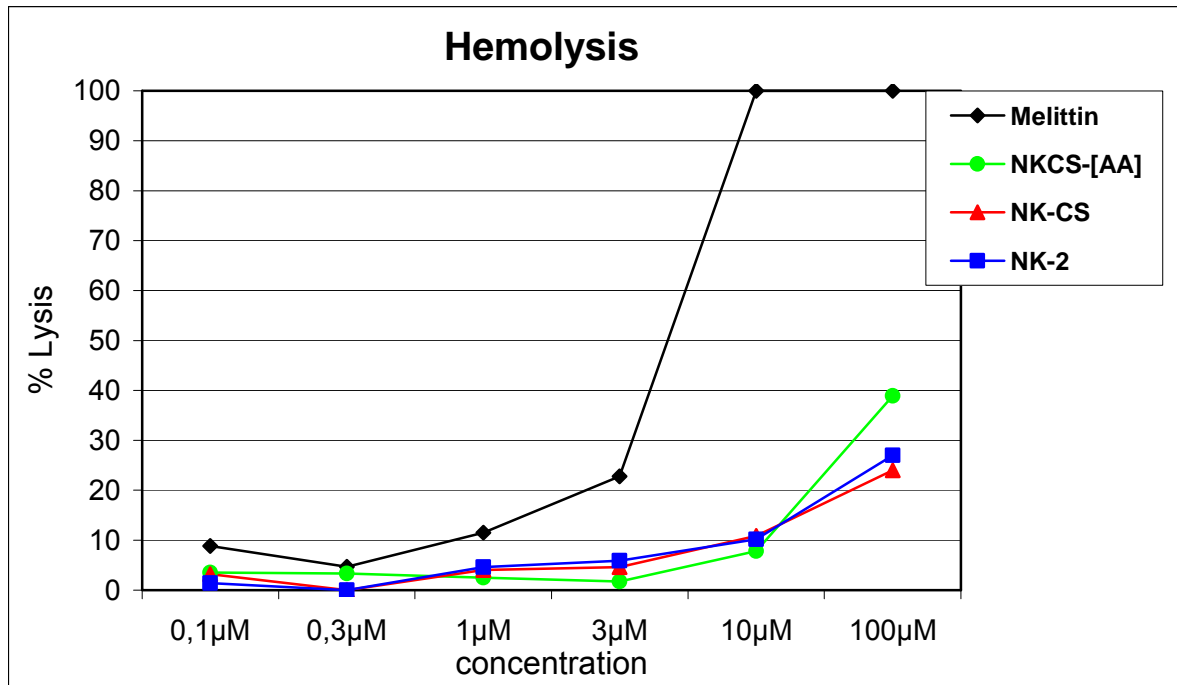


Figure 58: Hemolytic activity of NKCS-[AA] against human erythrocytes in comparison with NK-CS, NK-2 and melittin.

SAXS measurements for PE lipids

The interaction of NKCS-[AA] with phosphatidylethanolamine increases in a concentration dependent manner the transition temperature of POPE, while the repeat distance and the lamellar phase of POPE is not influenced (figure 59). At the highest peptide concentration of 100:1 [lipid:peptide] the transition temperature is increased by 9°C to 76°C (that is a shift of 13%) and the hexagonal phase of POPE is not fully reached.

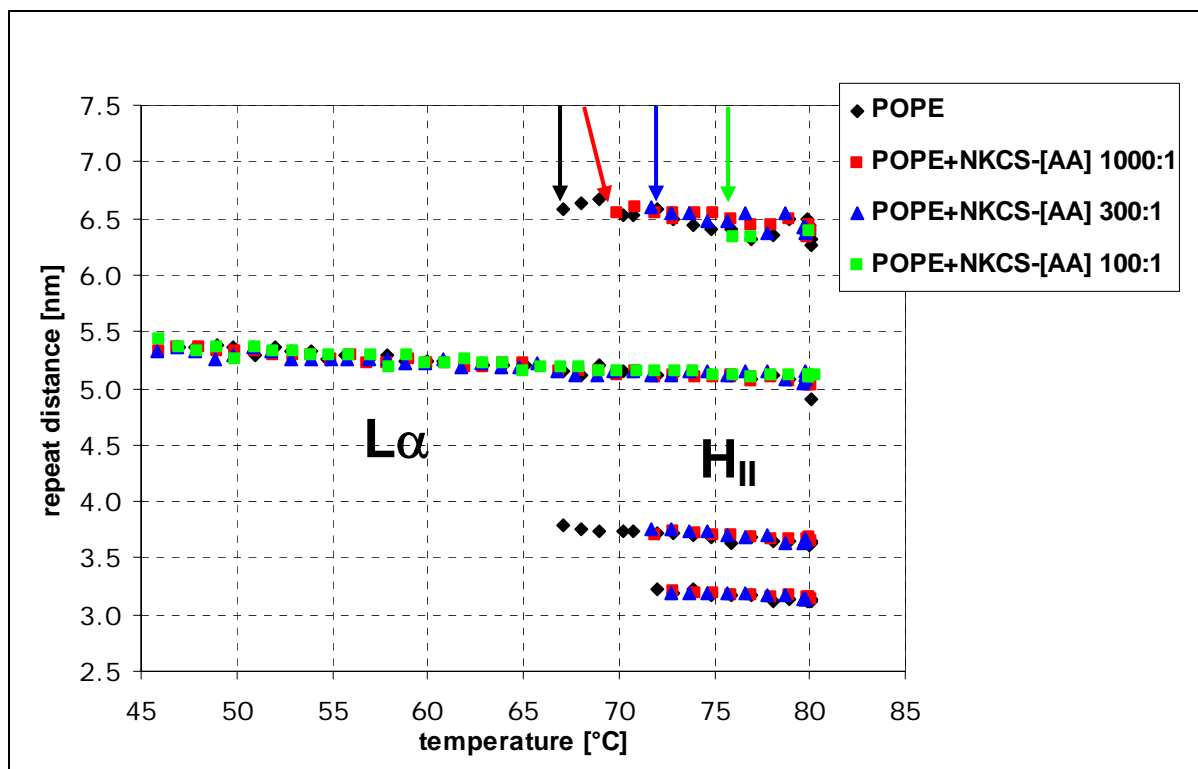


Figure 59: The repeat distance and the inverse hexagonal phase transition of POPE and after addition of NKCS-[AA] measured in 10mM sodium phosphate buffer (pH7,4) in a temperature range from 45 to 80°C. The phases are indicated.

Structural investigations with Circular Dichroism

The computer model suggests that the addition of two alanines in the middle of the peptide NK-CS will lead to an improved α -helical structure comparable to those of magainins. This was tested; and the changes in the structure of NKCS-[AA] were determined by CD measurements (figures 60 and 61). As reported for NKCS-[14] and NKCS-[15-27], also the peptide NKCS-[AA] has a random coil conformation if it is solved in water or sodium phosphate buffer (figure 60). In further measurements the structure of NKCS-[AA] was found to be alpha-helical after addition of SDS. At a concentration of 1mM SDS there is an interaction of the peptide with the detergent and the conformation of NKCS-[AA] changes and tends to be an alpha-helix. Above the CMC of SDS (10mM and 50mM) the typical CD spectrum for an alpha-helix can be observed. The alpha-helix is comparable to the helix found for NK-CS after addition of high concentrations of SDS, but it is more obvious for NKCS-[AA] than for the fragments NKCS-[14] and NKCS-[15-27].

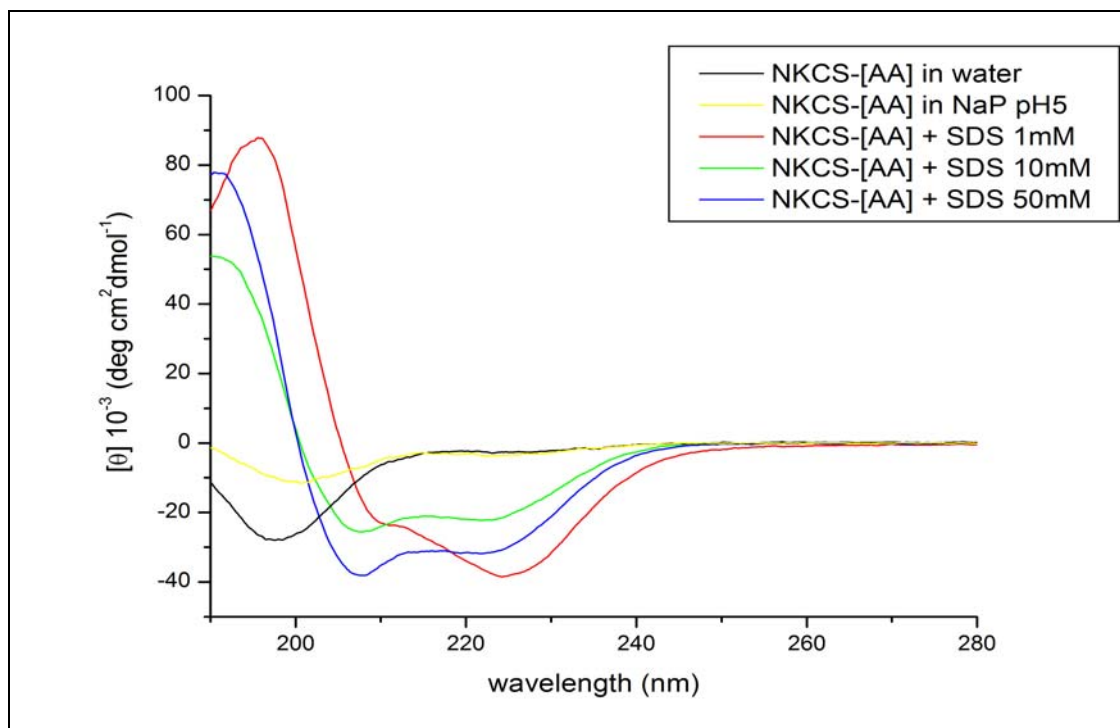


Figure 60: Circular dichroism (CD) measurements of NKCS-[AA] in ddH₂O and sodium phosphate buffer (pH5) and after addition of SDS.

Also in contact of vesicles of the zwitterionic lipid POPE the conformation of NKCS-[AA] changes (figure 61). Here the confirmation is starting to fold into a partial β -sheet (as reported for NKCS-[15-27] with high concentrations of SDS). A more detailed comparison between the CD measurements for the different peptides is given in table 9.

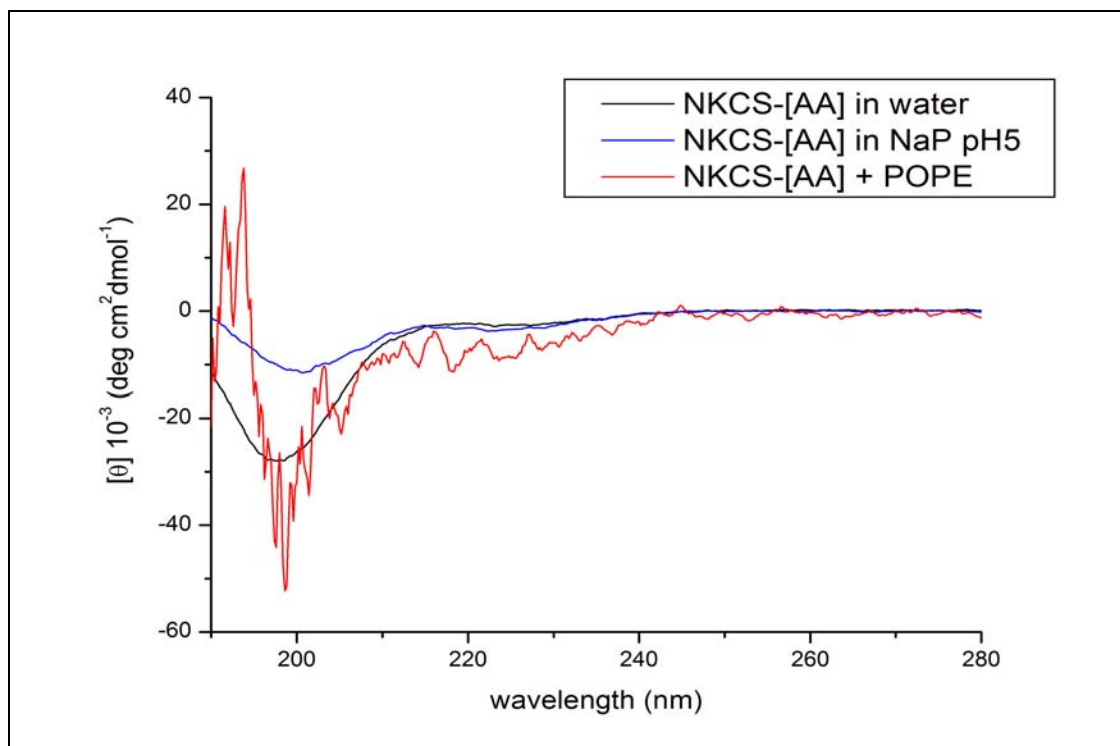


Figure 61: Circular dichroism (CD) measurements of NKCS-[AA] after addition of POPE liposomes. The liposomes were prepared in potassium phosphate buffer at pH7.

Table 9: Secondary structures of the peptides in various solutions. PPB is 10mM potassium phosphate buffer and NaP is 10mM sodiumphosphate buffer.

Peptide	Solvent	Molar ratio [peptide:solvent]	Structure
NK-CS	water	-	random coil
	PPB pH7	-	random coil
	SDS 1mM	1:17	beta-sheet
	SDS 10mM	1:167	beta-sheet
	SDS 50mM	1:854	alpha-helix
	SDS 100mM	1:1667	alpha-helix
NKCS-[14]	water	-	random coil
	NaP pH5	-	random coil
	NaP pH7	-	random coil
	POPE (water)	1:100	random coil
	POPE (PPB pH5)	1:17	random coil
	POPG (PPB pH7)	1:17	beta-sheet
	SDS 1mM	1:17	beta-sheet
	SDS 10mM	1:167	alpha-helix
	SDS 50mM	1:854	alpha-helix
	NKCS-[15-27]	water	-
NaP pH5		-	random coil
NaP pH7		-	random coil
SDS 1mM		1:17	(weak) beta-sheet
SDS 10mM		1:167	random coil (with a weak folding)
SDS 50mM		1:854	random coil (with a weak folding)
POPE (water)		1:100	random coil
POPG (PPB pH7)		1:17	random coil (with a weak folding)
SDS 50mM		1:854	alpha-helix
POPE (water)		1:100	random coil (with a weak folding)

Continuation of table 9.

NKCS-[AA]	water	-	random coil
	NaP pH5	-	random coil
	SDS 1mM	1:17	beta-sheet
	SDS 10mM	1:167	alpha-helix
	SDS 50mM	1:854	alpha-helix
	POPE (water)	1:100	random coil (with a weak folding)

Summary

The synthesis of the peptide NKCS-[AA] was based on computational modeling. The insertion of two alanines into the sequence of NK-CS was predicted to stabilize a more rod-like alpha-helical structure of the peptide. CD measurements showed a random coil structure in water and buffer solutions, and a complicated folded via a beta-sheet intermediate to an alpha-helical structure at higher concentrations of SDS micelles, what was also found for NK-CS before. The antibacterial activity of NKCS-[AA] was determined with a MIC at 1,25 μ M, which equals the values found for NKCS-[20K] and NKCS-[FR]; but for this peptide the hemolytic activity is higher than measured for NK-CS and most of the other modifications thereof (except for NKCS-[LP]). The interaction of this interesting peptide with POPE liposomes was also investigated; the former results for NK-CS and the modifications of this peptide were repeatable for NKCS-[AA]. Here the effect on the inverse hexagonal phase transition was very strong, the temperature was shifted by 13,4% after addition of the peptide and is the second strongest impact on the phase transition of the lipid (after NK-CS).

5.4. Peptidomimetics

In this work I concentrated on the investigation of one compound (LA-03-149), which was synthesized in the group of Gregory N. Tew at University of Massachusetts, Amherst, USA. LA-03-149 is a small oligomeric molecule with a MW of 595 Da; a more detailed description of the peptidomimetic was given in the materials and methods chapter before. More results found for this peptidomimetic with different techniques and the results for another oligomeric compound were published in Arnt, L., Rennie, J.R., Linser, S., Willumeit, R. and Tew, G.N. J. Phys. Chem. B, 2006.

Antibacterial and hemolytic activity

The peptidomimetic LA-03-149 was tested against *Escherichia coli* bacteria and a concentration of 1,25 μ M of the substance was necessary to inhibit the total bacteria growth. This value corresponds to the MIC found for a different strain of *E. coli* bacteria (D 31); here 0,8 μ g/ml of LA-03-149 was necessary, which equals a

concentration of 1,34 μ M (Arnt, L. et al, J. Phys. Chem. B, 2006). This activity is the same activity found for NKCS-[AA], but is not as good as the activity of NK-CS.

Furthermore, the selectivity of the molecule was tested against human erythrocytes like for antimicrobial peptides before (figure 62). The lysis at a concentration of 100 μ M was 33% for LA-03-149, which is a higher value as detected for NK-CS (24% lysis at this concentration), but the hemolytic activity is not as high as determined before for NKCS-[AA] (39% lysis). The group of Gregory N. Tew found a hemolytic value of 75 μ g/ml for LA-03-149, at which 50% of the erythrocytes were lysed (Arnt, L. et al, J. Phys. Chem. B, 2006). That equals a concentration of 126 μ M and fits also into the results found for LA-03-149.

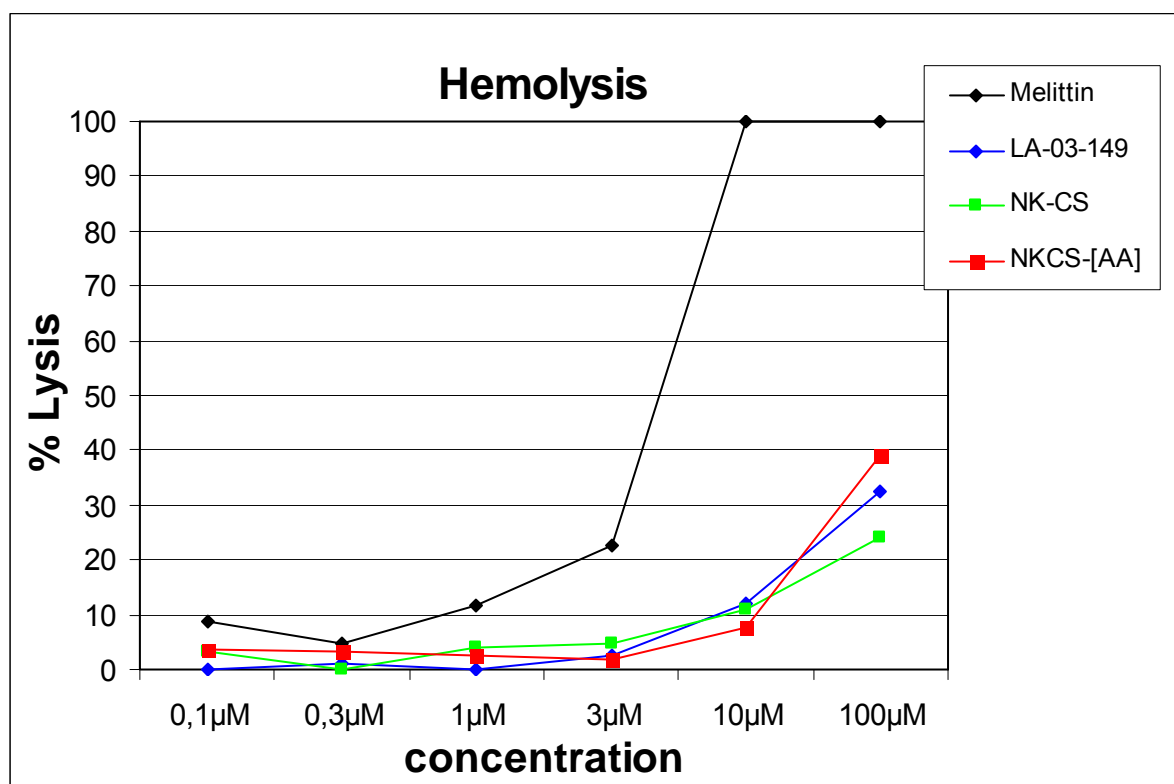


Figure 62: Hemolytic activity of LA-03-149 against human erythrocytes in comparison with NK-CS, NKCS-[AA] and melittin.

SAXS measurements for PE lipids

The previous tests showed that the peptidomimetic LA-03-149 is a potent imitation of an antimicrobial peptide, with a good activity against bacteria and also a good selectivity. Therefore, the molecule was investigated by SAXS measurements. The focus here was again put on phosphatidylethanolamine lipids in order to compare the influence of LA-03-149 with the previous results found for the peptides. Before the measurements, LA-03-149 dissolved in DMSO and then diluted in double distilled water, to minimize the influence of the solvent. For the lipids POPE and DOPE-trans the control measurements with lipid and DMSO showed no significant influence of the solvent (data not shown). Contrarily, during the measurements of DiPOPE a slightly influence of DMSO was obvious (figure 65). A difference in the phase transition

temperatures of the pure lipids compared to the previous measurements is probably due to the addition of sodium chloride to the buffer (with a final concentration of 90mM, respectively 130mM).

POPE

The influence of the peptidomimetic LA-03-149 on the gel to the liquid crystalline phase transition is again negligible as it was for the antibacterial peptides. Furthermore, the repeat distance of the multilayers is not altered after addition of the substance. But a significant change of the inverse hexagonal phase transition is visible. LA-03-149 decreases the transition temperature at high concentrations of the peptidomimetic (figure 63). The transition for pure POPE starts at 70°C, is increased by 1°C at a peptidomimetic concentration of 3000:1 [lipid:LA-03-149] and stays at 70°C at 1000:1 [lipid:LA-03-149]. At higher concentrations of LA-03-149 the transition temperature is decreased significantly. By 1°C at a molar ratio of 300:1 [lipid: LA-03-149] and by 3°C at 100:1 [lipid: LA-03-149], that equals a maximum decrease of 4%.

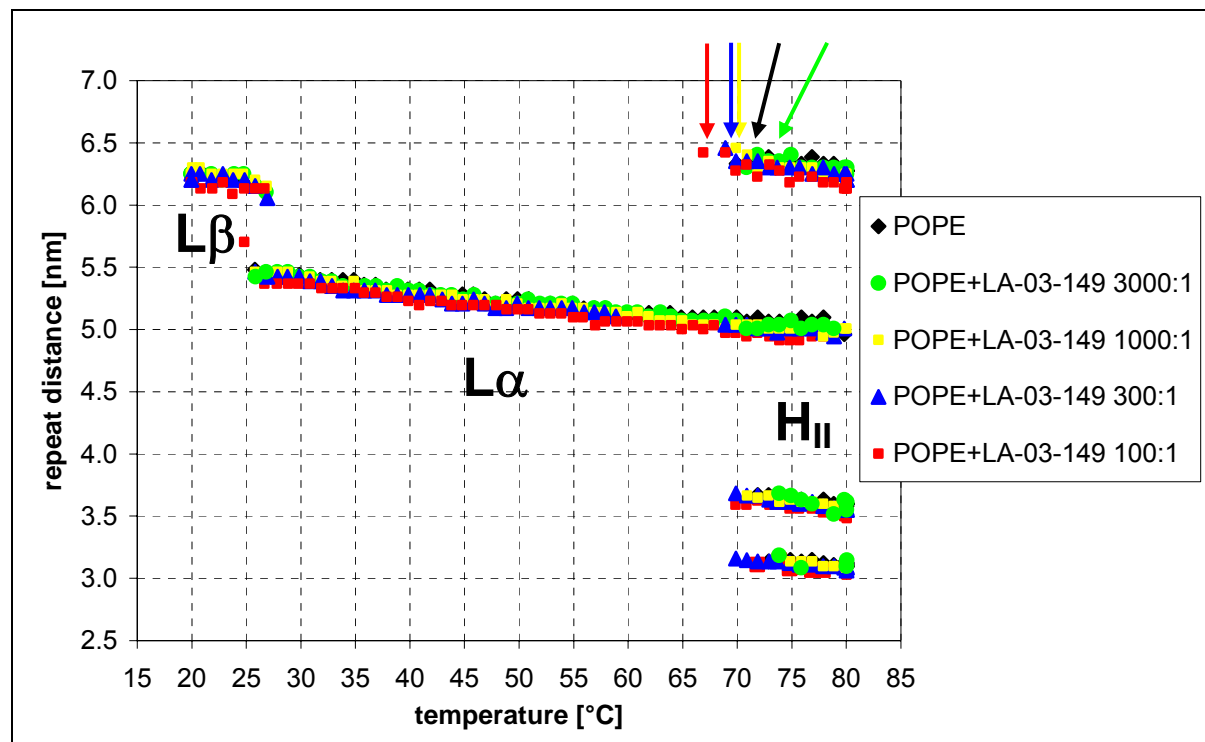


Figure 63: The repeat distance and the phase transitions of POPE and after addition of the peptidomimetic LA-03-149 measured in 10mM sodium phosphate buffer plus 130mM sodium chloride (pH6,8) in a temperature range from 20 to 80°C. The phases are indicated and the transition temperatures are marked with arrows.

This effect was also found for the peptide NK-2 before, but stays in contrast with the influence of NK-CS and the modifications thereof. In order to repeat the experiment with PE lipids and to investigate the influence of the acyl chain composition, the SAXS measurements were also done with DOPE-trans and DiPOPE liposomes.

DOPE-trans

Figure 64 shows the influence of LA-03-149 on DOPE-trans liposomes. The pre-transition at 36°C is not changed and also the RD of this lipid is not affected by LA-03-149, as it was observed for POPE before. But again the inverse hexagonal phase transition is influenced. The temperature for pure DOPE-trans starts at 66°C, is then increased by 1°C at the lowest concentration of LA-03-149, and at higher concentrations of the peptidomimetic decreased in a concentration dependent manner. At a molar ratio of 1000:1 [lipid:LA-03-149] by 1°C and at the highest concentration 100:1 [lipid:LA-03-149] by 4°C. The maximum decrease of the temperature for DOPE-trans is 6% and thus even more pronounced as calculated for POPE. Contrarily to the influence of NK-CS and the modification thereof the lamellar phase of DOPE-trans is not prolonged after addition of the peptidomimetic.

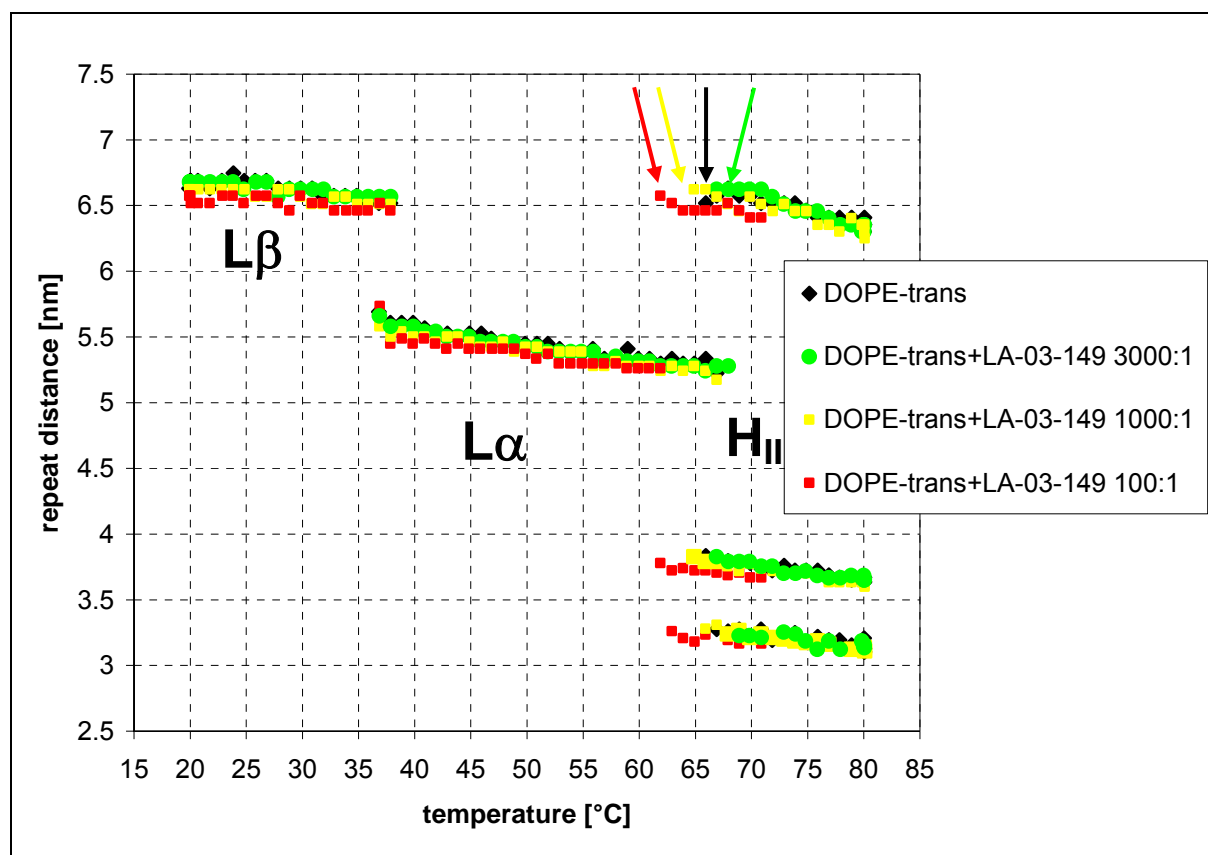


Figure 64: The repeat distance and the phase transitions of DOPE-trans and after addition of LA-03-149 measured in 10mM sodium phosphate buffer plus 90mM sodium chloride (pH7) in a temperature range from 20 to 80°C, respectively from 20 to 71°C for a lipid:LA-03-149 ratio of 100:1.

DiPOPE

The third lipid tested with the peptidomimetic LA-03-149 was DiPOPE (figure 65). The acyl chains are shorter compared with POPE and DOPE-trans and the inverse hexagonal phase transition temperature is lower for this lipid; it was determined at 58°C. The focus was put on this transition, because the former measurements showed that the influence of LA-03-149 on the pre-transition and the lamellar phase is not significant. From figure 67 it is obvious, that the solvent DMSO also has an effect on this phase transition. The transition temperature is decreased by 2°C. At a peptidomimetic concentration of 300:1 [lipid:LA-03-149] the temperature is lowered by only 1°C, and is negligible due to the influence of the solvent alone. But

nonetheless, at the highest peptidomimetic concentration of 100:1 [lipid:LA-03-149] the transition temperature is significantly changed, with a decrease of 6°C. The calculated influence of LA-03-149 at this concentration is then 10%, but as to be handled with care in order to the effect of DMSO. Furthermore, as mentioned above for DOPE-trans also for DiPOPE the lamellar phase is not prolonged and changed after addition of LA-03-149.

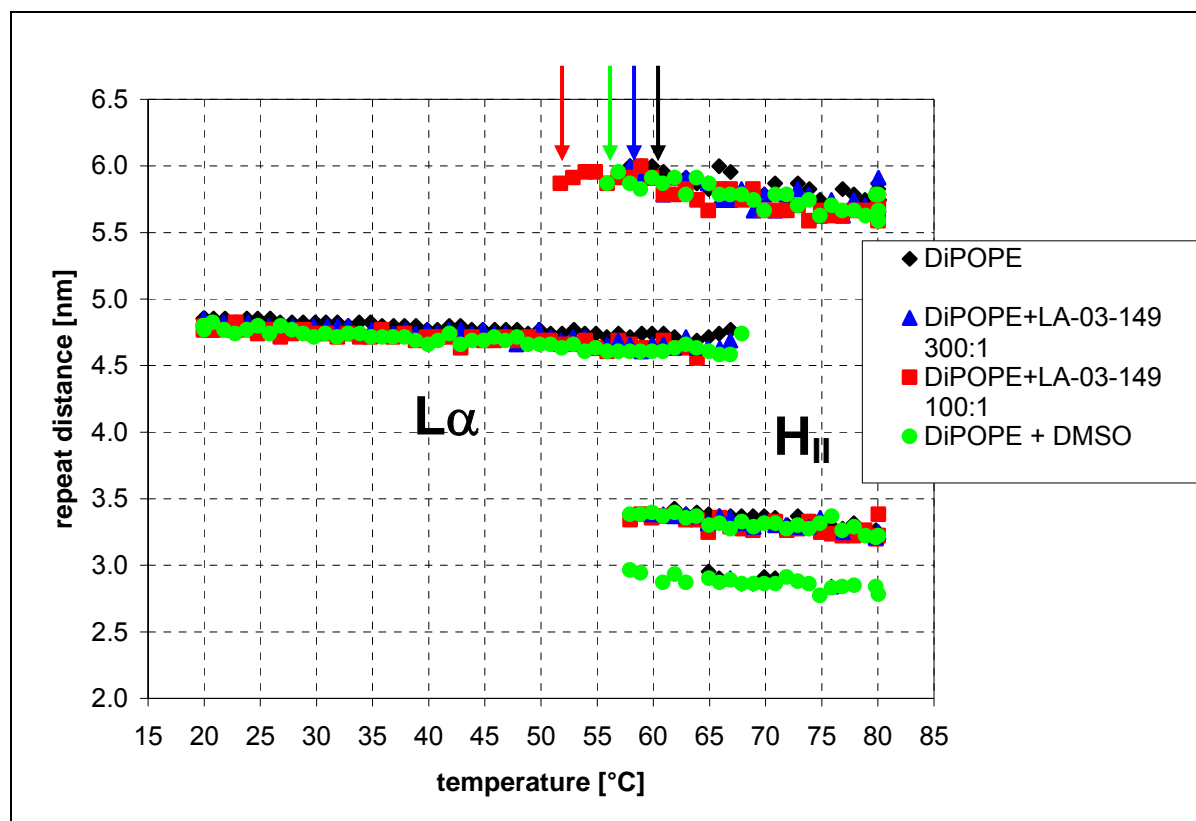


Figure 65: The repeat distance and the inverse hexagonal phase transition of DiPOPE and after addition of LA-03-149 measured in 10mM sodium phosphate buffer plus 90mM sodium chloride (pH7) in a temperature range from 20 to 80°C. The phases and transition temperatures are indicated.

Summary

To summarize the results found for the peptidomimetic LA-03-149, it can be concluded that the peptidomimetic is a good antibacterial molecule (MIC of 1,25 μ M) with potent properties (weak hemolysis) to imitate an antimicrobial peptide. The influence on PE lipids is comparable to the effect found for NK-2, and shows by decreasing the inverse hexagonal phase transition temperature the opposite effect as detected for NK-CS and the modifications thereof. Interestingly, there is a correlation between the transition temperature of the pure lipids and the influence of the peptidomimetic: The lower the transition temperature is, the more pronounced is the effect of LA-03-149.

5.5. Summary of peptide parameters

Table 10: Comparison of the peptides' antimicrobial and hemolytic activity at 100µM peptide concentration.

PEPTIDE	MIC [µM]	Lysis [%]
NK-2	2.5	27
<i>Reactive amino acids substitution</i>		
NK-CS	0.63	24
NKCS-[MS]	2.5	27
<i>Short fragments</i>		
NKCS-[14]	2.5	10
NKCS-[17]	2.5	16
NKCS-[20K]	1.25	28
NKCS-[RKK]	10	11
NKCS-[15-27]	>10	25
<i>Changes in the middle region</i>		
NKCS-[FR]	1.25	22
NKCS-[LP]	2.5	45
NKCS-[LP26]	5	8
<i>Modelled peptide</i>		
NKCS-[AA]	1.25	39
<i>Peptidomimetic</i>		
LA-03-149	1.25	33
<i>Control peptides</i>		
Magainin-II-amid	2.5	27
Melittin	2.5	100

Table 11: The maximal influence of the peptides and LA-03-149 on the L_{α}/H_{II} transition temperatures of PE lipids.

Lipid	Peptide/LA-03-149	Lipid/peptide (LA-03-149) concentration	Maximal influence [%]	comment
POPE	NK-2	1:100	5.6	decrease
POPE	LA-03-149	1:100	4.3	decrease
POPE	NK-CS	1:300	14.9	increase
POPE	NKCS-[MS]	1:1000	4.5	increase
POPE	NKCS-[14]	1:1000	3.0	increase
POPE	NKCS-[17]	1:1000	3.0	increase
POPE	NKCS-[20K]	1:300	7.5	increase
POPE	NKCS-[FR]	1:1000	4.5	increase
POPE	NKCS-[LP]	1:1000	6.0	increase
POPE	NKCS-[AA]	1:100	13.4	increase
POPE	Magainin-II	1:300	3.0	increase
POPE	Melittin	1:1000	0	no effect
DOPE-trans	NK-CS	1:100	10.7	increase
DOPE-trans	LA-03-149	1:100	6.1	decrease
DiPOPE	NK-CS	1:300	9.5	increase
DiPOPE	LA-03-149	1:300	10.3	decrease

6. Discussion

The aim of this work was to develop new antibacterial peptides based on the antibacterial peptide NK-2 and to understand their mechanism of interaction with model membranes. Eleven new peptides were synthesized and characterized (figure 66). From this data a probable mechanism of membrane disruption is suggested.

In order to get a better understanding about the mechanism of antibacterial peptides and their interaction with membranes, the development of new peptides was thought to answer seven important questions: (i) how important are the reactive amino acids cysteine and methionine within the sequence? (ii) which influence has the positive charge of the peptides? (iii) how strong is the impact of the hydrophobicity? (iv) how important is the alpha-helical structure of the peptides? (v) which role plays the assumed unstructured region in the middle of the peptide sequences? (vi) is it possible to predict the sequence of a very potent antibacterial peptide by computational modelling (vii) can small synthetic substances without any relation to naturally occurring peptides mimic the properties of antibacterial peptides?

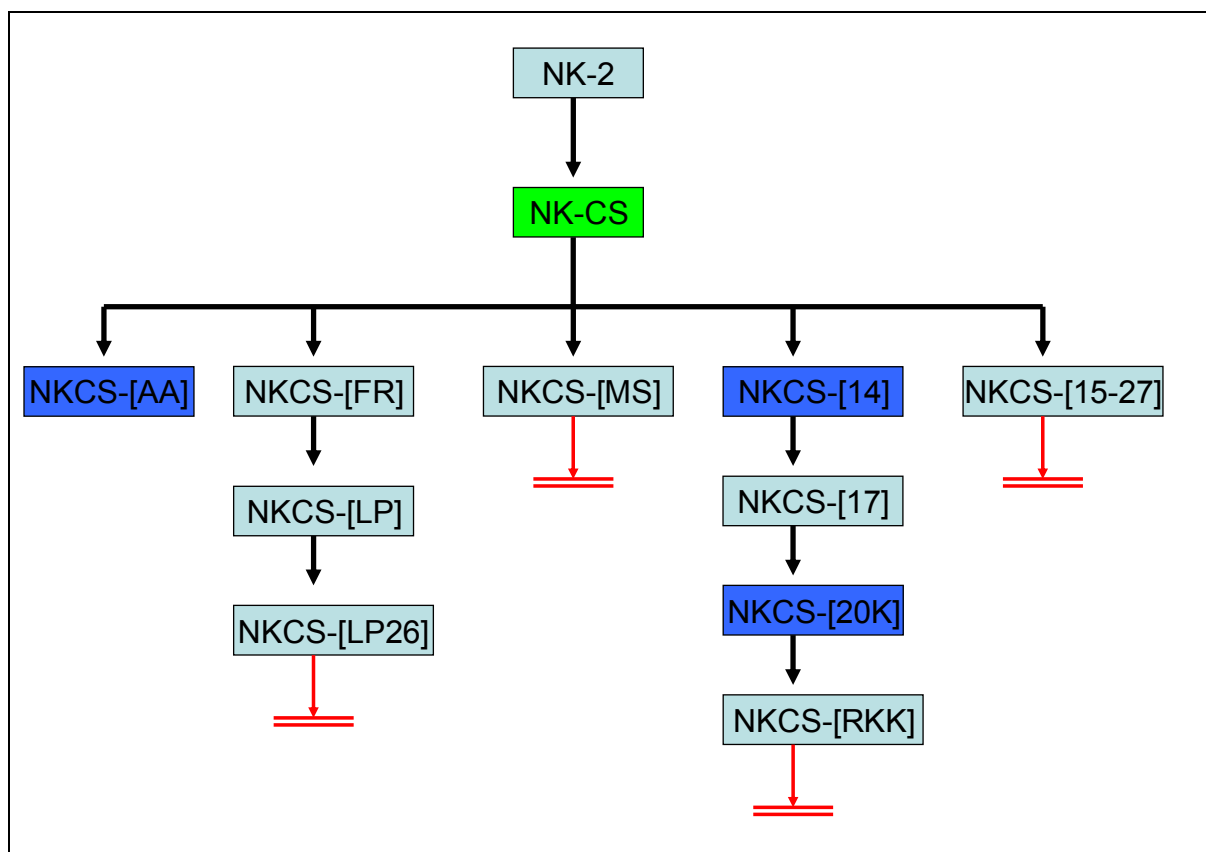


Figure 66: Schematic picture of peptide development. The most potent antibacterial peptide is marked in green, while the dark blue marked peptides are good candidates for further investigations and modifications. The red arrows mark dead ends of the development, where the activity of the peptides is decreased significantly and further developments are not reasonable.

Reactive amino acids

The replacement of the amino acid cysteine had a direct impact on the antibacterial activity. NK-CS was found to be significantly more active against Gram negative and Gram positive bacteria compared to NK-2. The replacement of cysteine for NK-CS resulted also in a change in the mode of action, which was also true for all modified peptides tested. Contrary to NK-2, for the new peptides a promotion of a positive membrane curvature was found. The change of the interaction with phosphatidylethanolamines must be due to the substitution of the amino acid cysteine. The dimerisation of NK-2 monomers will certainly decrease the activity of this peptide, but this is a time dependent effect and is not true for new peptide powder. Nonetheless, the cysteine is located on the first half of the peptide and is directed into the 'small pocket' that is build by the assumed unstructured region in the middle of the sequence (figure 67), and an interaction of the amino acid with a cysteine from different monomers or with amino acids in the sequence during the attraction and alignment to the membrane cannot be excluded.

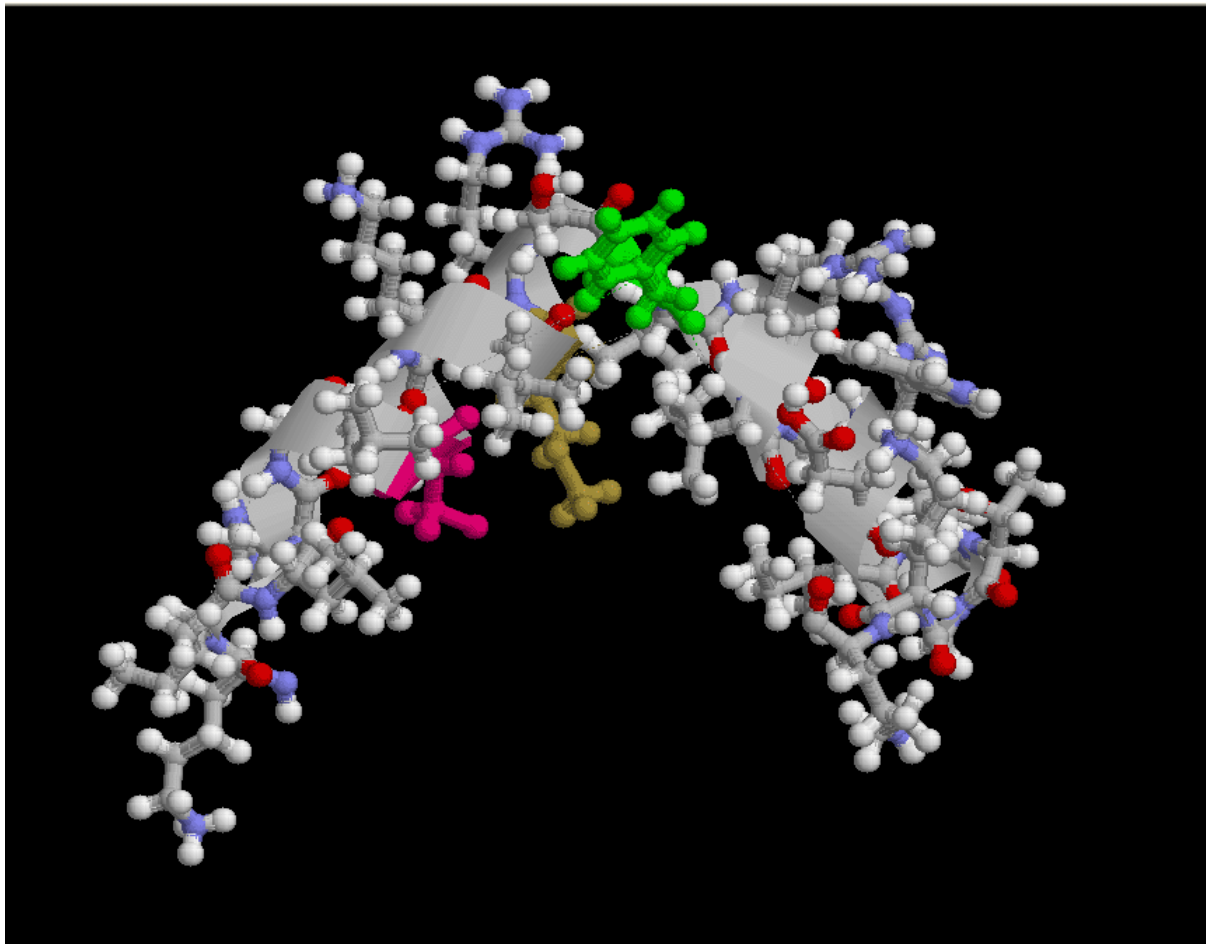


Figure 67: Secondary structure of NK-2. Prepared with the software RasMol. The amino acid cysteine is marked in magenta, the methionine in brown and the hydrophobic amino acid phenylalanine in green.

The substitution of methionine, which is also located in the middle region, decreased the antibacterial activity of the peptide. This amino acid is necessary for the optimal activity of the peptide indicating an interaction of methionine with amino acids within the sequence stabilizing the optimal structure of the peptide.

Charge

To investigate the influence of the charge of the peptide short fragments were developed. Due to the electrostatic interaction of cationic peptides with negatively charged lipids, it is not surprising that the charge is one important feature of antibacterial peptides. The negative charge of the head group of POPG and also of POPE, which was found to be negatively charged by Zeta-potential measurements (Willumeit, R. et al. BBA. 2005) and also reported before (Casals, E. et al. Chem. Phys. Lipids 2003) is one hint to explain the selectivity of the peptides. These lipids are more prominent in bacterial membranes, respectively for POPG absent in the membranes of erythrocytes.

Looking into the detailed distribution of the charges one can assume that the more equal the charges are distributed the better is the parallel alignment with respect to the membrane surface. For NKCS-[14] the charged amino acids are evenly distributed in the sequence (positions 1, 4, 8, 9 and 12) and the electrostatic interaction leads to a rather parallel orientation to the membrane surface. The activity for this small peptide is as good as the activity of NK-2 and furthermore the hemolytic activity is very low. A prolongation of the sequence of NKCS-[14] by three amino acids leads to an increase of the charge (again with a good distribution over the sequence), but the interaction is still not as strong as observed for NK-CS. But NKCS-[17] exhibited a very good selectivity and a good antibacterial activity compared to NK-2. If the sequence of NKCS-[17] is now prolonged again by three amino acids plus an additional lysine (NKCS-[20K]), the net charge of +9 is now close to the charge of the whole peptide sequence. Here the charge is again evenly spread over the sequence (positions 1, 4, 8, 9, 12, 16, 17, 20 and 21). The activity against bacteria is better compared to NK-CS, but not as good as observed for NK-CS. For the peptide NKCS-[RKK] the first three amino acids were excised, otherwise it equals the peptide NKCS-[20K]. The net charge has dropped by one. The second half of the whole sequence (NKCS-[15-27]) was inactive against bacteria. Although the level of charge is comparable to the first half, the distribution is rather unequal (positions 2, 3, 6, 12 and 13). The electrostatic attraction is basically due to an interaction with the beginning and the end of the sequence; the peptide is not parallel aligned and this could be a hint that the conversion into a helix is disturbed, leading to a lower activity. By increasing the net charge of NK-CS by one charged amino acid, the antibacterial activity was not increased. NKCS-[FR] exhibited nonetheless a better antibacterial activity than NK-2. From literature it is known that cationic peptides exhibit an electrostatic interaction with negatively charged lipids (Hancock, R.E.W. et al. Adv. Microb. Physiol. 1995 and Wu, M. and Hancock, R.E.W. J. Biol. Chem. 1999). This importance of the electrostatic attraction to the membrane was also found for cecropins (Wang, W. et al. J. Biol. Chem. 1998) and for defensins (Hristova, K. et al. J. Biol. Chem. 1997).

Hydrophobicity

The helical wheel diagrams in figure 68 demonstrate the amphipathicity of the molecules; although the wheel is **not** a structural picture of the sequence but instead the allocation of the charged and hydrophobic amino acids is demonstrated. The hydropathy analysis is based upon and incorporates principles of membrane protein stability (White, S.H. and Wimley, W.C. Annu. Rev. Biophys. Biomolec. Struct. 1999) and for the calculation of the hydrophobic moment the experiment-based Wimley-White whole-residue hydrophobicity scales are used in the plots. The octanol scale

used to draw the helical wheels measures a residue's free energy of transfer from water to the bilayer hydrocarbon core. From the figure it is obvious that both peptides have a distinct spatial charge on one side (marked by the blue balls in the picture), while the hydrophobic amino acids are more prominent on the opposite, with the strong hydrophobic amino acid phenylalanine in the centre. This amphipathic structure suggests a good hydrophobic and electrostatic interaction with membranes; where the random coil folded peptides start to fold into an alpha-helix in contact with cationic side of the peptide and subsequently a possible interaction with the (now structured) hydrophobic side starts.

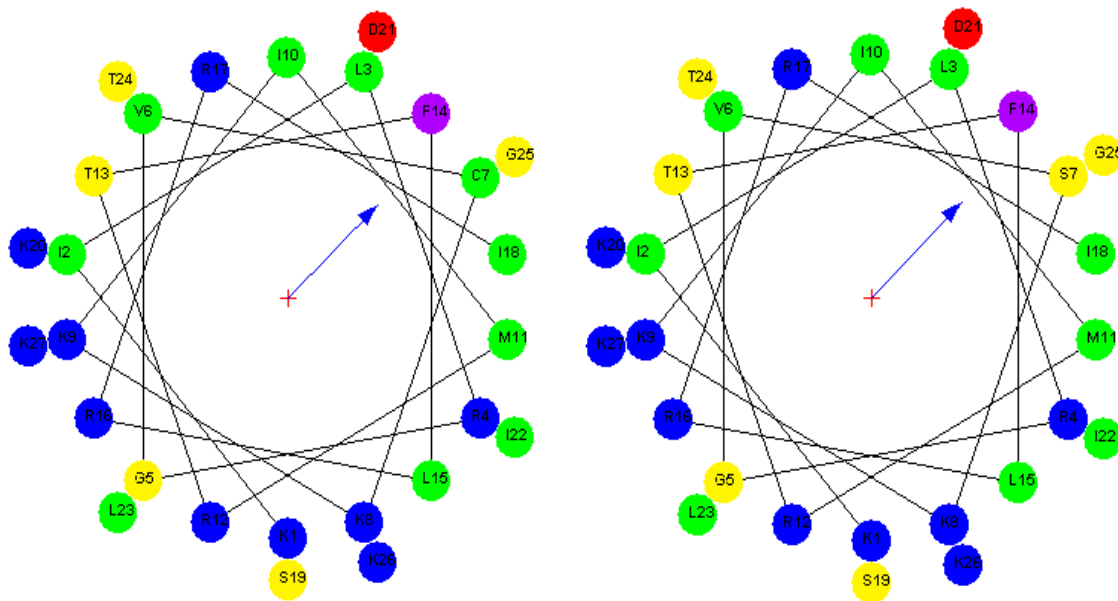


Figure 68: Helical wheel diagrams of NK-2 (left) and NK-CS (right) calculated resembling the octanol scale. The wheels were drawn with the software MPEX3.0 from Stephen Whites laboratory at the University of California, USA. Red balls are negatively charged amino acids, blue balls are positively charged and yellow balls are neutral amino acids. Green balls represent hydrophobic amino acids and the violet ball stands for strong hydrophobic residues and the hydrophobic moment is indicated by the blue arrows.

The amphipathicity of the helix is resulting in a hydrophobic moment, which is directed to the hydrophobic acyl chains of the membrane (indicated by the arrows in figure 68). The difference between NK-2 and NK-CS is, like mentioned above, marginal. The neutral amino acid serine of NK-CS is part of the hydrophobic side of the structure, but the hydrophobicity is only slightly decreased resulting in a slightly decreased hydrophobic moment.

The substitution of the amino acid phenylalanine by arginine implicated a loss in hydrophobicity of the peptide NKCS-[FR]; phenylalanine is a highly hydrophobic amino acid and it is reported that the aromatic ring within the amino acid structure is responsible for an interaction of peptides with membranes (Alberts, B. et al. 1994). Also for NK-2 it was shown that after the substitution of the phenylalanine in order to introduce a tryptophan for the measurements the amino acid was buried inside of the membrane (Schröder-Borm, H. BBA. 2003). The activity of NKCS-[FR] is slightly reduced compared with NK-CS, indicating that the phenylalanine is involved in the mechanism by which NK-CS kills bacteria.

A correlation between the charge and the hydrophobicity was obvious for the short fragment of NK-CS. By decreasing the size of the peptide and the net charge, an increase of the hydrophobicity was determined. This leads to the assumption that the weaker electrostatic interaction of the peptides is compensated by a higher hydrophobic moment to the membranes, which helps the peptides to align on the surface.

Importance of the alpha-helical structure

NK-CS is like all other investigated peptides random coil in aqueous solutions. When interacting with negatively charged SDS micelles, an alpha-helical structure is preferred (see also figure 67). Also NK-2 was found to be highly alpha-helical which was determined by FTIR spectroscopy measurements in a deuterium oxide solution (Schröder-Borm, H. BBA. 2003) and when interacting with trifluoroethanol (as a hydrophobic environment) determined by CD measurements (Andrä, J. and Leippe, M. Med. Microbiol. Immunol. 1999). The importance of a helical structure in combination with a high hydrophobicity is demonstrated for the first half of NK-CS. These fourteen amino acids adopted an alpha-helical structure which is sufficient to promote a positive membrane curvature when interacting with model membranes.

Contrary the second half of NK-CS exhibited just a weak folding; this is probably due to the disturbed parallel alignment of NKCS-[15-27] to the membrane resulting from the unequally distributed charges in the sequence. This more or less undefined alignment of the peptide leads to a significant decrease in the antibacterial activity.

Influence of the probable unstructured region of the peptide

The assumed 'small pocket' (figure 67) of the structure is basically formed by the middle region of the sequence. For NKCS-[FR] the phenylalanine within this region was replaced by arginine. The electrostatic attraction to the membrane is probably easier for this peptide due to the increase of the charge, but either the weaker hydrophobic interaction decreases the activity compared to NK-CS or a change of this region. The hypothetical unstructured region, which interrupts the alpha-helical structure of the peptides, was also changed by introducing the amino acid proline instead of leucine into the sequence. Proline can act as a structural disruptor for alpha-helices and as a turning point in β -sheets (Lehninger, A.L. et al. 1998). The alpha-helical structure of NK-2, respectively NK-CS, is even more interrupted in the middle region by proline. The secondary structure of NKCS-[LP] is therefore possibly more rigid than the helices of NK-CS and results in a decreased antibacterial activity and interaction with phosphatidylethanolamines. For the peptide NKCS-[LP26] one amino acids in this region was completely excised and again the leucine is substituted by proline. Now the efficiency to kill bacteria dropped even more compared to NKCS-[LP].

Computational modelling

Also the computational predicted peptide NKCS-[AA] was thought to inhibit the influence of the assumed unstructured region of the sequence of NK-CS. The insertion of two amino acids (alanine) at position 14 in front of the middle region

should stabilize the alpha-helical structure of NK-CS. Here the little kink in the sequence disappeared and a rod-like helical structure, similar to the structure of magainin (Zasloff, M. PNAS. 1987), is suggested by calculation. The CD measurements showed for NKCS-[AA] a similar behaviour compared to NK-CS; the peptide converts into an alpha-helical structure upon the interaction with the negatively charged detergent SDS. If the alpha-helix of NKCS-[AA] is more linear compared to the helical structure of NK-CS, remains unclear from this measurements. The activity against bacteria was not improved compared to NK-CS, what is possibly due to the slightly decreased hydrophobicity. Still, the activity is better than observed for NK-2. Although the antibacterial activities were not improved, the predicted peptide also had a strong influence on the inverse hexagonal phase transition of phosphatidylethanolamines, suggesting further investigations of computational modelled peptides.

Peptidomimetic

The investigated peptidomimetic LA-03-149 is based on the amphipathic property of the antibacterial peptides and proofed the assumption that it is possible to mimic the effects of peptides with small molecules very well. The antibacterial activity is better compared to NK-2, but slightly worse than the value for NK-CS; weak hemolysis shows a sufficient selectivity of oligomeric substance. The influence on phosphatidylethanolamine lipids is comparable to the effect found for NK-2, and shows a decrease of the inverse hexagonal phase transition temperature. Interestingly, there is a correlation between the transition temperature of the pure lipids and the influence of the peptidomimetic: The lower the transition temperature is, the more pronounced is the effect of LA-03-149. The molecule is very small (MW 595), but the charge attracts it to the membrane. Further experiment with different phospholipid bilayers showed that the lipid head group and the concentration of lipid molecules within the bilayer have a significant impact on overall activity (Arnt, L. et al, J. Phys. Chem. B, 2006).

Probable mechanism

Before the results for the modified peptides will be discussed, an overview about the know mechanism of NK-2 will be given. It was shown that NK-2 had no influence on the zwitterionic phosphatidylcholine liposomes demonstrated by SAXS measurements. Furthermore, NK-2 did not bind to zwitterionic phosphatidylcholine monolayers (Schröder-Borm, H. BBA. 2003). This leads to the general conclusion that NK-2 does not interfere with phosphatidylcholine lipids. Surface Plasmon resonance measurements showed that the initial interaction of NK-2 is primarily an electrostatic interaction (Schröder-Borm, H. BBA. 2003). Upon closer contact, hydrophobic effects and the amphipathicity of the peptide come into play as well as the biophysical properties of the membrane lipids. SAXS in combination with DSC and FTIR showed that for phosphatidylethanolamines the membrane becomes more fluid and that a negative curvature is induced (Willumeit, R. et al. BBA. 2005). The same methods elucidated for phosphatidylglycerins a rigidification of the membrane.

The mode of NK-2 interaction was thus described in the following way: The peptide promotes a negative curvature of phosphatidylethanolamine model membranes, such an effect was also observed for other antimicrobial peptides before: gramicidin A and S (Szule, J.A. and Rand, R.P. Biophys. J. 2003 and Staudegger, E. et al.

BBA. 2000), the wasp venom mastoparan (Epand, R.M. and Vogel, H.J. BBA. 1999) and alamethicin (Angelova, A. et al. Arch. Biochem. Biophys. 2000). In phosphatidylethanolamine rich regions this curvature in combination with a different degree of fluidity for phosphatidylglycerin rich regions will induce a strong tension at the surfaces between phosphatidylethanolamine and phosphatidylglycerin moieties, which disrupts the membrane at these borderlines. We can speculate if the peptides behave detergent like at these fraction points. In conclusion the interaction of NK-2 follows in general the carpet model mechanism, but the final membrane disruption has a different mode of action (Willumeit, R. et al. BBA. 2005). Still it remained unclear how NK-2 is able to induce a negative curvature.

The attraction of NK-CS to the membrane and the hydrophobic interaction with the membrane afterwards is similar to NK-2. But contrary to the mechanism suggested for NK-2, NK-CS interacts in a different manner with the membrane after attraction, which leads to a positive membrane curvature, which resembles the physiological curvature of a biological membrane and does not automatically lead to mechanical stresses at the interfaces of phospholipid moieties. But by inhibiting the inverse hexagonal phase of phosphatidylethanolamines for example the cell division of the bacteria is also inhibited, leading to a potent bacteriostatic or antibacterial effect. The pivotal role of the impact on the curvature is proved by a direct correlation the antibacterial activity and the impact on the phase transition of phosphatidylethanolamine lipids was found (table 12). Except for NKCS-[LP] for all peptides is a linear correlation between the MIC values and the temperature shift observable. The higher the activity against bacteria, the higher is the impact on the phase transition temperature.

Table 12: Correlation between the antibacterial activity against *E. coli* and the impact on the POPE inverse hexagonal phase transition temperature (ΔT) of the tested peptides.

Peptide	MIC [μM]	ΔT [$^{\circ}\text{C}$]
NKCS	0,63	10
NKCS-[AA]	1,25	5
NKCS-[20K]	1,25	5
NKCS-[FR]	1,25	3
NKCS-[MS]	2,5	3
NKCS-[LP]	2,5	4
NKCS-[14]	2,5	2
NKCS-[17]	2,5	2
Magainin-II-amide	2,5	2

A positive curvature was also observed for several antimicrobial peptides, for example in the mechanism of the human antimicrobial peptide LL-37, which disrupts the membrane subsequently by a toroidal pore (Henzler Wildman, K.A. Biochem. 2003), for magainin (Epand, R.M. and Vogel, H.J. BBA. 1999 and Matsuzaki, K. et al. Biochem. 1998) and an analogue of magainin called MSI-78 (Hallock, K.J. et al. Biophys. J. 2003). For magainin it was suggested that the peptide is killing bacteria in a concentration dependent manner starting from the carpet model and ending by the formation of a toroidal-like pore as proposed by the Shai-Matsuzaki-Huang model (Oren, Z. and Shai, Y. Biopolymers. 1998, Matsuzaki, K. et al. BBA. 1998 and Huang, H.W. Biochem. 2000).

In regard to the questions from the beginning of the discussion, the developed peptide provided results that are capable to answer these questions:

(i) The replacement of the reactive amino acid cysteine by serine resulted in a surprisingly high increase of the antibacterial activity.

(ii) A balanced distribution of the charge is necessary for a good antibacterial activity rather than the overall charge of the peptide. The distribution of the charged amino acids is important for the parallel alignment of the peptides to the membrane surface.

(iii) Hydrophobic interactions are important for the function of the peptides. The decreased electrostatic interaction of the short peptide fragments was compensated by the increase of the hydrophobicity to gain a potent antibacterial activity.

(iv) The alpha-helical structure is necessary for the antibacterial activity of the peptides. A proper folding of the sequence could be correlated with the equal distribution of the charges within the sequence.

(v) The assumed unstructured region seems to be important for the optimal alignment of the peptide on the membrane and the subsequent antibacterial activity.

(vi) Although the antibacterial activity of the predicted peptide was not improved, the strong interaction with the membrane makes further studies reasonable.

(vii) The small molecule LA-03-149 exhibited a good antibacterial activity and proved the idea to mimic the amphipathic property of antimicrobial peptides.

7. Conclusion

The development of new antimicrobial peptides and the characterisation of their antibacterial and hemolytic activity, peptide structure and their impact on biological model membranes in order to achieve a better understanding of the structure-function relationship was the goal of this work.

The excision of the amino acid cysteine from the sequence of the basic peptide NK-2 led to a significant increase of the antibacterial activity of the peptide NK-CS and this effect was accompanied by a change in the mode of action of all modified peptides: Contrary to NK-2, the modifications of the peptide promoted a positive membrane curvature after attraction to the membrane, what must be due to the missing interaction of the amino acid cysteine. The concept of mimicking basic properties of antimicrobial peptides in order to achieve a similar biological effect was proven to be correct for the small molecule LA-03-149 which exhibits a good activity and interacts with model membranes in a peptide-comparable fashion. For all peptides a correlation between the antibacterial activity and the impact on the inverse hexagonal phase transition of phosphatidylethanolamine lipids was found.

The membrane destructive mechanism can be divided into several parts:

- (i) The cationic peptides (and also the peptidomimetic LA-03-149) are attracted to the membrane by an electrostatic interaction with negatively charged lipids.
- (ii) The peptides subsequently fold into an alpha-helix and a rearrangement of the peptides promotes the hydrophobic interactions with the membranes, which was observable for all investigated substances.
- (iii) If the concentration of the molecules is high enough, the interaction with phosphatidylethanolamines introduces a curvature in distinct parts of the membrane. Contrary to NK-2, all modified peptides promote a positive curvature.
- (iv) This positive curvature and the inhibition of the inverse hexagonal phase disturbs the cell division and probably also the function of membrane proteins, which results in the killing of bacteria or the inhibition of bacterial growth.

Beside NK-CS, also the short fragments NKCS-[14] and NKCS-[20K], which are definitely cheaper to produce and therefore easier to use for a clinical application, are good basic peptides for further modifications. Here also an application on antibacterial surfaces, where the peptides are connected to polymers is conceivable. The antibacterial effect of the peptides could inhibit bacteria biofilm production on clothing. Furthermore the coating of materials for implantations with the antibacterial peptides is feasible and would help to protect the implants from bacterial infections. The prediction of the amino acid sequence for the peptide NKCS-[AA] proved the ability of rational computational peptide design, and also the peptidomimetic offered good qualities to imitate the properties of antibacterial peptides and is a very promising basis for further modifications.

8. References

8.1. Own publications

Peer reviews

Willumeit, R., Kumpugdee, M., Funari, S.S., Lohner, K., Pozo Navas, B., Brandenburg, K., Linser, S. and Andrä, J. Structural rearrangement of model membranes by the peptide antibiotic NK-2. *Biochimica et Biophysica Acta (BBA)* 1669 (2005), 125-134

Arnt, L., Rennie, J.R., Linser, S., Willumeit, R. and Tew, G.N. Membrane Activity of Biomimetic Facially Amphiphilic Antibiotics. *Journal of Physical Chemistry Part B (J. Phys. Chem. B)* 110 (2006), 3527-3532

Talks

Linser, S., Funari, S.S. and Willumeit, R. Development Of New Antimicrobial Peptides And Their Interaction With Model Membranes. Talk, 31st FEBS congress, 24.-29.06.2006, Istanbul, Turkey

Linser, S., Kumpugdee-Vollrath, M., Funari, S.S. and Willumeit, R. The structure of phosphatidylethanolamine model membranes is Influenced by antimicrobial peptides. Workshop 'Biophysics of Membrane-Permeabilising and Membrane-Translocating Peptides', 13.-16.04. 2005, Berlin, Germany

Linser, S. Interactions of antibiotic peptides with model membranes. MPI für Polymerforschung, 05.07.-09.07.2004, Mainz, Germany

Linser, S., Pozo Navas, B., Andrä, J., Kumpugdee, M., Funari, S.S., Lohner, K. and Willumeit, R. The influence of NK-2 on the inverted hexagonal phase transition of phosphatidylethanolamine model membranes investigated by SAXS and DSC. Applications of Biocalorimetry IV, 31.08. - 03.09.2004, Art'otel, Budapest, Hungary

Posters

Linser, S., Funari, S.S. and Willumeit, R. Antimicrobial Peptides and the disruption of model membranes. International Workshop on dynamics of artificial and biological membranes, 20.-22.03.2006, Gomadingen, Germany

Linser, S., Funari, S.S. and Willumeit, R. The interaction of peptide antibiotics with model membranes investigated by SAXS measurements. 5th European Biophysics Congress, 27.08.- 01.09.2005, Montpellier, France

Linser, S., Andrä, J., Kumpugdee-Vollrath, M., Funari, S.S. and Willumeit, R. The effect of antimicrobial peptides on the structure of phosphatidylethanolamine model membranes as investigated by Small Angle X-Ray Scattering. Hercules Trainingscourse, 20.02.05 - 25.03.05, Grenoble, France

Linser, S., Andrä, J., Kumpugdee-Vollrath, M., Funari, S.S. and Willumeit, R. The peptide antibiotic NK-2 influences the inverted hexagonal phase transition of phosphatidylethanolamine model membranes. International Workshop on Biophysics of Cellular Communication: Networks and molecular interactions, 22.03.-24.03.2004, Gomadingen, Germany

Linser, S., Kumpugdee, M., Andrä, J., Funari, S.S. and Willumeit, R. Influence of antimicrobial peptides on the curvature strain and lateral pressure of phosphatidylethanolamine model membranes. Hasylab User Meeting 2004, Hamburg, Germany

Others

Linser, S., Funari, S.S. and Willumeit, R. The antibacterial peptide NKCS and derivatives thereof change the inverse hexagonal phase transition temperature of phosphatidylethanolamine membranes. Hasylab Annual Report (2005)

Linser, S., Funari, S.S. and Willumeit, R. Influence of antibacterial peptides on the structure of PE model membranes, Hasylab Annual Report 2004 (2005)

Linser, S., Kumpugdee, M., Andrä, J., Funari, S.S. and Willumeit, R. The antimicrobial peptide NK-2 enhances the negative curvature strain in phosphatidylethanolamine model membranes. Hasylab Annual Report 2003 (2004)

Linser, S., Andrä, J., Kumpugdee, M., Funari, S.S. and Willumeit, R. The antimicrobial peptide NK-2 enhances the negative curvature strain in phosphatidylethanolamine model membranes. Hasylab Annual Report (2003)

8.2. Articles and books

Janeway, C. A., Travers, P., Walport, M. and Shlomchik, M. In Mahlke, K. (eds), Immunologie. Spektrum Akademischer Verlag, Heidelberg, Germany (2002)

Zasloff, M. Antimicrobial peptides in health and disease. N. Engl. J. Med. 347 (2002), 1199-1200

Janeway, C.A., Jr and Medzhitov, R. Introduction: The role of innate immunity in the adaptive immune response. Sem. Immunol. 10 (1998), 349-350

Fleming, A. On the antibacterial action of cultures of a penicillium, with special reference to their use in the isolation of B. influenzae. Br. J. Exp. Pathol. 10 (1929), 226-236

Alberts, B., Bray, D., Lewis, J., Raff, M., Roberts, K. and Watson, J.D. Molekularbiologie der Zelle. VCH, Weinheim, Germany (1994)

Leeb, M. Antibiotics: A shot in the arm. Nature 431 (2004), 892-893

Nature Biotech. Supplement. 18 (2000); reprinted from Nature Biotech. 17 (1999), 1141-1142

Hancock, R.E.W. Peptide antibiotics. Lancet. 349 (1997), 418-422

Bush, K., Macielag, M. and Weidner-Wells, M. Taking inventory: antibacterial agents currently at or beyond Phase 1. Curr. Opin. Microbiol. 7 (2004), 466-476

Giles, F.J., Redman, R., Yazji, S., Bellm, L. Iseganan HCl: a novel antimicrobial agent. Expert Opin. Investig. Drugs 11 (2002), 1161-1170.

Vizioli, J. and Salzet, M. Antimicrobial peptides from animals: focus on invertebrates. Trends Pharmacol. Sci. 23 (2002), 494-496

Hancock, R.E.W. and Chapple, D.S. Peptide antibiotics. Antimicrob. Agents Chemother. 43 (1999), 1317-1323

Ganz, T. Defensins and host defense. Science. 286 (1999), 420-421

Lai, R., Liu, H., Lee, W.H. and Zhang, Y. An anionic antimicrobial peptide from toad *Bombina maxima*. Biophys. Res. Commun. 295 (2002), 796-799

Schittek, B., Hipfel, R., Sauer, B., Bauer, J., Kalbacher, H., Stevanovic, S., Schirle, M., Schroeder, K., Blin, N., Meier, F., Rassner, G. and Garbe, C. Dermcidin: a novel human antibiotic peptide secreted by sweat glands. Nature Immunol. 2 (2001), 1133-1137

Steiner, H., Hultmark, D., Engstrom, A., Bennich, H. and Boman, H.G. Sequence and specificity of two antibacterial proteins involved in insect immunity. Nature 292 (1981), 246-248

Habermann, E. Bee and wasp venoms. Science 177 (1972), 314-322

Zasloff, M. Magainins, a class of antimicrobial peptides from *Xenopus* skin: isolation, characterization of two active forms, and partial cDNA sequence of a precursor. Proc. Natl. Acad. Sci. U.S.A. 84 (1987), 5449-5453

Pouny, Y., Rapaport, D., Mor, A., Nicolas, P. and Shai, Y. Interaction of antimicrobial dermaseptin and its fluorescently labeled analogues with phospholipid membranes. Biochem. 31 (1992), 12416-12423

Park, C.B., Yi, K.S., Matsuzaki, K., Kim, M.S. and Kim, S.C. Structure-activity analysis of buforin II, a histone H2A-derived antimicrobial peptide: the proline hinge is responsible for the cell-penetrating ability of buforin II. Proc. Natl. Acad. Sci. U.S.A. 97 (2000), 8245-8250

Johansson, J., Gudmundsson, G.H., Rottenberg, M.E., Berndt, K.D. and Agerberth, B. Conformation-dependent antibacterial activity of the naturally occurring human peptide LL-37. J. Biol. Chem. 273 (1998), 3718-3724

Boman, H.G. Peptide antibiotics and their role in innate immunity. *Annu. Rev. Immunol.* 13 (1995), 61-92

Shamova, O., Brogden, K.A., Zhao, C., Nguyen, T., Kokryakov, V.N. and Lehrer, R.I. Purification and properties of proline-rich antimicrobial peptides from sheep and goat leukocytes. *Infect. Immun.* 67 (1999), 4106-4111

Boman, H.G., Agerberth, B. and Boman, A. Mechanisms of action on *Escherichia coli* of cecropin P1 and PR-39, two antibacterial peptides from pig intestine. *Infect. Immun.* 61 (1993), 2978-2984

Zhao, C., Ganz, T. and Lehrer, R.I. Structures of genes for two cathelin-associated antimicrobial peptides: prophenin-2 and PR-39. *FEBS Lett.* 376 (1995), 130-134

Selsted, M.E., Novotny, M.J., Morris, W.L., Tang, Y.Q., Smith, W. and Cullor, J.S. Indolicidin, a novel bactericidal tridecapeptide amide from neutrophils. *J. Biol. Chem.* 267 (1992), 4292-4295

Basir, Y.J., Knoop, F.C., Dulka, J., Conlon, J.M. Multiple antimicrobial peptides and peptides related to bradykinin and neuromedin N isolated from skin secretions of the pickerel frog, *Rana palustris*. *BBA* 1543 (2000), 95-105

Kokryakov, V.N., Harwig, S.S., Panyutich, E.A., Shevchenko, A.A., Aleshina, G.M., Shamova, O.V., Korneva, H.A. and Lehrer, R.I. Protegrins: leukocyte antimicrobial peptides that combine features of corticostatic defensins and tachyplesins. *FEBS Lett.* 327 (1993), 231-236

Ganz, T. Defensins: antimicrobial peptides of innate immunity. *Nat. Rev. Immunol.* 3 (2003), 710-720

Lehrer, R.I. Primate defensins. *Nat. Rev. Microbiol.* 2 (2004), 727-738

Tang, Y.Q., Yuan, J., Miller, C.J. and Selsted, M.E. Isolation, characterization, cDNA cloning, and antimicrobial properties of two distinct subfamilies of alpha-defensins from rhesus macaque leukocytes. *Infect. Immun.* 67 (1999), 6139-6144

Andersson, M., Gunne, H., Agerberth, B., Boman, A., Bergman, T., Sillard, R., Jörnvall, H., Mutt, V., Olsson, B., Wigzell, H., Dagerlind, A., Boman, H.G., Gudmundsson, G.H. NK-lysin, a novel effector peptide of cytotoxic T and NK cells. Structure and DNA cloning of the porcine form, induction by interleukin 2, antibacterial and antitumor activity. *Embo J.* 14 (1995), 1615-1625

Fehlbaum, P., Bulet, P., Michaut, L., Lagueux, M., Broekaert, W.F., Hetru, C. and Hoffmann, J.A. Insect immunity. Septic injury of *Drosophila* induces the synthesis of a potent antifungal peptide with sequence homology to plant antifungal peptides. *J. Biol. Chem.* 269 (1994), 33159-33163

Kuwata, H., Yip, T.T., Yip, C.L., Tomita, M. and Hutchens, T.W. Bactericidal domain of lactoferrin: detection, quantitation, and characterization of lactoferricin in serum by SELDI affinity mass spectrometry. *Biochem. Biophys. Res. Commun.* 245 (1998), 764-773

Zucht, H.D., Raida, M., Adermann, K., Magert, H.J., Forssmann, W.G. Casocidin-I: a casein-alpha s2 derived peptide exhibits antibacterial activity. FEBS Lett. 372 / 2-3 (1995), 185-188

Csordas, A. and Michl, H. Isolation and structure of a haemolytic polypeptide from the defensive secretion of European Bombina Species. Monatsheft Chem. 101 (1970), 182-189

Kreil, G. Antimicrobial peptides from amphibian skin: an overview. Ciba Found. Symp. 186 (1994), 77-90

Boman, H.G., Wade, D., Boman, I.A., Wahlin, B. and Merrifield, R.B. Antibacterial and antimalarial properties of peptides that are cecropin-melittin hybrids. FEBS Lett. 259 (1989), 103-106

Tossi, A., Tarantino, C. and Romeo, D. Design of synthetic antimicrobial peptides based on sequence analogy and amphipathicity. Eur. J. Biochem. 250 (1997), 549-558

Blondelle, S.E., Perez-Paya, E. and Houghton, R.A. Synthetic combinatorial libraries: novel discovery strategies for identification of antimicrobial agents. Antimicrob. Agents Chemother. 40 (1996), 1067-1071

Hancock, R.E.W. Cationic peptides: effectors in innate immunity and novel antimicrobials. Lancet Infect. Dis. 1 (2001), 156-164

Piers, K.L., Brown, M.H. and Hancock, R.E.W. Improvement of outer membrane-permeabilizing and lipopolysaccharide-binding activities of an antimicrobial cationic peptide by C-terminal modification. Antimicrob. Agents Chemother. 38 (1994), 2311-2316

Bello, J., Bello, H.R. and Granados, E. Conformation and aggregation of melittin: chirality, antimicrobial activity and proteolytic resistance. Biochem. 21 (1982), 461-465

Falla, T.J., Karunaratne, D.N. and Hancock, R.E.W. Mode of action of the antimicrobial peptide indolicidins. J. Biol. Chem. 271 (1996), 19298-19303

Wieprecht, T., Dathe, M., Krause, Beyermann, M., Molloy, W.L., MacDonald, D.L. and Bienert, M. Modulation of membrane activity of amphipathic, antibacterial peptides by slight modifications of the hydrophobic moment. FEBS Lett. 417 (1997), 7934-7941

Brodgen, K.A. Antimicrobial peptides: Pore formers or metabolic inhibitors in bacteria? Nature Rev. Microbiol. 3 (2005), 238-250

Cantor, R.S. Size distribution of barrel-stave aggregates of membrane peptides: influence of the bilayer lateral pressure profile. Biophys. J. 82 (2002), 2520-2525

- Bechinger, B. The structure, dynamics and orientation of antimicrobial peptides in membranes by multidimensional solid-state NMR spectroscopy. *BBA*. 1462 (1999), 157-183
- Shai, Y. Mechanism of the binding, insertion and destabilization of phospholipid bilayer membranes by alpha-helical antimicrobial and cell non-selective membrane-lytic peptides. *BBA*. 1462 (1999), 55-70
- Matsuzaki, K., Murase, O., Fujii, N. and Miyajima, K. An antimicrobial peptide, magainin 2, induced a rapid flip-flop of phospholipids coupled with pore formation and peptide translocation. *Biochem*. 35 (1996), 11361-11368
- Yang, L., Harroun, T.A., Weiss, T.M., Ding, L. and Huang, H.W. Barrel-stave model or toroidal model? A case study on melittin pores. *Biophys. J.* 81 (2001), 1475-1485
- Giannis, A. and Kolter, T. Peptidmimetica für Rezeptorliganden - Entdeckung, Entwicklung und medizinische Perspektiven. *Angew. Chem.* 105 (1993), 1303-1326
- Porter, E.A., Wang, X., Lee, H.S., Weisblum, B. and Gellman, S.H. Non-haemolytic beta-amino-acid oligomers. *Nature* 404 (2000), 565-566
- Liu, D. and DeGrado, W.F. De novo design, synthesis, and characterization of antimicrobial beta-peptides. *J. Am. Chem. Soc.* 123 (2001), 7553-7559
- Patch, J.A. and Barron, A.E. Helical peptoid mimics of magainin-2 amide. *J. Am. Chem. Soc.* 125 (2003), 12092-12093.
- Oren, Z. and Shai, Y. Selective lysis of bacteria but not mammalian cells by diastereomers of melittin: structure-function study. *Biochem*. 36 (1997), 1826-1835
- Tew, G.N., Liu, D., Chen, B., Doerksen, R.J., Kaplan, J., Carroll, P.J., Klein, M.L. and DeGrado, W.F. De novo design of biomimetic antimicrobial polymers. *Proc. Natl. Acad. Sci. U.S.A.* 99 (2002), 5110-5114
- Arnt, L., Nüsslein, K. and Tew, G.N. Nonhemolytic Abiogenic Polymers as Antimicrobial Peptide Mimics. *J. Polym. Sci. A, Polym. Chem.* 42 (2004), 3860-3864
- Böhm, H.J., Klebe, G. and Kubinyi, H. In: *Wirkstoffdesign*. Spektrum Akademischer Verlag, Heidelberg, Germany (1996)
- Böhm, H.J. Towards the automatic design of synthetically accessible protein ligands: peptides, amides and peptidomimetics. *J. Comput-Aided Mol. Design* 10 (1996), 265-272
- Andrä, J. and Leippe, M. Candidacidal activity of shortened synthetic analogs of amoebapores and NK-lysin. *Med. Microbiol. Immunol.* 188 (1999), 117-124
- Liepinsh, E., Andersson, M., Ruysschaert, J.M., Otting, G. Saposin fold revealed by the NMR structure of NK-lysin. *Nature Struct. Biol.* 4 (1997), 793-795

- Lehrer, R.I., Lichtenstein, A.K., Ganz, T. Defensins: antimicrobial and cytotoxic peptides of mammalian cells. *Annu. Rev. Immunol.* 11 (1993), 105-128
- Garcia-Penarrubia, P. In Lewis, C.E. and McGee, J.O.D. (eds), *The natural immune system: The natural killer cell.* Oxford University Press, Oxford, UK (1992), 68-105
- Andrä, J. Amoebapores, cytolytische und antibakterielle Peptide aus *Entamoeba Histolytica*. Untersuchung der Struktur-Funktionsbeziehungen. PHD-thesis (1996), University of Hamburg, Germany
- Singer, S.J. and Nicholson, G.L. The fluid mosaic model of the structure of cell membranes. *Science* 173 (1972), 720-731
- Israelachvili, J.N., Marcelja, S. and Horn, R.G. Physical principles of membrane organisation. *Q. Rev. Biophys.* 13 (1980), 121-200
- Frömter, E. In Hoppe, W., Lohmann, W., Markl, H. Ziegler, H. (eds), *Biophysik.* Springer Verlag, Heidelberg, Germany (1982), 480-531
- Cotterill, R. In: *Biophysics. An introduction.* Wiley, New York, USA (2004), 161-186
- Cevc, G. and Marsh, D. (Eds.) In: *Phospholipid Bilayers - Physical Principles and Models, Vol. 5,* Wiley, New York, USA (1987)
- Gennis, R.B. In: *Biomembranes: Molecular Structure and Function,* Springer Verlag, Heidelberg, Germany (1989)
- Silvius, J.R. Thermotropic phase transitions of pure lipids in model membranes and their modification by membrane proteins. *Lip. Prot. Interact.* 2 (1982), 239-281
- Arnt, L., Nüsslein, K. and Tew, G.N. Nonhemolytic Abiogenic Polymers as Antimicrobial Peptide Mimics. *J. Polym. Sci. A: Polym. Chem.* 42 (2004), 3860-3864
- Lee, T. and Fitzgerald, V. Phase transitions of alkyl ether analogs of phosphatidylcholine. *BBA.* 598 (1980), 189-192
- Curatolo, W., Sears, B. and Neuringer, L.J. A calorimetry and deuterium NMR study of mixed model membranes of 1-palmitoyl-2-oleylphosphatidylcholine and saturated phosphatidylcholines. *BBA* 817 (1985), 261-270
- Boyd, P. and Tirrell, D. American Chemical Society Meeting 21 (1980), 188-190
- Rudolph, A.S., Crowe, J.H. and Crowe, L.M. Effects of three stabilizing agents--proline, betaine, and trehalose--on membrane phospholipids. *Arch. Biochem. Biophys.* 245 (1986), 134-143
- Fleming, B.D. and Keough, K.M. Thermotropic mesomorphism in aqueous dispersions of 1-palmitoyl-2-oleoyl- and 1,2-dilauroyl-phosphatidylglycerols in the presence of excess Na⁺ or Ca²⁺. *Can. J. Biochem. Cell Biol.* 61 (1983), 882-891

Jaworsky, M. and Mendelsohn, R. Fourier-transform infrared studies of CaATPase partitioning in phospholipid mixtures of 1,2-dipalmitoylphosphatidylcholine-d62 with 1-palmitoyl-2-oleoylphosphatidylethanolamine and 1-stearoyl-2-oleoylphosphatidylcholine. *Biochem.* 24 (1985), 3422-3428

Rujanavech, C., Henderson, P.A. and Silbert, D.F. Influence of sterol structure on phospholipid phase behavior as detected by parinaric acid fluorescence spectroscopy. *J. Biol. Chem.* 261 (1986), 7204-7214

Sanderson, P.W., Lis, L.J., Quinn, P.J. and Williams, W.P. The Hofmeister effect in relation to membrane lipid phase stability. *BBA* 1067 (1991), 43-50

Leventis, R., Fuller, N., Rand, R.P., Yeagle, P.L., Sen, A., Zuckermann, M.J. and Silvius, J.R. Molecular organization and stability of hydrated dispersions of headgroup-modified phosphatidylethanolamine analogues. *Biochem.* 30 (1991), 7212-7219

Van Dijck, P.W., De Kruijff, B., Van Deenen, L.L., De Gier, J. and Demel, R.A. The preference of cholesterol for phosphatidylcholine in mixed phosphatidylcholine-phosphatidylethanolamine bilayers. *BBA* 455 (1976), 576-587

Nosedá, A., Godwin, P.L. and Modest, E.J. Effects of antineoplastic ether lipids on model and biological membranes. *BBA* 945 (1988), 92-100

Van Echteld, C.J.A., Van Stigt, R.; de Kruijff, B.; Leunissen-Bijvelt, J.; Verkleij, A. and De Gier, J. Gramicidin promotes formation of the hexagonal HII phase in aqueous dispersions of phosphatidylethanolamine and phosphatidylcholine. *BBA* 648 (1981), 287-291

Mabrey, S. and Sturtevant, J.M. Incorporation of saturated fatty acids into phosphatidylcholine bilayers. *BBA* 486 (1977), 444-450

Mendelsohn, R. and Koch, C.C. Deuterated phospholipids as Raman spectroscopic probes of membrane structure. Phase diagrams for the dipalmitoyl phosphatidylcholine (and its d62 derivative)-dipalmitoyl phosphatidylethanolamine system. *BBA* 598 (1980), 260-271

Harlos, K. and Eibl, H. Hexagonal phases in phospholipids with saturated chains: phosphatidylethanolamines and phosphatidic acids. *Biochem.* 20 (1981), 2888-2892

Lewis, R.N., Mannock, D.A., McElhaney, R.N., Turner, D.C. and Gruner, S.M. Effect of fatty acyl chain length and structure on the lamellar gel to liquid-crystalline and lamellar to reversed hexagonal phase transitions of aqueous phosphatidylethanolamine dispersions. *Biochem.* 28 (1989), 541-548

Epand, R.M. Hydrogen bonding and the thermotropic transitions of phosphatidylethanolamines. *Chem. Phys. Lipids* 52 (1990), 227-230

Ashcroft, A.E. *Ionization Methods in Organic Mass Spectrometry.* (1997) The Royal Society of Chemistry, UK

Yamashita, M. and Fenn, J.B. Electrospray ion source. Another free jet theme. *J. Phys. Chem.* 88 (1984), 4451-4459

Greenfield, N. and Fasman, G. Computed circular dichroism spectra for the evaluation of protein conformation. *Biochem.* 8 (1969), 4108-4116

Guinier, A. and Fourier, G. In: *Small Angle Scattering of X-Rays*. Wiley, New York, USA (1955)

Svergun, D.I. and Koch, M.H.J. *Rep. Prog. Phys.* 66 (2003), 1735–1782

Lindblom, G. and Rilfors, R. Nonlamellar phases formed by membrane lipids. *Adv. Colloid Interface Sci.* 41 (1992), 101-125

Boulin, C., Kempf, R. Koch, M.H.J. and McLaughlin, S.M. Data appraisal, evaluation and display for synchrotron radiation experiments: hardware and software. *Nucl. Instrum. Methods A.* 249 (1986), 399-407

Schröder-Borm, H., Willumeit, R., Brandenburg, K. and Andrä, J. Molecular basis for membrane selectivity of NK-2, a potent peptide antibiotic derived from NK-lysin. *Biochim. Biophys. Acta* 1612 (2003), 164-171

Hauser, H. Some aspects of the phase behaviour of charged lipids. *BBA* 772 (1984), 37-50

Deme, B., Dubois, M., Gulik-Krzywicki, T. and Zemb, T. Giant collective fluctuations of charged membranes at the lamellar-to-vesicle unbinding transition: 1. Characterization of a new lipid morphology by SANS, SAXS, and electron microscopy. *Langmuir* 18 (2002), 997-1004

Waterhous, D.V. and Johnson, W.C. jr. Importance of environment in determining secondary structure in proteins. *Biochem* 33 (1994), 2121-2128

Casals, E., Galan, A.M., Escolar, G., Gallardo, M. and Estelrich, J. Physical stability of liposomes bearing hemostatic activity. *Chem. Phys. Lipids* 125 (2003), 139-146

Hancock, R.E., Falla, T. and Brown, M. Cationic bactericidal peptides. *Adv. Microb. Physiol.* 37 (1995), 135-175

Wu, M. and Hancock, R.E. Interaction of the cyclic antimicrobial cationic peptide bactenecin with the outer and cytoplasmic membrane. *J. Biol. Chem.* 274 (1999), 29-35

Wang, W., Smith, D.K., Moulding, K. and Chen, H.M. *J. Biol. Chem.* 273 (1998), 27438– 27448.

Hristova, K., Selsted, M.E. and White, S.H. *J. Biol. Chem.* 272 (1997), 24224–24233.

White, S.H. and Wimley, W.C. Membrane protein folding and stability: physical principles. *Annu. Rev. Biophys. Biomolec. Struct.* 28 (1999), 319-365

Szule, J.A. and Rand, R.P. The effects of gramicidin on the structure of phospholipid assemblies. *Biophys. J.* 85 (2003), 1702-1712.

Staudegger, E., Prenner, E.J., Kriechbaum, M., Degovics, G., Lewis, R.N., McElhaney, R.N. and Lohner, K. X-ray studies on the interaction of the antimicrobial peptide gramicidin S with microbial lipid extracts: evidence for cubic phase formation. *BBA* 1468 (2000), 213-230

Epand, R.M. and Vogel, H.J. Diversity of antimicrobial peptides and their mechanisms of action. *BBA* 1462 (1999), 11-28

Angelova, A., Ionov, R., Koch, M.H.J. and Rapp, G. Interaction of the peptide antibiotic alamethicin with bilayer- and non-bilayer-forming lipids: influence of increasing alamethicin concentration on the lipids supramolecular structures. *Arch. Biochem. Biophys.* 378 (2000), 93-106.

Henzler Wildman, K.A., Lee, D.K. and Ramamoorthy, A. Mechanism of lipid bilayer disruption by the human antimicrobial peptide, LL-37. *Biochem.* 42 (2003), 6545-6558

Matsuzaki, K., Sugishita, K., Ishibe, N., Ueha, M., Nakata, S., Miyajima, K. and Epand, R.M. Relationship of membrane curvature to the formation of pores by magainin 2. *Biochem.* 37(1998), 11856-11863

Hallock, K.J., Lee, D.K. and Ramamoorthy, A. MSI-78, an analogue of the magainin antimicrobial peptides, disrupts lipid bilayer structure via positive curvature strain. *Biophys. J.* 84 (2003), 3052-3060

Oren, Z. and Shai, Y. Mode of action of linear amphipathic alpha-helical antimicrobial peptides. *Biopolymers.* 47 (1998), 451-463

Matsuzaki, K. Magainins as paradigm for the mode of action of pore forming polypeptides. *BBA* 1376 (1998), 391-400

Huang, H.W. Action of antimicrobial peptides: two-state model. *Biochem.* 39 (2000), 8347-8352

8.3. Useful internet addresses

- 1) <http://www.wikihealth.com/Antibiotic>
- 2) <http://www.genaera.com/clinicaltrials.html>
- 3) <http://www.diabetes-mellitus.org/locilex.htm>
- 4) <http://www.clinicaltrials.gov>
- 5) <http://www.lipidlibrary.co.uk/>
- 6) <http://blanco.biomol.uci.edu/>

9. Acknowledgements

In the process of writing this thesis many people have contributed their time and effort in assisting me. I would like to express my gratitude towards them for making this possible.

First of all I want to acknowledge my supervisor Dr. Regine Willumeit for her never ending patience and Prof. Dr. Ulli Hahn for also being in charge of correcting this thesis.

I give a special thank to Dr. Jörg Andrä for the preliminary work on NK-2 and the discussions about the peptide on which this thesis was based.

My participation on the interesting subject of peptidomimetic substances was possible due to the cooperation with Gregory N. Tew and Jason R. Rennie. The computational modelled peptide was provided from Nir Ben-Tal and Dalit Bechor. I thank Stephan Lassen for the technical discussions and the mass spectroscopy experiments and Claudia Olak for her help during the CD measurements.

Furthermore, I gratefully acknowledge the group of macromolecular structure research at the GKSS Research Centre for the help and assistance.

Especially, I would like to give my thanks to my family whose encouragement enabled me to complete this work. I dedicate this work to my girlfriend Constanze Duisman and my daughter Ida Duisman.

Thank you!